ENGINEERING RESEARCH UNIT
UNIVERSITY OF MORATUWA
SRI LANKA

RESEARCH FOR INDUSTRY

Proceedings of the Annual Symposium 1998

November 1998

ISSN 1391-3999

ENGINEERING RESEARCH UNIT
UNIVERSITY OF MORATUWA
SRI LANKA

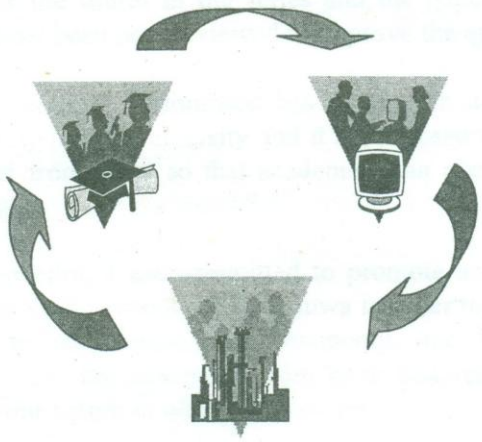

RESEARCH FOR INDUSTRY

Proceedings of the Annual Symposium 1998

November 1998

ISSN 1391-3999

These proceedings comprise papers presented at the 4th Symposium on Research for Industry organised by the Engineering Research Unit of the University of Moratuwa and held in the premises of the University in November 1998.

The views and findings presented in the papers are those of the authors, and do not reflect those of the Engineering Research Unit, Moratuwa.

Edited by

Premini Hettiarachchi

Published by

Engineering Research Unit
University of Moratuwa

Moratuwa, Sri Lanka 1998

Message from the Vice Chancellor
ERU Symposium on Research for Industry

The University of Moratuwa emphasizes Research in its Mission Statement. Research especially Industry oriented research is all the more relevant and important in the face of rapid technological change that is taking place to-day. This is an era of the knowledge-worker as knowledge is becoming the world's major source of development and wealth. Under the circumstances Universities which are knowledge-based institutions by design will have to play a key role in research and generation of new knowledge.

The University of Moratuwa with its dominance in Engineering and Architecture has established Research Units both in Engineering and Architecture. The Engineering Research Unit (ERU) was established in 1990 to promote engineering research and disseminate findings of research. In 1995 the first Annual Symposium on Research for Industry was held and then onwards it had been an annual event. The 1998 Symposium is the fourth in the series and the papers presented at this symposium have been peer reviewed to improve the quality of research.

The Senate Research Committee has been activated to enhance the research activity in the University and it is proposed to have an adequate annual budget from 1999 so that academics can plan and conduct their research activity.

As Vice Chancellor, I am committed to promote and enhance research activity within the University of Moratuwa in order to make a meaningful contribution to our industry and economy, and I expect a similar commitment from the academics who have that research capability to contribute to our nation in no small measure.

I pay a tribute to all those who have strived to make this Symposium a success and I appeal to industry to appreciate our effort and utilize the findings of our research as far as possible.

I wish the Symposium every success.

Prof. S Karunaratne
Vice Chancellor

Message from the Dean/Faculty of Engineering
ERU Symposium on Research for Industry

I am very happy to note that the Engineering Research Unit (ERU) of the Faculty is organising an Engineering Research Symposia in the fourth year in succession. The Faculty of Engineering and the University of Moratuwa as a whole have been trying to promote research activities in many possible directions. In the recent part our major trust had been to promote industry based research in the Faculty. In order to accomplish this we have been encouraging the Faculty members to undertake research in collaboration with the industry in different forms.

Since we were unable to attract full time M. Phil/Ph.D. students the Faculty embarked as a programme to have one year full time M.Sc./M.Eng. students with an enhanced component of research. We expect a large number of engineers from the industry to register in this programme and staff are planning to undertake research projects directly relevant to industry needs. We hope this will act as a catalyst to promote industry based research in the University. With an active industry based research in the University. With an active industry based research, it is hoped that the industry will sponsor major research projects in future which will have direct benefit to them.

We expect the ERU to be a major partner in promoting industry based research in the Faculty and assist the researchers as well as the administration to strengthen the research capabilities in the Faculty of Engineering at University of Moratuwa.

I wish the 1998 ERU Symposium a great success.

Professor L.L. Ratnayake
Dean/Faculty of Engineering

Message from Chairman, ERU

This annual symposium, the fourth in a series that commenced in 1995, has been progressively upgraded to the point that all the papers that are published and presented have been successfully peer-reviewed. We would therefore like to congratulate the authors, not only for the utilitarian value of their contributions but also for their academic content. Peer-reviewing has meant of course that not all submitted papers have been accepted; in fact we had a rejection rate of around 30%. We would like to encourage more of our colleagues to submit papers next time around.

We also publish abstracts of some poster papers, which are being displayed on the day of the symposium. These posters too will have many useful ideas and applications and we would encourage symposium participants to spend some time at these displays.

I would also like to make use of this opportunity to inform participants and others reading these proceedings that we are about to publish a directory of research; this too will hopefully be an annual exercise. If you wish to receive a directory, please get in touch with us. Also let us know if you would like to receive our ERU newsletter that is published once in two months.

Finally, it is my pleasant task to thank all the other members of the Engineering Research Unit who have worked hard to make this Symposium a reality, especially Dr Thishan Jayasinghe, our Secretary; and more especially Dr Premini Hettiarachchi, our Editor, who worked tirelessly and effectively to nurse all these papers from their original submission, through the peer-review process into the final form that is before you. I also wish to place on record the assistance rendered by our clerk, Mr. Menaka Jayawardena.

Priyan Dias
Chairman, Engineering Research Unit
(priyan@civil.mrt.ac.lk)
November 1998

CONTENTS

Pricing of electricity from renewable energy sources in Sri Lanka 1
Priyantha DC Wijayatunga
Combined symbolic and numerical methods for solving equational systems. 11
Visakha Nanayakkara & Gihan Dias

Computer simulation of buildings with passive elements for energy efficiency 25
MTR Jayasinghe, PTP Jayatunga & RA Attalage
Use of reinforced brickwork for crack free load-bearing construction 38
MTR Jaysinghe & DPK Maharachchi
A design method for prismatic pre-stressed concrete continuous box girder bridges 52
WMDN Ranasinghe & MTR Jayasinghe

An appropriate latex -bitumen emulsion blend for road surfacing 69
K Subramaniam & TK Sivarajan
The use of saltern bitterns for manufacturing magnesia refractories 77
WLW Fernando
Modified clay as a filler in rubber compounding 91
PY Gunapala & M Sivasundaram

Investigation of wave reflection from coastal structures 99
SSL Hettiarachchi & PD Mirihagalla
A surface source singularity model for time averaged flow around cylindrical structures 121
AGT Sugathapala

Design and construction of a bending tester for textiles 136
Nirmali Perera
Investigation of the use of water by the textile industry in Sri Lanka – Part 1 145
NGH de Silva
Positive environmental management via waste minimization in a textile washing facility 157
Samudrika Wijayapala, NGH de Silva & Ajith de Alwis

POSTER PAPERS

Billest: Computer aided estimating software 168
AADAJ Perera

Measurement of ocean wave height
using a capacitance-based liquid level sensor 169
GK Watugala, WA Dilhara, NGDI Perera, KKKC Ariyathilake, & SCR Perera

Earthquake resistant detailing of reinforced concrete structures 170
DFU Perera & MTR Jayasinghe

Electromagnetic effects on a human brain due to cellular phones 171
IJ Dayawansa

Future Prospects for a New Industry 172
Nirmali Perera

PRICING OF ELECTRICITY FROM RENEWABLE ENERGY SOURCES IN SRI LANKA

Priyantha D C Wijayatunga
Department of Electrical Engineering, University of Moratuwa

PRICING OF ELECTRICITY FROM RENEWABLE ENERGY SOURCES IN SRI LANKA

Priyantha D C Wijayatunga
Department of Electrical Engineering, University of Moratuwa

ABSTRACT

This paper examines the area of purchase pricing of electricity generation from renewable energy sources with emphasis on micro/mini-hydro and wind turbine plants. It also presents an overview of different types of new and renewable energy sources available in Sri Lanka along with their associated costs. The prospects and quantum of future development of these resources are investigated considering both existing and a restructured electricity industry in Sri Lanka. The applicability of established pricing techniques with appropriate modifications for power purchase from different renewable sources is also discussed with case studies involving a typical wind turbine plant and a microhydro plant in Sri Lanka.

1. INTRODUCTION

The main indigenous commercial energy source available in Sri Lanka is hydroelectric power, which accounted for 91% of the total electrical energy supply in 1995. More than half of the estimated hydropower potential of 2000MW has been already harnessed through major hydropower schemes and small scale micro/mini hydro schemes [1] with a gross generation standing around 5300 GWh a year. The only conventional alternative thermal options available for electricity generation are coal-fired stations, diesel plants and gas turbines where imported fossil fuels are used. This situation demands the power planners to pursue a balanced path of energy sector development where an optimal mix of thermal, hydro and renewable energy sources is present not only to minimise the impact of heavy dependence on imported fuels envisaged in the future but also to minimise the environmental impact by future thermal plant additions[2].

The main alternative energy sources available for exploitation are wind energy, solar energy, micro-hydro power, ocean wave and thermal energy, geothermal energy, biogas and biomass which includes saw dust, paddy husk and coir dust. Though some of these are not very appropriate in the context of Sri Lanka due to problems in the areas of technical and economic viability others such as wind energy, micro/mini-hydro power, dendro power[1] and solar photovoltaics are very likely to contribute to the local energy supply [3].

2. WIND ENERGY

At present, wind power is the most mature renewable energy technology for application in large-scale electricity generation. In Sri Lanka systematic studies involving the development of wind energy by the CEB have revealed that the coastal belt from Hambantota to Kirinda offer an exploitable wind turbine capacity of 200MW with an

[1] Fuel-wood fired power plants

annual yield of 350GWh. Also it is expected that a substantial wind energy potential is available on the coastal belts from Puttlam to Jaffna and from Jaffna to Trincomalee on the east coast. In addition, certain areas such as Ambewela and Uva-basin experience strong wind speeds which can be exploited for possible wind turbine plants.

Even though the average wind speeds in possible sites are as low as 6m/s to 6.5m/s, wind power is still an option to be considered in future power development since the cost of turbines gradually decreases with technological advances making them economically viable in many circumstances.

3. MICROHYDRO POWER

In the early part of this century many of the small water streams flowing through the highlands had been tapped for small-scale power generation mainly to fulfil the electricity requirement of the tea industry. Later, with the penetration of the national electricity grid into these tea estates most of these micro-hydro plants were abandoned in late sixties. It is noted that there had been around 500 micro-hydro plants with capacities varying between 10kW to 250kW and a combined capacity of around 20MW, during this period. The exploitable capacity at these sites can be as high as 40MW. In addition to these there are other large scale sites resulting in a total exploitable small-hydro potential of around 100MW to 120MW [2].

The CEB has now allowed grid connection of small hydro plants and offers to buy all the energy injected to the system by such plants at a pre-published power purchase tariff meant for small power producers below 10MW. This has generated a considerable interest among investors and presently, studies are being carried out with regard to development of many of the sites already identified [2].

Also non-governmental organisations like the Intermediate Technology Development Group (ITDG) have been involved in developing very small hydro plants at remote villages with no access to grid electricity. These plants are in the order of 1kW to 25kW capacities.

4. BIOMASS

Though as in the case of many other developing countries, biomass is the most widely used source of primary energy in Sri Lanka with total biomass consumption standing at 9.6 million metric tons in the year 1995, very little of this indigenous primary source is used to generate electricity.

In Sri Lanka, the only large scale electricity production with biomass can be seen only in the sugar industry where baggase resulting from sugar production is almost completely utilised for electricity generation within the sugar factories themselves.

Several studies are being carried out at present with regard to energy plantations aimed at satisfying the energy requirements in various sectors including that of possible dendro power plants [4].

It is estimated that if one third of the available 1.6 million hectares of scrub land identified in the Forestry Master Plan is used for an energy plantation, it will produce

around 10 million tons of fuelwood annually. If this is used for electricity generation, it can produce 10 TWh of energy, which is equivalent to the expected electricity demand addition to the system within the next 13 years in Sri Lanka [8]. It is estimated that electricity from a 10MW dendro-thermal station would cost around Rs 2.80 to Rs 3.00 per kWh [5].

5. SOLAR PHOTOVOLTAICS (PV)

The main solar PV applications identified for Sri Lanka are in domestic lighting, small scale refrigeration and water pumping in remote rural areas with no access to the national electricity grid within a foreseeable future.

A typical 40W solar PV system which can operate around four 8W lamps, radio and a black & white TV costs around Rs 25000 including all the accessories for internal wiring and a local battery. If this is financed through a normal bank loan the monthly repayment is such that the rural poor find it hard to honour it unless such an energy supply is coupled with an income generating activity [6].

Due to these economic implications it is necessary to introduce a component of subsidy if solar PV systems are to proliferate in Sri Lanka.

6. PURCHASE PRICE OF ELECTRICITY

It is important that electricity from different renewable energy sources is carefully costed before deciding the purchase price. The prices so decided should result in encouraging more private sector participation in electricity generation while providing electricity to the consumers at the least possible cost. In other words the actual costs of production need to be properly reflected in the final purchase price.

When deciding the purchase price of electricity it is possible to choose from established techniques available for the calculation of electricity costs.

Since electricity from renewable sources is fed into the main grid from the low voltage network supplying mainly local energy requirements, the transmission and distribution loss which amounts to 17% of generation, is saved. This effect need to be included in the cost calculations based on any of the techniques involved.

6.1 Long Run Marginal Cost (LRMC)

The cost of electricity calculated with this method is based on the long term least cost generation expansion plan. LRMC is defined as the incremental cost associated with increased capacity and energy requirements as a result of an increment in the system demand sustained in to the future. This involves LRMC of generation, transmission and distribution.

The LRMC of generation in the Sri Lanka system is around Rs 3.75 per kWh and when the effect of transmission and distribution losses is considered it rises to Rs 4.39 per kWh.

6.2 Short Run Marginal Cost (SRMC)

SRMC is based on the least cost operating schedule of the generators in the system. The investment costs are not considered. SRMC is defined as the incremental cost of operation due to an increased demand at a given point in the system. Typical variation of SRMC of generation in the Sri Lanka system is given in Figure 1. Here it has been considered that the cost of energy not served is approximately Rs 18 per unit (1998) with a loss of load probability (LOLP) in each month as 1%.

Figure 1: Variation of SRMC in a typical year

6.3 Avoided Cost

The cost what the supply authority avoids as a result of power purchase from these outside sources is known as the avoided cost. In theory this is the maximum that the supply authority should pay to the power producers since higher payment will result in automatic price increases at the consumer end. The most important function during avoided cost calculation is that all the components of the avoided cost are carefully identified and accurately determined.

Capacity cost

With the installation of power plants operating with renewable energy sources the supply authority may avoid or defer installation of new generation facilities of different types. Also it is important to note that in certain cases the supply authority avoids costs associated with transmission and distribution capacity expansion which also need to be carefully determined and included in the final value.

Operating Cost

These renewable energy sources introduced to the system result in the operating cost of the supply authority owned power plants being reduced in terms their fuel costs and transmission & distribution losses.

Environmental Cost

Though it is difficult to quantify the avoided environmental cost with the introduction of renewable sources one has to recognise the need to include a cost component in this regard due to wide range of generation options considered in the electricity industry. For instance the installation of a micro/mini hydro plant avoids harmful emissions at the thermal generating stations while the installation of a dendro power plant with an associated energy plantation will result in reduced soil erosion. These environmental benefits need to be included when deriving the purchase price.

Avoided cost – Ceylon Electricity Board (CEB)

The purchase price offered to small power producers by the CEB is based on seasonal avoided operating costs. Two seasons, dry and wet are identified for this purpose.

Purchase price:
Wet season (May 01 to January 31) - 2.89 Rs/kWh
Dry season (February 01 to April 30) - 3.38 Rs/kWh

7. CASE STUDY

7.1 Wind Energy

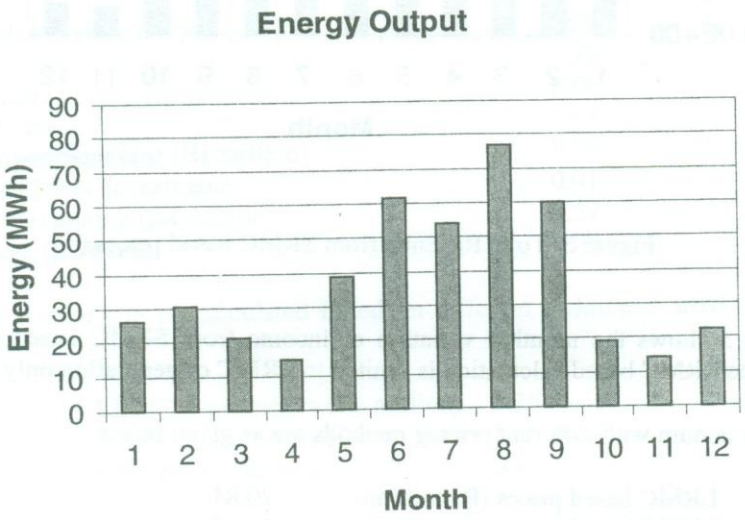

Figure 2: Energy Output from the 250kW wind turbine

The first part of the case study involves a hypothetical wind farm in Hambantota with a capacity of 3MW. The wind farm consists of twelve 250kW turbines. The wind pattern in the wind farm location during the year is such that the energy generation per wind turbine is as given in Figure 2.

It assumed that the plant has an availability of 90% during one year operation.

Sample calculation

Investment cost (Rs million)	224.12
Life time (Years)	**20**
Discount rate	10%
Annuity factor	8.51
Annual invest cost (Rs million)	26.33
Annual O&M cost (3% of Investment)	0.79
Total cost per annum (Rs million)	27.12
Per unit cost (Rs/kWh)	5.71

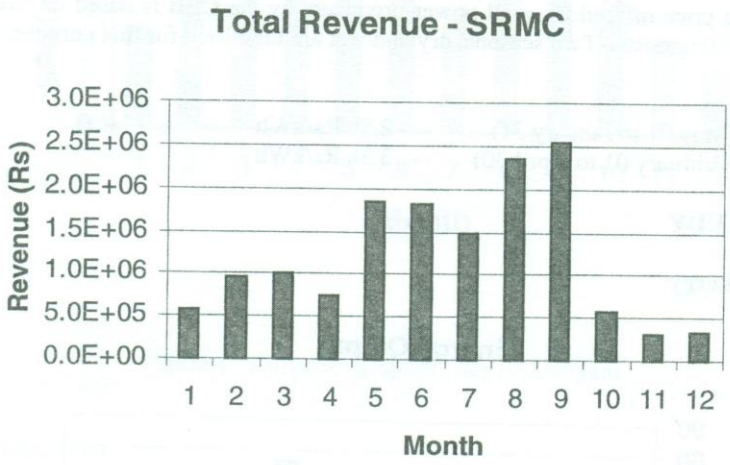

Figure 3: Total Revenue from SRMC based prices

The figure 3 shows the monthly variation of income from SRMC based prices. For convenience LRMC based calculation is limited to LRMC of generation only.

Income per annum with different pricing methods are as given below.

LRMC based prices (Rs million)	20.84
SRMC based prices (Rs million)	19.60
CEB prices (Rs million)	14.07

7.2 Microhydro power

A typical microhydro plant in the highlands with a capacity of 75kW has been considered for case study 2. The variation of energy output during the year is shown in Figure 4.

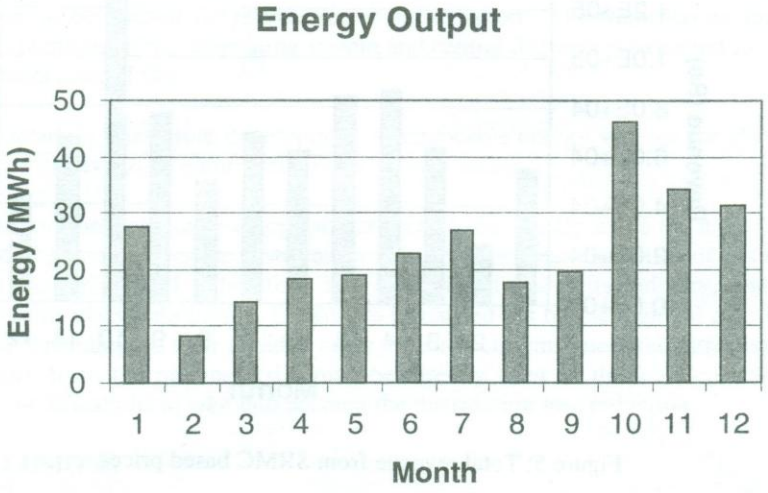

Figure 4: Total energy output from micro-hydro plant

Sample calculation

Investment cost (Rs million)	5.29
Life time	**30**
Discount rate	10%
Annuity factor	9.43
Annual investment cost (Rs million)	0.56
O&M cost (2% of Investment)	0.01
Total cost per annum (Rs million)	0.57
Per unit cost (Rs/kWh)	2.00

The total income can be calculated based on different techniques used for purchase pricing.

LRMC based prices (Rs million)	1.25
SRMC based prices (Rs million)	1.06
CEB prices (Rs million)	0.85

LRMC based calculation has ignored the effect of transmission and distribution capacity cost components for convenience.

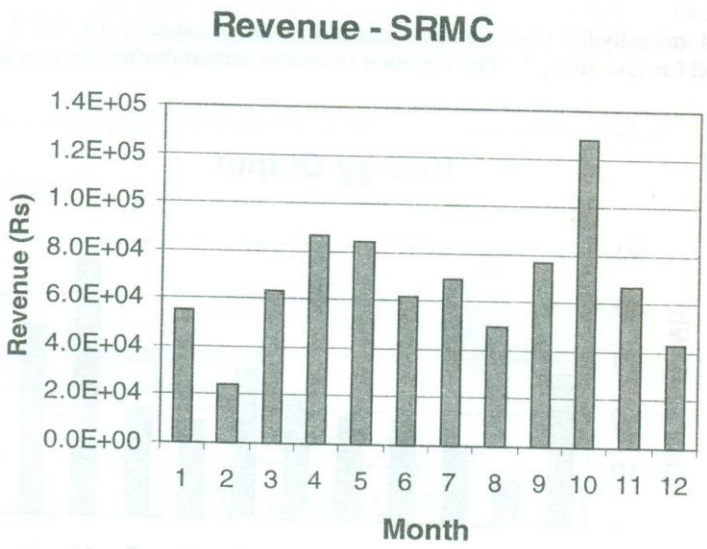

Figure 5: Total revenue from SRMC based prices

8. DISCUSSION

8.1 Case Study Results

It can be seen from the results that the cost of the wind turbine plant (Rs million 27.12 per annum) at 10% discount rate cannot be recovered through any of the power purchase prices based on the given approaches. In case of the micro-hydro plant presented in the case study all three pricing schemes manage to recover the costs associated with the plant.

It is important to note that the monthly varying prices of the SRMC scheme do not always follow the pattern of the energy output of individual plants. Therefore such a pricing scheme encourages those who generate during times of energy shortages or higher operating costs.

The strict avoided cost based prices, as discussed in a previous section, need to include avoided capacity costs, operating costs and environmental costs. The avoided operating costs are equivalent to the SRMC given in Figure 1 adjusted to take account of avoided transmission and distribution losses amounting to 17% of generation.

The avoided environmental costs considering emission of pollutants from thermal power stations can be calculated based on the findings in [9]. A recent study has revealed that this component of the avoided cost is around Rs 0.08 per kWh [10].

In general there will not be a significant avoided capacity cost without a substantial input from the renewable energy sector.

8.2 Restructuring and Renewable Energy

The proposed structure for the electricity industry in Sri Lanka is that the industry is to be split horizontally as generation, transmission and distribution businesses. Except large hydropower development, the rest of generation and whole of distribution business are to be opened for private sector participation. The transmission business along with planning of the generating system and central dispatch is expected to remain in government control [8].

In such a scenario, the future development of renewable energy sources for electricity generation will have to be completely by the private sector.

The electricity from renewable energy sources tend to be usually fed to the national grid as embedded generation in the distribution network since the capacities of associated plants are relatively small. Therefore, in a restructured electricity industry, pricing of electricity from renewable sources is likely to be carried out by the regional distribution companies depending on their avoided costs. In such circumstances the purchase price of electricity from the national grid, may be directly used as the avoided cost with necessary modifications to take into account the distribution loss reduction.

9. CONCLUSIONS

It is difficult to justify the use of an LRMC based pricing formula for electricity from renewable energy sources due to their insignificant impact on the system capacity costs unless the total generation from these sources increases considerably. Also possible deviations from the least cost generation expansion plan in a restructured framework with more private sector participation in the electricity industry will make it inappropriate to use LRMC in price calculations.

Also it is apparent from the results of the case studies and the discussion that the existing avoided cost based purchase price of electricity from renewable energy sources needs to be improved to take account of actual cost components.

It is recommended that the SRMC with an adjustment for transmission and distribution losses is used as the avoided operating cost while a reasonable value for avoided environmental cost is included based on the presented analysis. This gives a proper cost reflective purchase price regime that is independent of the type of structure in the electricity industry, for electricity from renewable energy sources.

ACKNOWLEDGEMENT

The author gratefully acknowledges the help extended by the Pre-electrification Branch, Generation Planning Branch and the System Control Centre of the CEB by providing necessary technical assistance for the analysis presented in the paper.

REFERENCES

1. "Long Term Generation Expansion Planning Studies:1996-2010", Generation Planning Branch, CEB, July 1996.

2. K Sunith Fernando, "Small Thoughts and Experiences on Wind and Micro Hydro Power", Economic Review, August 1996.

3. KKYW Perera, "Energy Status in Sri Lanka: Issues-Policy-Suggestions", Institute of Policy Studies, Sri Lanka, 1992

4. Priyantha D C Wijayatunga, "Prospects of Renewable Energy Sources in Sri Lanka: Pricing and Other Issues", Workshop on Energy and Environment, LIFE/German Cultural Institute, January 1998, Colombo, Sri Lanka.

5. Ray Wijewardena, P G Joseph, " Energy Plantations: Complementing hydro-power for sustainable thermal energy and rural employment in Sri Lanka", Achievers, September 1997.

6. "Report of the Regional Workshop on Selection of Pilot Projects", Asian and Pacific Development Centre, Malaysia, August 1997,

7. Lalith Gunaratne, "Solar Photovoltaics in Sri Lanka: a Short History", Progress in Photovoltaics: Research and Applications, Vol-2, 1994

8. "Power Sector Policy Directions", Ministry of Irrigation and Power, 1997.

9. Peter Meier and Mohan Munasinghe, "Incorporating Environmental Concerns into Power Sector Decision Making: A Case Study for Sri Lanka", World Bank Environment Paper No 5, The World Bank, 1994.

10. "Study on the Environmental & Economic Impact of using Micro-hydro and Biomass power in the Tea plantation sector in Sri Lanka", Intermediate Technology Development Group, Sri Lanka, September 1998.

11. "Energy Policy for Sri Lanka", Ministry of Irrigation Power and Energy, Sri Lanka, 1997

COMBINED SYMBOLIC AND NUMERICAL METHODS FOR SOLVING EQUATIONAL SYSTEMS

Vishaka Nanayakkara and Gihan Dias
Department of Computer Science & Engineering
University of Moratuwa, Moratuwa.
Email: vishaka@cse.mrt.ac.Ik, gihan@cse.mrt.ac.lk

COMBINED SYMBOLIC AND NUMERICAL METHODS FOR SOLVING EQUATIONAL SYSTEMS

Vishaka Nanayakkara and Gihan Dias
Department of Computer Science & Engineering
University of Moratuwa, Moratuwa.
Email: vishaka@cse.mrt.ac.lk, gihan@cse.mrt.ac.lk

ABSTRACT

In this paper we discuss systems developed to assist scientists and engineers to solve their problems based on mathematical models using numerical and symbolic methods. Numerical library routines for numerical algorithms and Computer Algebra Systems (CASs) for symbolic computation are both now well established areas. The recent research interest in these areas is oriented towards combining these solvers, rather than on improving the individual solvers. We analyse the state of research in numerical and symbolic solvers as well as the area of these combining methods or coupled (or combined) systems as they are commonly referred to. We evaluate these coupled systems to identify their essential features and various methods of integration. Based on our analysis we then propose a new strategy for integration which can enhance the facilities provided by the existing symbolic and numerical systems.

INTRODUCTION

Engineers and scientists use equations to model the problems arising in their work, and then try to solve them. If the solution cannot be obtained by symbolic simplifications alone, the equations are transformed to a form in which they can be solved using numerical algorithms. Before computers became available both tasks were done manually. The desire to mechanise the tedious, often repetitive numerical calculations and to increase speed and accuracy was one of the driving forces behind the development of computers.

To exploit the advantages of computers for numerical calculations, users started developing new algorithms; which could make more efficient use of their power. Many algorithms were developed to solve the most common types of numerical problems. Collections of such algorithms, coded in various high level programming languages, have long been available. These numerical programs have frequently been refined to increase their efficiency and accuracy and hence are usually superior to any code a non-expert user might write for the same purpose. In order to use such a standard algorithm users need to transform their original problem to an instance of the one solved by the algorithm.

Symbolic computation can be used in the transformation of the initial mathematical description into an equivalent form that is either itself the solution or an instance of a problem for which a numerical solution algorithm exists. This process requires mathematical knowledge about transformation rules. Computer Algebra Systems are increasingly becoming capable to carry out these transformations without the risk of error and at far greater speed than would be possible if the same transformations were done by hand.

Given that there are tools to perform both numerical and symbolic calculations, the users have developed many solution algorithms which can efficiently be implemented using these solvers from both numerical and symbolic domains. However the absence of an environment to use these solvers interactively may hinder the efficient implementation of these algorithms. Coupled systems, systems which allow the

interactive use of symbolic and numerical solvers, can overcome this problem. Such systems allow the users to work using equations, formulae, symbols and numerical computations, evaluate results using graphical facilities provided by CASs and automatic or semi-automatic selection of numerical algorithms.

Design and development of these systems is still at an early stage. During the last two decades many researchers have approached this problem with different methods and many coupled systems have been designed and implemented. However one common characteristic of these attempts are that the systems are being developed only for particular applications. These application domain specific combined solvers have some drawbacks. The models, which cannot be fitted into one of these application areas or the ones, which require, more than one mathematical domain cannot benefit from such environments. The cost involved in developing custom built environments prohibits users from developing combined solvers specifically for an application. Therefore the requirement is to have an environment where both symbolic and numerical systems are used interactively without restrictions on the problems it can be used for. We propose a method to build an environment for using symbolic and numerical solvers for various application areas.

NUMERICAL LIBRARIES

The solvers available for numerical calculations largely consist of high level programming language subroutines implemented using the algorithms developed by various mathematicians. These subroutines have been organised into various libraries available as commercial or public domain software. In addition to the libraries there are systems developed with easy to use interfaces to similar types of subroutines. Numerical library routines in general are built using subprograms collected over the years. The available libraries are either general purpose or specific for some area of mathematics. The criteria used in classification of the subroutines are their scope, numerical stability, accuracy and speed.

NAG library routines [*http: www.nag.co.uk*] and Numerical Recipes [1] are examples for general-purpose numerical libraries. These libraries consist of subroutines developed using the most commonly used algorithms in mathematics, and covering the most frequently occurring mathematical problems. However these routines may not in certain situations achieve the same efficiency as some of the more specific ones. There are some libraries available to provide numerical solutions to problems that can be grouped into particular areas of Mathematics. The areas are selected to allow a large cross section of problems to be treated under the same area but are specific in such a way that most of the algorithms in any area can be programmed under one library. Examples of these area specific libraries are BLAS (Basic Linear Algebra Subprograms) [2,3], LAPACK (Linear Algebra PACKage) [4,5] and Templates [6] for Linear Algebra and IMSL (International Mathematical and Statistical Library) for Statistics.

Methods for Selecting Routines

The large number of algorithms and implementations available can make it difficult for users find the one best suited for a given problem. Especially non-expert users need assistance in the selection and the use of the available software. The traditional method of written documentation can sometimes be difficult to use for inexperienced

users. If these libraries are to be used in automated solution processes there must be methods to search for algorithms to match the problem requirements using keywords.

GAMS (Guide to Available Mathematical Software) developed by the NIST (National Institute of Standards and Technology, USA) provides a large tree-structured database of mathematical and statistical software which is available on-line. GAMS allows users to search based on library and subroutine names and keywords. Users can access GAMS using the web browsers at the URL http://gams.nist.gov.

Using an expert system oriented approach to subroutine selection is another possibility. NAXPERT [7] claims to be a prototype expert system, which gives advice to users about a small mathematical library based on Fortran for IBM personal computers. Users need to select the mathematical domain of the problem at hand and then either give the keywords describing the problem or respond to the keywords suggested by NAXPERT.

A more recent approach to select the subroutines is the use of Computer Algebra Systems. ARC (Automatic Routine Chooser) [8] is a package developed to exploit this idea. This system which is implemented in REDUCE [9] chooses the best routines to match the user's description of the problem. It is implemented for a part of the NAG library.

SYMBOLIC SOLVERS

With symbolic solvers users from Science and Engineering work with computers in their natural working environments, (i.e. using equations and algebraic terms). Apart from the long tedious sequence of mathematical manipulations, inappropriateness of approximate numerical solutions (for example, in computing real roots of polynomials), easy interpretation of partial results in symbolic form are also reasons for the need for symbolic computing. Most modern day Engineers and Scientists use symbolic preprocessing in order to ensure the efficiency and accuracy in carrying out the algebraic simplifications in their work.

The concept of symbolic computing (or non-numerical computing) is not restricted only to manipulation of algebraic equations. Program compiling, logic programming, word processing, expert systems and other artificial intelligence applications are some examples. But in the context of Computer Algebra (Symbolic Computing) in this paper we discuss only the algebraic manipulation of mathematical terms. A Computer Algebra System (CAS) can be defined as a collection of an algorithm with a data structure for representing non-numerical data, a language making it possible to manipulate them, and a library of effective functions for carrying out the necessary symbolic operations.

The two major requirements expected from CASs are to provide a set of basic pre-programmed commands which instruct the computer to carry out the algebraic calculations and to offer a programming language which enables the users to define higher level commands or procedures to enlarge the original set of commands. In order to fulfill these requirements CASs usually provide the following functions.

- Operations on integers, rational, real and complex numbers to (in principle) any desired accuracy.

- Simple analysis such as differentiation, expansion of series, etc and manipulation of formulae and operations on polynomials.
- Matrix algebra with numerical and/or symbolic elements.

Window based environments and graphical outputs are now becoming standard features of CASs. The field of CASs has now grown such that there are a large number of general purpose CASs available. Maple [10] and Mathematica [11] can be considered as the leaders among the commercial packages. The various news groups formed on the Internet for different CASs are examples for widespread user communities of these packages. In addition there are many special purpose CASs, which were developed for specific problem domains. CAYLEY [12] and Macaulay [13] are examples for such special purpose CASs.

MOTIVATION FOR COUPLED SYSTEMS

Efficient solutions of many problems encountered in Engineering and Science require combination of methods from numerical analysis and symbolic computation. Computers have long handled numerical calculations and as a result large libraries of numerical routines are available. As an alternative to the traditional approach of often tedious and error prone symbolic calculations by hand, CASs have become widely used in the last 20 years. However, in applications, which require a high level of both symbolic and numerical processing, the user is still forced to alternate between both types of solvers. Instead it could be desirable to have both capabilities combined. This has motivated various attempts at combined systems. In this section we will discuss features of such systems, existing research work towards integrating different solvers and problems related to producing efficient coupled systems.

Coupled systems can be defined as systems which provide facilities to implement solutions to a given domain of applications using both symbolic and numerical methods interactively, and without the necessity for the user to have specialised knowledge of the underlying systems. These systems can help the user to solve problems that need specialised knowledge and expertise. The merits of coupled systems can be summarised as:

- Computational efficiency: Where appropriate symbolic computation can reduce the numerical workload, for instance by pre-processing symbolic input to a form which is numerically tractable.
- Reduction of errors: Limits and approximations can be handled better symbolically than numerically.
- Automation: Simplified programming with automated solution process (e.g. automated code generation).
- User guidance: Systems can be developed which allow even the non-expert users to use them.
- Resource efficiency: Developing interfaces between existing numerical and symbolic solvers costs less human and other resources than an entirely new system.
- Reuseability of results: Combined systems allow recursive refinement of the problem solving process without leaving the system.

Existing Coupled Systems

The realization of the need for combined the symbolic and numerical solvers has led to a growing research effort in this direction and to the development of number of systems. ELLPACK [14, 15], Sinapse [16, 17], ObjectMath [18, 19], FRISCO [20], CAS/PI [21, 22] and OpenMath [23] are examples of some of the existing systems which are presently available as complete systems or systems in the research stage.

Depending on the type and the area covered the existing work can broadly be classified into two categories as *Software Environments* and *Protocols for Data Interchange*.

Software: Driven by the necessity of having systems which can solve specific applications using both symbolic and numerical solvers many people have designed systems using ad-hoc integration methods to communicate with solvers. But in spite of the fact that there is no general method for communication among solvers such systems can be considered as coupled systems. ELLPACK is an example for this category. Sinapse, ObjectMath and FRISCO also exhibit similar features.

The systems in this area show two different trends in the domains they cover. Some systems are developed to solve applications having similar mathematical problems. For example ELLPACK can be used only to solve problems of PDEs. The aim of the developers of FRISCO is to provide a solver for polynomials. On the other hand some solvers are developed to solve problems in a certain application area. ObjectMath is used to generate programs to design components for a certain industrial partner. SciComp using SciNapse develops solvers customised for certain applications.

Protocols: Realising the lack of an efficient general method to transform data types and handle other communication related issues in combining the solvers, recently there have been several attempts to remedy this. The earlier attempts of ASAP [24] and MP [25] have been followed by a more general method in the OpenMath project.

Functions that can be provided by coupled systems:

- Interactive access to both CASs and numerical library routines.
- Facilities for the users to work at various levels of abstraction, without leaving the system, using equations, formulae, symbols and numerical computation.
- Facilities to evaluate results using extensive graphical facilities provided by CASs.
- Automatic or semi-automatic selection of suitable numerical algorithms.

Efficient integration of systems from different origins involves dealing with many complex issues. Some of these are

- Hiding command language variations between the different solvers by developing a common interface.
- Transparent management of remote computations.
- Automated programming environments to interactively communicate with solvers providing easy and fast communication among solvers.

The existing approaches use different methods in addressing these issues. Also when developing application-specific coupled systems the extent to which these issues has to be met vary with the applications and the requirements of the users.

Most of the coupled systems have an aim of capturing the application knowledge necessary in the field in which they are applicable. This makes reuse of knowledge in those domains feasible without much trouble. Also the interactive use of solvers in one environment facilitates the reuse of partial results generated for the same problem.

In many coupled symbolic-numerical systems, the symbolic analysis of a problem is used to determine which of a given menu of numerical procedures needs to be performed. The symbolic routines then call the chosen numerical procedures with the appropriate numerical parameters. The output of the numerical computation is either the desired results themselves, or is passed back to the symbolic routines for further analysis and action. The link between symbolic and numerical components is static in the sense that the numerical routines are chosen from a pre-selected collection. The only degree of freedom is the choice of input parameters to them.

A more flexible way to couple symbolic and numerical computation is to use a CASs to generate numerical code automatically, on demand, from the symbolic component. The automatically generated code could be a complete computation itself, or could include calls to existing numerical libraries. The symbolic component then compiles, loads and executes the code. The numerical results could either be given to the user, or used as part of further symbolic analysis.

A FRAMEWORK FOR GENERAL INTEGRATION

As discussed in the previous section the existing approaches towards integrated solvers do not provide a solution to the requirement of a general integration environment. The aim of the proposed approach is to design a framework for integrating solvers in a general way without restricting them to specific application areas. We are proposing to build a common environment for using existing CASs and numerical library routines to enable the users to access the functionality of both interactively.

Most of the CASs available today are self-contained systems for general requirements. But a problem arises when an application requires extensive mathematical calculations, which are not provided by the embedded mathematical routines. We believe that the best way to overcome this restriction is to build an interface from which users can use the functions provided by both symbolic and numerical solvers interactively.

The most general solution would have many CASs and numerical libraries working under a common command level. With this in mind, the aim of this section is to show how such an environment can be developed using a single CAS and some numerical library routines.

A perfect automated programming environment would automatically transform the algebraic problem into efficient symbolic and numerical programs. It would select the required CAS functions, guide the CAS to do the simplifications, select the necessary

numerical routines and do the required transformations. Though such an automated system is the ideal, it is more realistic to assume some user interaction, with the user supplying information to decide which functions are needed in CASs, the extent to which these functions can be applied, and the type of transformations required. The knowledge given by an expert user can to a certain extent be replaced by a rule-base.

Among the reasons for not totally excluding the human interaction are the following:

- Accuracy versus speed tradeoff: the choice of algorithms may depend on the desired accuracy of the results, or on a user-imposed execution time limit.
- Indeterminacy of the rule-base: the situation where more than one algorithm is applicable, leaving the choice to the user is certainly preferable to imposing a selection rule not suggested by the problem at hand.
- Flexibility: new algorithms can be added and tested.

The self-contained nature of CASs requires efficient and effective techniques of transformation methods from problems to CASs and of partial results from these to numerical library routines. The common features of various application domains will be evaluated and then transformation rules to use the required symbolic and numerical methods will be defined. Figure 1 shows a diagrammatic representation of the proposed system.

The proposed system has to make use of the defined functions of CASs to suit the requirements of the given task, decide the extent to which symbolic simplification can be applied, make a correspondence between the output of CAS and the input to the numerical library routines; and also to provide for human interaction, where necessary.

The functionality of such a system will be illustrated using a case study from linear optimisation. Existing work by Manocha and Canny [30] on using symbolic and numerical calculations in solving the problem of inverse kinematics in robotics is another good example. Since the proposed method is general, it can be extended to handle problems from any number of application areas.

Description of Functions:

The various steps need to be performed by the proposed system are described below.

Problem Specification: This is the phase in which the user specifies the problem to be solved in mathematical terms.

Example: Solve ***apde***
Subject to ***boundary and initial conditions***
Where ***apde and boundary and initial conditions*** are valid mathematical expressions.

Pre-processing: The system simplifies the equations given where possible and transforms them to a standard type. This is required to ensure the necessary degree of uniformity in the problem specification in order to find solution methods.

Example: Cancel identical factors from the coefficient and right hand side of a PDE.

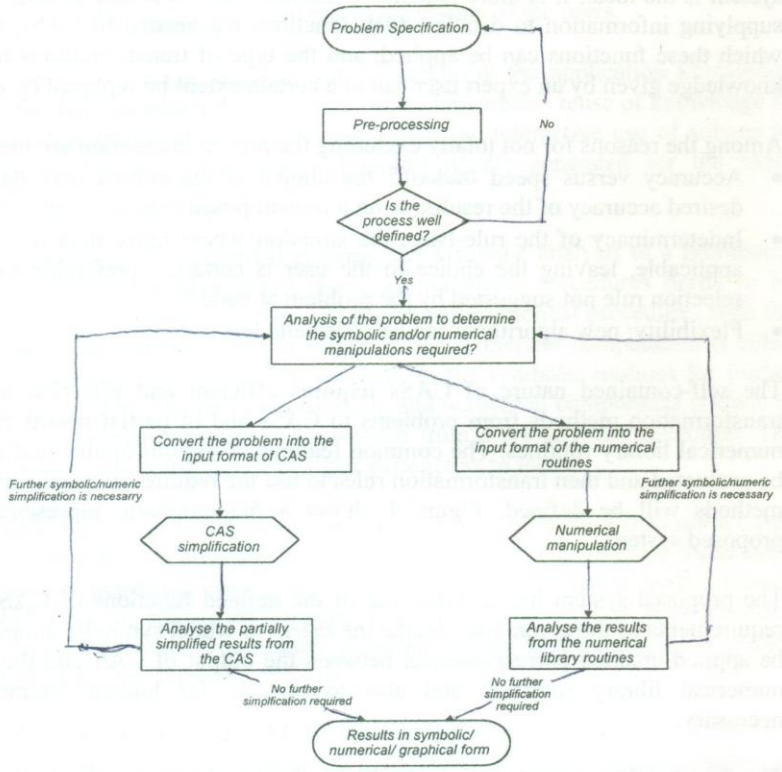

Figure 1 – Flow diagram of the proposed system

Problem Analysis and Algorithm Selection:

Problem Analysis

The system analyses the problem to identify the "type" of the problem. (E.g. In PDEs whether the given PDE is hyperbolic, parabolic or elliptic by analysing the discriminant.) Also the system must check whether the problem is well defined, i.e. whether it has a unique solution. Inappropriate specifications should be detected at this stage. As far as possible the analysis should be done using symbolic methods rather than resolving to numerical calculations.

Example: The possible geometry of the boundary conditions depends on the type of PDE; inappropriate boundary conditions should be rejected at this stage.

Algorithm Selection

The complete problem specification given by the user should then be passed to a knowledge base in order to find a suitable solution algorithm. Whenever the problem specification is incomplete the system ought to prompt the user to give more information. Also if there are more than one solution algorithm available the system should seek assistance from the users in order to make the decision.

If the system is to be useful for the users unfamiliar with CASs and numerical libraries there has to be a technique to decide the method of solution suitable for the given problem. We propose to achieve this by building up a knowledge base. The mathematical solutions that can be used depend very much on the nature of the parameters in the given equations.

For example the methods that can be used to solve a system of equations given by $\boldsymbol{A}\underline{x} = \underline{\boldsymbol{b}}$ depend on the size and the characteristics of $\boldsymbol{A}$. The database will have the solution methods needed for all the cases of $\boldsymbol{A}$. The user need not be aware of the different solution methods. These decisions can be handled by CASs. The advantage of using CASs in selecting the algorithm is that the analysis of the parameters can be done efficiently using symbolic manipulation.

In order to implement the solution the algorithm has to be properly analysed to identify the sections that can be implemented symbolically. One disadvantage of using only one CAS is that the level of symbolic manipulation that can be achieved is restricted to the functions of that CAS. Providing an interface that can include more than one CAS would help to overcome this restriction.

Implementation of the Solution: The outcome of the problem analysis phase is either a solution method, or the system has not been able to find one, in which case the system ought to seek the user's help. Once the algorithm has been selected, the system has to pass the required parameters to these sub routines. When the problem analysis phase has identified the required algorithm, the next step is to implement it using symbolic and numerical solvers. A major problem faced in integrating the solvers is the closed nature of CASs. CASs are developed for end user interaction and therefore it is hard to use them in any other platform to behave as intermediate systems.

The design issues related to calling the symbolic and/or numerical sub routines are not discussed in this paper.

Modularity and Re-usability: An advantage of the proposed method is these sub routines are not specific to any method of solution. The same subroutine can be used by more than one method of solution.

Partially simplified results from the subroutines may be reused for instance when a formula resulting from symbolic manipulation is evaluated repeatedly with different sets of parameters. This saves time which could otherwise have to be spent on redoing the time consuming symbolic preprocessing.

Evaluation of Results: The idea here is to use the extensive graphical capabilities of CASs to present the results in a user friendly and easy to analyse method. Also users may want to rerun or use a different solution method after evaluating the results. We aim to provide facility for re-evaluating partial results where necessary. This enables the user to change the algorithm or reformulate part of the problem while retaining reusable structures as possible.

Implementation Issues

Integrating Solvers

As described earlier the system design involves designing a method for integration of CAS and numerical routines and providing means of user interaction. The integration between different solvers can be achieved in many ways. A very general approach is to build up a common interface to communicate with the solvers. This facilitates a complete integration transparent to users (Figure 2).

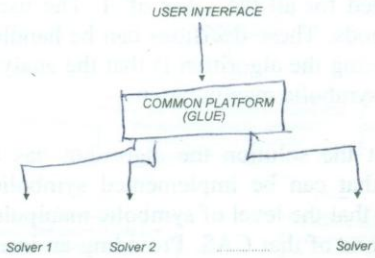

Figure 2: Overview of the system architecture

The common platform can be designed in a modular way to achieve the following functions.

- Communication with the solvers: passing them the sub-problems to be solved, getting the results and passing these results onto other solvers (if necessary), passing information between solvers, etc.
- Synchronisation of the solvers, formulating the output from partial solutions received from solvers.
- User interaction with the user in order to get the necessary user intervention.
- Pattern matching, transformations etc. between the output from one solver and input to another.

These functions can be achieved by implementing the common command level in the way of a submodule architecture. The submodule architecture will facilitate modifications to the system easily.

Users will use a common language to give the instructions to the system and the system will, depending upon the user instructions, issue the commands to solvers. The matching between these two will have to be done by the submodule. For example:

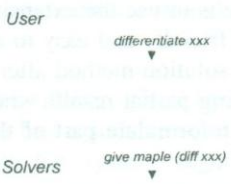

The front end of the system may be implemented either as a part of a knowledge base or the language of the symbolic solver used. Examples for both techniques are among the systems discussed under existing coupled systems.

These implementation issues need to be discussed in detail at implementation stage. Such a detailed description of system design will have to also address the following issues of

- identifying all the required data types
- how to define the abstract data types (ADTs)
- how to implement these data types etc.

Use of a knowledge base

A knowledge base oriented approach can be used to select the appropriate algorithms. The knowledge base that can be used here is based on a database of solution algorithms indicating the symbolic and numerical subroutines and under which conditions each of them is suitable. The knowledge can be extracted from presently available algorithms. Then an expert system can be built to access the knowledge base.

Knowledge bases for the integration of symbolic and numerical methods have been considered by many researchers [26]. Russo, Peskin and Kowalski [27] have shown how to use a knowledge based system to automatically generate the numerical programs for the solution of problems based on continuous partial differential equations. A CAS called PRESS (PRolog Equation Solving System) [28] is used for symbolic manipulations. Re-write rules for symbolic simplifications are written in PROLOG. The problem is analysed by the knowledge based system and then a numerical method is selected based on the problem characteristics. The system uses symbolic methods to discretise and rearrange the set of equations to obtain a form suitable for the numerical method. Mutrie, Char and Bartels [29] have also discussed the use of a knowledge based system in combining symbolic algebra and numerical computations. They have also given attention to expression optimising in such systems. Techniques similar to these can be used in the proposed method to select the algorithms required.

Case Studies

Newton's Method for Unconstrained Optimisation

This example shows how manual calculations can be achieved symbolically and how such symbolic solutions can then be used in numerical methods.

Problem:

Find the optimum value of a given expression with n variables without any constraints. This is called unconstrained optimisation.

$$Minimise \{g(x) \mid x \in R^n\}$$

In Newton's method, we start with an initial guess for the set of variables and keep on changing these values in order to minimise the function value. Let $g(x_i)$ be the given function.

Algorithm:

It is assumed that an initial estimate $x^{(0)}$ of $x^{(k)}$ is known.

Step 1: Set $k=0$

Step 2: Compute $g^{(k)}$ and $G^{(k)}$ from

$$g_i^{(k)} = \partial_i g(x^{(k)}) \qquad (i=1,\ldots,n)$$

$$G_{ij}^{(k)} = \partial_i \partial_j g(x^{(k)}) \qquad (i=1,\ldots,n)$$

Step 3: Compute $p^{(k)}$ by solving the system of linear equations:
$G_{ij}{}^{(k)} p^{(k)} = - g_i{}^{(k)}$

Step 4: Compute $x^{(k+1)} = x^{(k)} + p^{(k)}$

Step 5: Check whether $p^{(k)} \leq$ required tolerance, if so stop; otherwise set $k = k+1$ and go to step 2.

Implementation:

The Symbolic computing tools such as Maple [10] can perform Step 2 (or rather the symbolic partial differentiation). So we can have the grad ($g_i{}^{(k)}$) and Hessian ($G_{ij}{}^{(k)}$) and also inverse of the Hessian matrix ($[G_{ij}{}^{(k)}]^{-1}$) in symbolic form as output from a Maple session. Maple allows the users to convert output to a Fortran 77 format. Then we can make use of numerical methods to perform the rest of the algorithm.

CONCLUSION

We have proposed a method that can be used to implement an environment to combine symbolic and numerical methods in solving equational systems. We have implemented the proposed method with some examples. With the help of these examples we have identified the requirements of the different phases of the method. However this paper does not include the extensive implementation details of these phases. The proposed method allows the users to interactively use the features of both symbolic and numerical solvers in many application areas.

REFERENCES:

[1] W Press, B Flannery, S Teukolsky, and W Vetterlin, *Numerical Recipes: The Art of Scientific Computing*, Cambridge University Press, 1989.

[2] C Lawson, R Hanson, D Kincaid, and F Krough, "Basic Linear Algebra Subprograms for Fortran usage", in *ACM transactions on Mathematical Software*, pages 308--323, September 1979.

[3] J Dongarra, J Croz, S Hammarling, and I Duff, "A set of level 3 Basic Linear Algebra Subprograms", in A*CM Transactions on Mathematical Software*, March 1990.

[4] J Dongarra and S Ostrouchov, *LAPACK Working Note 81 - Quick Installation Guide for LAPACk on Unix Systems*, Technical report, University of Tennessee, 1994.

[5] E Anderson and et.al. *LAPACK Users' Guide: 2nd Edition*, SIAM, 1995.

[6] R Barrett, M Berry, T F Chan, J Demmel, J Donato, J Dongarra, V Eijkhout, R Pozo, C Romine, and H Van der Vorst, *Templates for the Solution of Linear Systems: Building Blocks for Iterative Methods*, 2nd Edition, SIAM, Philadelphia, PA, 1994.

[7] K Schulze and C Cryer, "NAXPERT: a prototype expert system for numerical software", in *SIAM Journal of Scientific and Statistical Computing*, May 1988.

[8] M Dewar, "Using computer algebra to select numerical algorithms", in *ISSAC 92*, 1992.

[9] G Rayna, *REDUCE: software for algebraic computation*, Springer-Verlag, 1987.

[10] B Char, K Geddes, G Gonnet, B Leong, M Monagan, and S Watt, *Maple V - Library Reference Manual*, Springer-Verlag, 1991.

[11] S Wolfram, *Mathematica: A System for Doing Mathematics by Computer*, Addison-Wesley Publishing Company, 1991.

[12] E Engeler and R Mader, "Scientific Computation: The Integration of Symbolic, Numeric and Graphic Computation", in *EUROCAL '85: European Conference on Computer Algebra, Vol.1. Invited lectures, Lecture notes in computer science 203,* B Buchberger, editor, Springer-Verlag, 1984, pages 185-200.

[13] D Bayer and M Stillman, "The design of Macaulay: A system for computing in algebraic geometry and commutative algebra", in *proceedings of the 1986 Symposium on Symbolic and Algebraic Computation: SYMSAC '86*, Bruce W Char, editor, Association for Computing Machinery: New York, 1986.

[14] J Rice and R Boisvert, *Solving Elliptic Problems using ELLPACK*, Springer-Verlag, 1984.

[15] S Weerawarna, E N Houstis, and J R Rice, "An interactive symbolic-numeric interface to parallel ELLPACK for building general PDE solvers", in *Symbolic and Numerical Computation for Artificial Intelligence*, Academic Press, 1992, pages 303-321.

[16] E Kant, "Synthesis of mathematical modeling software", in *IEEE Software*, May 1993.

[17] R Akers, E Kant, C Randall, S Steinberg, and R Young, *Problem solving environments and solution of partial differential equations, Version 1*, Technical report, SciComp Inc., 1997.

[18] P Fritzson, L Viklund, J Herbert, and D Fritzson, "Industrial application of object-oriented mathematical modelling and computer algebra in mechanical analysis", in *TOOLS EUROPE '92*, 1992.

[19] V Engleson, P Fritzson, and L Viklund, "Variant handling, inheritance and composition in the ObjectMath computer algebra environment" in *DISCO '93*, 1993.

[20] P Iglio, *Applying software components technology to computer algebra*, Technical report, NAG/FRISCO Consortium, 1997.
http://extweb.nag.co.uk/projects/FRISCO/reports/component.ps.

[21] N Kajler, "CAS/PI: a portable and extensible interface for computer algebra systems", in *ISSAC '92*, 1992.

[22] N Kajler, "User interfaces for symbolic computation: a case study", in *UIST '93*, 1993.

[23] S Dalmas, M Gaetano, and S Watt, "An Openmath 1.0 implementation", in *ISSAC '97*, 1997.

[24] S Dalmas, M Gaetano, and A Sausse, *ASAP: a protocol for symbolic computation systems*, Technical report, INRIA, Sophia-Antipolis, March 1994.

[25] S Gray, N Kajler, and P Wang, "MP: A protocol for efficient exchange of mathematical expressions", in *ISSAC '94*, 1994.

[26] N Jacobstein, C Kitzmiller, and J Kowalik, "Integarting symbolic and numerical methods in knowledge-based systems: Current status, future prospectus, driving events", in *Coupling Symbolic and Numerical Computing in Expert Systems II*, J Kowalik and C Kitzmiller, editors, Elsevier Science Publishers, 1988.

[27] M Russo, R Peskin, and A Kowalski, "Using symbolic computation for the automatic development of numerical programs", in *Coupling Symbolic and Numerical Computing in Expert Systems II*, J Kowalik and C Kitzmiller, editors, Elsevier Science Publishers, 1988.

[28] A Bundy and B Welham "Using Meta-Level Inference for Selective Application of Multiple Rewrite Rules in Algebraic Manipulation", in *5th Conference on Automated Deduction, Lecture notes in computer science 87*, W Bibeland and R Kowalski, editors, Springer-Verlag, July 1980 pages 24--38.

[29] M Mutrie, B Char, and R Bartels, "Expression optimization in a symbolic-numeric interface", in *Coupling Symbolic and Numerical Computing in Expert Systems II*, J Kowalik and C Kitzmiller, editors, Elsevier Science Publishers, 1988.

[30] D Manocha and J Canny, "*Real time inverse kinematics for general 6R manipulators*", Technical report, University of California, Berkeley.

COMPUTER SIMULATION OF BUILDINGS WITH PASSIVE ELEMENTS FOR ENERGY EFFICIENCY

M T R Jayasinghe*, P T P Jayatunga*, R A Attalage**
* Department of Civil Engineering, University of Moratuwa.
** Department of Mechanical Engineering, University of Moratuwa.

COMPUTER SIMULATION OF BUILDINGS WITH PASSIVE ELEMENTS FOR ENERGY EFFICIENCY

M T R Jayasinghe*, P T P Jayatunga*, R A Attalage**
* Department of Civil Engineering, University of Moratuwa.
** Department of Mechanical Engineering, University of Moratuwa.

ABSTRACT: Conservation of energy used for thermal and visual comfort in the building sector using passive techniques has both short and long term benefits. In short term, passive solar buildings can mean lower capital cost due to smaller equipment and in the longer run, the life cycle cost of the buildings would be lower. Since major decisions that affect the thermal performance are taken by the architect at the pre-design stage, it is essential to provide him with a set of tools on passive techniques that can be integrated to his design. These tools can be as important as detailed computer simulations since those can be adopted only when the architectural design of the structure is completed to a considerable extent. Therefore, detailed computer simulations are better suited to optimise a building where the architect has already incorporated some of the energy conservation options. This paper explains the development of a set of graphical aids for hot humid climates using the results of computer simulations. The possibility of developing artificial neural networks with such results also has been highlighted.

INTRODUCTION

The building industry is one of the largest industrial sectors world-wide. In Europe, it is the second largest industry accounting for around 12% of gross domestic product. However, little progress has been made towards the improvements of energy efficiency of buildings. According to Kennington & Monaghan (1993), the main reasons for this is as follows:

1. The design of energy efficient buildings is a complex task involving many different design disciplines requiring expertise that takes many years of study and practice to acquire.

2. There is little communication between professionals involved in the different design domains especially in the early stages of a project where the decisions taken have the greatest impact on future energy usage in the building. For example, architects and HVAC engineers may not interact at the very early stages of the design. In many instances, many design professionals are not recruited until the later stages of the project, resulting in major decisions being made without full knowledge of their consequences.

3. Software tools currently available may not provide sufficient information in a readily usable form at appropriate times in the design process, particularly in the early stages of a project.

Due to its vast usage of energy, energy conservation in the building sector can be identified as one of the major sources for the reduction of the fossil and nuclear fuel. Building designs with passive techniques has an important potential for energy conservation by reducing the heating and cooling needs in both residential and

commercial buildings (Wouters et al., 1993). Generally, the architects work on the basis of whole to detail while the computer simulations for the thermal performance need information from detail to the complete building. Therefore, it is necessary for the architect to have a set of simple graphical tools that can be used in the pre-design stage when integrating the passive solar concepts. This will allow the inclusion of as many passive concepts as possible to conserve energy from the pre-design stage.

The development of graphical tools could be done by carrying out a large number of computer simulations on typical buildings. This paper explains one such simulation and the associated analysis to develop the graphical tools for hot humid climates prevailing in tropical countries. The use of Perimeter Annual Value concept in preference to Overall Thermal Transmission Value for hot humid climates is also highlighted.

These graphical tools also can be used to develop Artificial Neural Networks as well. The use of neural networks for this purpose will have certain advantages over representing the computer simulations in graphical form.

1. The graphical tools can be prepared only for selected cases. In the case of intermediate values of parameters, it would be necessary to resort to linear interpolation between two graphs, where the relationship may not be linear. In such situations, the neural network could be a better tool to predict an approximate annual air conditioning load.

2. The results from the neural network can be checked approximately with available graphical tools to determine the validity of the answers. It they are acceptable, those results also can be incorporated to further improve the neural network.

It will be possible to carryout similar simulations for a large number of buildings with different dimensions and these data can be used to train the neural network. Once trained, the neural network will be able to predict the energy consumption for a wide variety of buildings, which would be difficult to cover with graphical tools. This will be another application of computer simulations that can be carried out on proposed buildings.

ENERGY SAVINGS IN BUILDINGS

It is a primary requirement in buildings to provide visual, thermal and acoustic comfort together with other services. The desirable levels of these comforts are generally achieved by using energy, where there would be only a few buildings where the usage of energy is optimised without constraining the function of the building. In Western Europe, a massive 52% of energy delivered is consumed to maintain acceptable environmental conditions within buildings (Clark and Maver, 1991). In Taiwan, more than 30% of the total electrical power of the country is consumed by residential and commercial sectors. Of this, 40% is for providing lighting, 40% for air-conditioning and 20% for other functions (Yang and Hwang, 1993).

In Sri Lanka, the commercial sector consumes about 20% of the total energy demand at present, and this is expected to grow up to about 28% by 2013. Of this energy, 20% is for lighting, 5% for ventilation and 55% for air-conditioning (Attalage and Wijetunga, 1997).

Studies on possible energy savings have shown that in United States, a sum of US $ 100 billion a year can be saved by doubling the energy efficiency by the year 2010 (Bevington & Rosenfeld, 1990). The United Kingdom Department of Energy suggests that better design of new buildings could result in 50% reduction in energy consumption and that appropriate design intervention could yield reductions of 25% (Mathews & Richards, 1993). It is shown by Attalage and Wijetunga (1997) that in Sri Lanka, the commercial sector has a total energy conservation potential of 20% - 40% of the total consumption by the year 2013 if state of the art energy efficient equipment gradually replaces the existing equipment. Of this saving, air conditioning accounts for 14.4%-26.5%. It would be possible to make further savings if future buildings incorporate more and more passive solar techniques. This clearly shows that there is a considerable potential for saving energy by adopting appropriate techniques, specially of passive nature for buildings.

There is another important reason to seek energy savings in buildings in the context of preserving the environment. A major cause responsible for the global environmental degradation is the release of refrigeration gases and combustion products of fossil fuel into the atmosphere. These gases are primarily responsible for the depletion of the atmospheric ozone layer, global warming and acid rains, which can have serious effects on humans, animals and plant if left to progress unchecked.

Therefore, determination of methods that ensure thermal efficiency to limit the refrigeration loads in buildings are thus of paramount importance for the future. Achieving indoor thermal comfort with small capital investment is another subject area requiring earnest attention in the future.

When designing, architects follow the whole concept and proceed towards detailed design. Therefore, the main decisions are taken in the pre-design stage. Those decisions will generally determine the major thermal characteristics of the building. When computer simulations are used for buildings, those are performed starting from details, leading step by step to the complete design. Therefore, the procedure moves from the constituent parts towards the whole. This is in the opposite direction to the architectural design approach. Thus, for a proper simulation, the architectural design should run a full course (Holm, 1993). Usually towards the end of the architectural design, the building owner and the architect may have been inspired by the design in which case any extra energy cost may be of little significance.

Therefore, it is essential that the concepts that give the thermal efficiency are available to the architect in simple terms so that he can integrate at least some of the concepts into his design. One way to develop these concepts is to carry out computer simulations for typical buildings with the adoption of various energy conservation concepts, especially

adopting passive techniques. The results of these computer simulations can be presented as graphical tools for the use of architects at the pre-design stage.

Since the climates and perceptions of thermal comfort can vary from one country to another or even within a country, it is very important to carry out detailed studies and then to produce these rules for various local climatic conditions.

USE OF PERIMETER ANNUAL LOAD VALUE FOR COMPARISONS

In hot humid environments, shading devices are far more effective than thermal insulation (Yang and Hwang, 1993). One of the parameters available for evaluating the thermal performance of building envelope is Overall Thermal Transmission Value (OTTV). This is of particular application to temperate climates where insulation is important in minimising the building energy use, which primarily comes from the conductive heating load.

As described by Yang and Hwang (1993), for hot humid climates, the use of Perimeter Annual Load value (PAL value) is more appropriate and offers more flexibility for the architect in adopting passive concepts. PAL value evaluates the heat gain per floor area, taking account of all external and internal heat gains including those from the building envelope. Thus, the architects have the option of adopting some features such as large glass facades that may not be the optimum, but to adopt some other concepts like adequate shading which will give a PAL value that is low enough.

PAL value also can be used as an indicator of the efficiency of the passive concepts adopted and also to compare the results of computer thermal simulations.

COMPUTER SIMULATIONS

In this study, the computer simulations have been carried out using the software package CASAMO developed as part of Ademe-AIT RUE Project at Asian Institute of Technology. It is a tool for designing buildings with one of the following objectives. It could be used to design buildings with comfortable thermal conditions, determine the methods available for reducing the energy consumed for air conditioning or calculating the air-conditioning loads of proposed or existing buildings. In hot humid tropical climates, the main sources of heat gains are due to effects of radiation transmitted through glazed areas and absorbed by roofing and exposed facades. The conduction component is not very dominant due to low temperature difference. In commercial buildings, considerable heat gains are also possible due to occupants, lighting and appliances (casual gains).

In this research work, CASAMO has been used to determine the air conditioning loads for different facade conditions, indoor temperatures throughout the year at an interval of two months. The annual air conditioning loads are calculated without considering the casual gains due to occupants and usage since the idea is to determine the effects of the

facade on the thermal performance of the building. The air conditioning loads have been calculated for every two months since the sun path varies throughout the year. Although an interval of one month is preferable, it was not considered in order to keep the number of computer simulations at a manageable level.

Thermal gains in an air conditioned building can be due to reasons such as thermal gains due to direct solar irradiance through external glass facade, indirect solar irradiance through shaded or unshaded glass facades, solar gains through the solid walls, etc. Some of these have been considered in more detail.

Thermal Gains due to Direct Irradiance

This is specially applicable for facades facing east and west since solar altitude angle changes from about 0^{o} at 0600 hours to 60^{o} - 90^{o} at noon depending on the day under consideration and then to about 0^{o} at 1800 hours. Thus, it is quite difficult to control the direct solar irradiance gains by having large glass facades facing east or west.

Therefore, it is desirable to use solid walls for facades facing east and west. When solid walls are used, those are useful in maximising the time lag taken by any heat absorbed by the external facade reaching the interior face. Generally, a wall thickness of 200 mm with solid materials is sufficient to provide a time lag of about 6 hours when no insulation is used (Szololay, 1991). This thickness is also would be able to provide sufficient resistance against rainwater penetration and also could be cast either with bricks or precast concrete. Therefore, a wall thickness of 200 mm was used for the computer simulations, when no glass panels were provided. The effects of having glass facades of different window to wall ratios (WWR) without any shading were evaluated in the case studies.

Due to location of Sri Lanka, it is possible to control the direct solar radiation gains through windows facing north or south by providing appropriate shading devices. It has been shown by Jayasinghe et al (1997) that horizontal shading devices on north and south facades should subtend an angle, ϕ (see Figure 1), less than or equals to 50^{o} to provide sufficient shading from 0800 hours until 1600 hours.

In many buildings in Sri Lanka, the present trend is to have large glass facades without any shading devices. When such a facade faces north or south, each of them will receive direct irradiance for nearly 10 hours from 0700 hours until 1700 hours for nearly six months of the year. However, it is possible to provide the external glass facades of these buildings with shading by using shading devices arranged horizontally and vertically as shown in Figure 2 a and b. In large glass facades, the projection required from the face of the building can be minimised by forming recessed windows where a large window will be formed by a large number of small windows as shown in Figure 2 c. Thus, for modelling, glass facades that have been shaded and unshaded were considered.

CASAMO does not allow the simulation of shaded windows consisting of large number of small windows. It allows only one horizontal shading device to be assigned for a given window. Therefore, a horizontal shading device has been specified where the projection of it was calculated by considering the full height of the glass facade between two consecutive floors. For example, the overhang of a shading device used in computer simulations for a window of height 1.8 m was 1.5 m.

Thermal Gains due to Indirect Solar Irradiance

Indirect solar irradiance on a building consist of diffused irradiance and ground reflected irradiance. The intensity of these irradiances are lower than the direct irradiance. When large glass facades are provided for buildings, irrespective of the presence of shading devices, heat gains due to indirect solar irradiance will take place. The heat gains due to indirect irradiance can be minimised when solid facades are used without windows.

Case Studies

Two case studies that have been carried out to model two different buildings are presented here. The details of the case studies are as follows.

1. Building details: Two building shapes have been considered. A square building of 24 m x 24 m and a rectangular building of approximately the same area of 20 m x 30 m. These two cases were considered to check the shape that is thermally more efficient. Both buildings were of ten storeys. The floor to floor height was 3.6 m. The square building was denoted as X and rectangular as Y. These are shown in Figures 3 & 4. The core area of the square building is of 12 m x 12 m. Thus the effective rentable area was 432 m^2 per floor. The core area of the rectangular building was 8 m x 18 m. Thus the effective rentable area was 456 m^2. The air conditioning load was calculated considering that the core area will not be air conditioned.

2. Facade details: It is quite common to use large glass panels in building facades generally without shading. However, it is explained above that even in multi-storey buildings, the external facade can be provided with shading devices. Therefore, the possibility of providing shading is also considered. For the computer simulations, the cases with shading was denoted as S. However, these shading devices will be effective only for the glass facades facing north and south. Two types of glass facades have been considered where type of glass was *3 mm clear glass*. Those having a height of 3.0 m per floor (denoted as A) and those having a height of 1.8 m with the sill level at 1.2 m (denoted as B), thus giving a total height of 3.0 m as shown in Figure 5. The length of a facade has been the length between two grid lines, thus 6.0 m for both these cases. The floor to floor height was considered as 3.6 m. Thus, A gives a window to wall ratio of 0.83 and B gives a window to wall ratio of 0.5.

3. Glazed facades: For each building, it is considered that glass facades of Types A and B will be provided on sides facing north and south. The effects of providing

additional windows on east (denoted by E), west (denoted by W) and east and west (denoted by EW) also have been considered. The shading devices were not considered for these three cases since those would not be effective. When glass was not used, a wall thickness of 200 mm was provided.

4. Temperatures and humidities maintained indoors: The temperatures maintained indoors were 22, 24, 26, 28 and 29. The relative humidity has been maintained at 60%.

5. The outdoor temperature from March 21st to September 21st is considered to vary between 27°C at 0600 hours to 34°C at 1400 hours. It varies between 25°C at 0600 hours to 32°C at 1400 hours from September 21st to March 21st. The outdoor humidity varies between 90% at 0600 hours to 60% at 1400 hours. These values have been selected using the temperature and humidity variation charts given for few typical days in Jayasinghe and Attalage (1997) which indicated that the average temperature variation in a typical day is about 7°C and a humidity variation as given above for low altitudes in Sri Lanka.

The air conditioning loads calculated at two month intervals have been added up to determine the annual air conditioning load and this value has then been divided by the total air conditioned area of the building to determine the annual air conditioning load per square metre.

In this study, the annual air conditioning load is calculated instead of Perimeter Annual Load value (PAL value) since the calculation of annual air conditioning load helps the designer to evaluate the economic consequences of his decisions.

Determination of Annual Air Conditioning Load

The air conditioning load of the building was calculated for 21st day of January, March, May, July, September, November, thus representing the climatic variations and the movement of the sun with some degree of accuracy. Then, the total air conditioning load (kWh) of the building for a two month period was calculated by multiplying each value by sixty. Thus a total of six such values were obtained. These were added to obtain the annual air conditioning load of the building. This value was divided by the total area of the building excluding the core to obtain the air conditioning load per m^2 per year.

ANALYSIS OF RESULTS

The results of the computer simulations for square and rectangular buildings are give in Tables 1 and 2, respectively. These results have also been presented in graphical form in Charts 1 and 2, respectively. The following notations have been used.

X = square building with glass facade facing north and south
Y = rectangular building with longer axis in east west direction and glass facade as in X

A = glass facade of height 3.0 m
B = glass facade of height 1.8 m
S = glass facade provided with shading devices
E = glass facade facing east
W = glass facade facing west

Thus, XASEW means square building with window type A on north and south provided with shading. It also has unshaded windows on E and W.

Internal temperature °C	XA	XAS	XB	XBS	XASE	XASW	XASEW
22	308.75	261.0	281.29	263.10	295.97	294.0	307.34
24	218.16	198.62	225.10	180.61	208.20	207.21	235.81
26	169.63	116.31	143.98	123.09	141.21	140.05	164.73
28	105.56	53.98	89.28	56.11	80.88	76.34	109.55
29	80.29	35.41	73.21	42.58	51.90	48.52	80.26

Table 1: Annual air conditioning load values for a square building - notations as given above. The unit is kWh/m^2/year

Internal temperature °C	YA	YAS	YB	YBS	YASE	YASW	YASEW
22	308.16	243.0	263.16	257.76	280.44	264.24	306.36
24	214.52	182.88	208.80	178.56	208.08	207.00	234.00
26	165.85	106.56	144.52	107.28	133.56	131.76	162.36
28	99.36	47.52	82.10	47.88	75.96	74.52	107.64
29	73.8	24.84	56.29	25.20	48.60	48.24	77.40

Table 2: Annual air conditioning load values for a rectangular building - notations as given above. The unit is kWh/m^2/year

It can be seen from Tables 1 and 2 that the energy consumption of rectangular buildings with longer axis in east west direction is generally less than the energy consumption in square buildings with same window to wall ratios and approximately the same floor area. This stems from the fact that it is easier to control the external energy gains through the facades facing north and south than those facing east and west. Thus, it is advantageous to have rectangular buildings with minimum facade areas on east and west. It can also be seen that having shaded windows can always help to reduce the energy consumption for air conditioning.

The indoor temperature that is maintained for thermal comfort also has a significant effect on the energy consumption. For example, in the case of a rectangular building with shading, with indoor temperature being maintained at 27°C, the annual air conditioning load is about 75 kWh/m^2/year (from Chart 2) whereas when the same building is maintained at 24°C, the air conditioning load is about 180 kWh/m^2/year (from Chart 2). This indicates nearly 2.5 times increase. It should be noted that 27°C with 60% humidity and wind velocity less than 0.25 m/s can just provide thermally comfortable conditions

for Sri Lankans as indicated by the comfort zones marked on psychrometric chart provided in Figure 6 (Jayasinghe et al., 1997).

These comfort zones have been suggested for Sri Lankans by Jayasinghe and Attalage (1997) on the basis of a comfort survey covering about 3000 subjects. Few modifications have been incorporated for the methods suggested in Szokolay (1991) to suit Sri Lankans. It was shown that when combined ventilation and air conditioning is used, it is possible to maintain buildings even at higher temperatures such 29°C with about 70% relative humidity and air velocity above 0.6 m/s while providing thermal comfort to a majority of people.

When the same building is provided with windows on east and west without shading in addition to shaded windows facing north and south, the air conditioning load is about 235 kWh/m^2/year at 24°C internal temperature, thus indicating a nearly three fold increase in the energy consumption.

Thus the annual air conditioning loads caused by thermal gains for the ten storey rectangular building shown in Figure 2 for maintaining 27°C and 24°C indoors are 342 MWh and 820.8 MWh respectively. If the coefficient of performance of the air conditioning system is 4.0, the total electrical energy consumptions will be 85.5 Mwh and 205.2 MWh. Thus, it would be possible to achieve an energy saving of 120.2 MWh by maintaining the building at 27° C instead of 24°C.

If an average size house consumes 1000 units of electricity per year (1 MW hour), these energy savings of a ten storey building will be sufficient to provide electricity to 120 households. It has been reported by Perera (1997) that the annual energy consumption of rural house holds will be below 350 units per house. These energy savings in a ten storey building will be able to provide electricity to 343 rural households.

It is possible to compare the case of a building maintained at 24°C with windows provided on east and west facades. The total air conditioning load of such a building due to the considered thermal gains is 1071.6 MWh. The corresponding electricity usage is 267.9 MWh with a coefficient of performance of 4.

These figures indicate the importance of proper design of buildings and the need to maintain the interior of the buildings at just the sufficient thermally comfortable conditions for a country like Sri Lanka which has already tapped most of its hydro-power potential and has to depend on fossil fuels for further increases in generation capacity.

CONCLUSIONS

In this paper, the application of computer simulations to buildings with passive solar elements to determine the air conditioning loads resulting from external thermal gains has been presented. This is of particular advantage at the preliminary design stage, since the designer has the ability to change and rearrange the passive elements that have already

been adopted with minimum effort. In such instances, it is invaluable to be able to predict the effects of such decisions. The results of computer simulations that have been carried out using CASAMO were presented in graphical form for quick reference by architects and service engineers. Once the preliminary design is over, it will be possible to use a more sophisticated software for further improvements in energy efficiency. It will also be possible to further improve these charts by including the internal loads due to occupancy and also by using a more sophisticated package which can take account of the dynamic nature of the environment more precisely than CASAMO.

It was shown that due to the location of Sri Lanka, extensive use of shading devices on facades facing north and south can be of particular advantage in minimising the thermal gains due to solar irradiance. Avoiding windows on facades facing east and west also can be used. It was also shown that the energy usage can be minimised by maintaining the buildings at thermally comfortable, but at elevated temperatures that suits Sri Lankans, when air conditioning is used.

REFERENCES

ATTALAGE, R.A., WIJETUNGA, P.D.C. 1997, "Energy conservation potential in the Commercial Sector in Sri Lanka", Proceedings of symposium at Open University of Sri Lanka - An Energy Policy for Sri Lanka, OUR Engineering Technology, Vol 3 -#1, March, pp 47-53.

BOVINGTON, R., ROSENFIELD, A.H. 1990, "Energy for buildings and homes" Scien.Amer., September, pp 39-45.

CASAMO - Version 2.0, Ademe-AIT RUE Project, Asian Institute of Technology.

CLARK, J.A., MAVER, T.W. 1991, "Advanced design tools for energy conscious building design: Development and disseminations", Building and Environment, Vol 26, 25-34.

HOLM, D. 1993, "Building thermal analysis: What the industry needs - The architects perspective", Building and Environment, Vol 28, No 4, pp 405-407.

JAYASINGHE, M.T.R., SUJEEWA, L.C., FERNANDO, K.K.J.S., WIJAYAPRIYA, R.A. 1997, "Passive solar techniques for Sri Lanka", Proceedings - Research for Industry - 1997, University of Moratuwa, Sri Lanka, 21st November, pp 11/1 - 11/14.

JAYASINGHE, M.T.R., ATTALAGE, R.A. 1997, "Minimisation of energy usage in commercial sector", Proceedings of symposium at Open University of Sri Lanka - An Energy Policy for Sri Lanka, OUR Engineering Technology, Vol 3 -#1, March, pp 131-137.

KENNINGTON, J., MONAGHAN, P.F. 1993, "COMBINE: The HAVC - Design Prototype, Building and environment, Vol: 128, No: 4, pp 453-463.

MATHEWS, E.H., RICHARDS, P.G. 1993, "An efficient tool for future building design", Building and Environment, Vol: 28, No 4, pp 409-417.

PERERA, H.Y.R. 1997, "Rural electrification policy in Sri Lanka", Proceedings of symposium at Open University of Sri Lanka - An Energy Policy for Sri Lanka, OUR Engineering Technology, Vol 3 -#1, March, pp 54-57.

SZOKOLAY, S.V. 1991, Heating and Cooling of Buildings - *Handbook of Architectural Technology*, Ed. Cowan, H. J., Van Nostrand Reinhold, New York, pp 323-365.

WOUTERS, P., VANDAELE, L., VOLT, P., FISCH, N. 1993, "The use of out door test cells for thermal and solar building research within the PASSYS project", Building and Environment, Vol: 28, No: 2, pp 107-113.

YANG, K.H., HWANG, R.L. 1993, "The analysis and design strategies on building energy conservation in Taiwan", Building and Environment, Vol 28, No 4, pp 429-438.

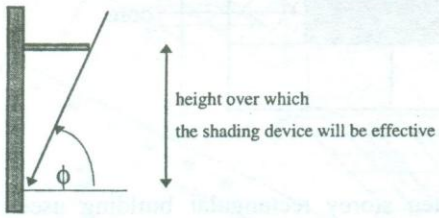

Figure 1: Effectiveness of shading devices

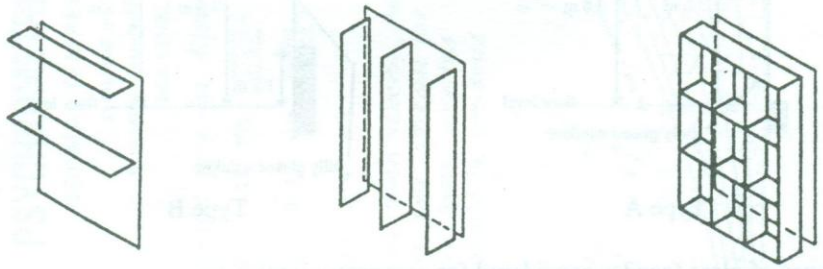

Figure 2: a. Horizontal shading devices; b. Vertical shading devices; c. A combination of horizontal and vertical shading devices

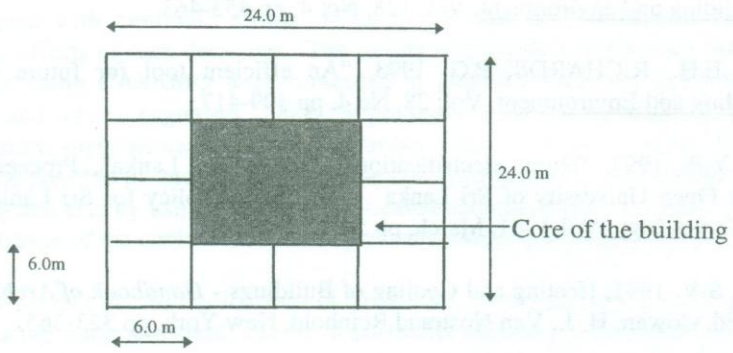

Figure 3: The plan view of the ten storey square building used for computer simulations

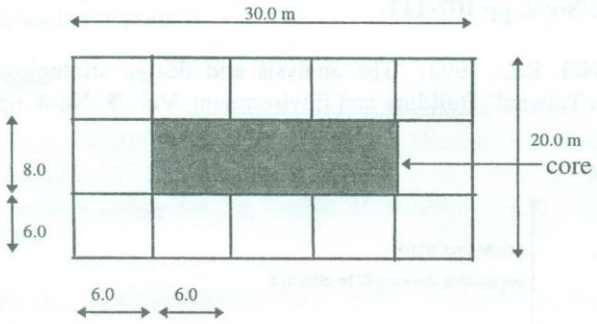

Figure 4: The plan view of the ten storey rectangular building used for computer simulations

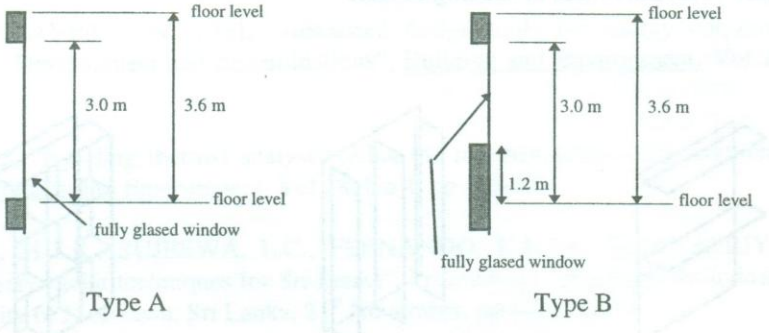

Figure 5: Types of glass facades considered for computer simulations

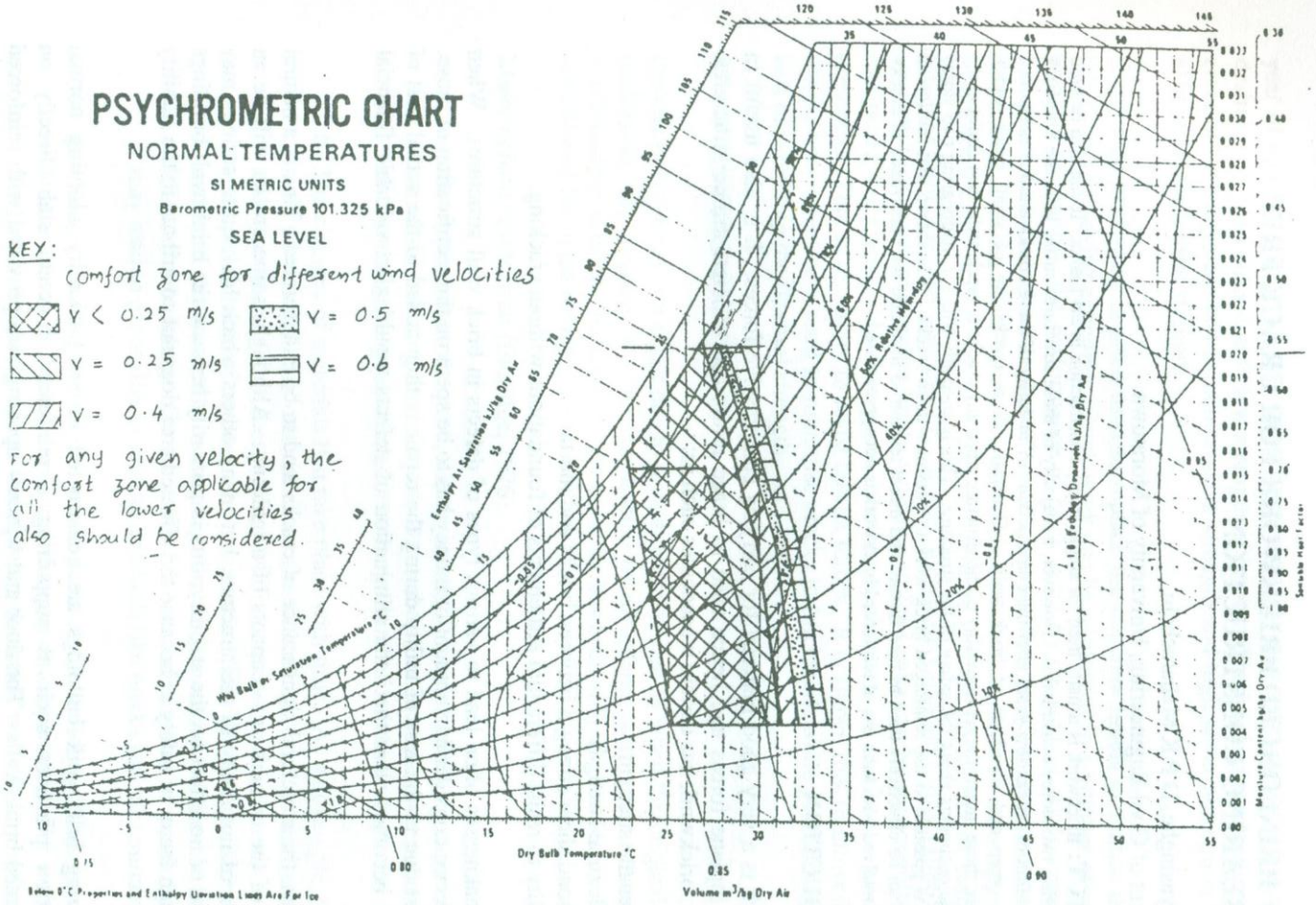

Figure 6: Psychrometric chart showing the comfort zones obtained with different internal air velocities

USE OF REINFORCED BRICKWORK FOR CRACK FREE LOADBEARING CONSTRUCTION

M T R Jayasinghe, D P K Maharachchi
Department of Civil Engineering, University of Moratuwa.

USE OF REINFORCED BRICKWORK FOR CRACK FREE LOADBEARING CONSTRUCTION

M T R Jayasinghe, D P K Maharachchi
Department of Civil Engineering, University of Moratuwa.

ABSTRACT: Brickwork is usually used for single storey construction in Sri Lanka. It can also be used for loadbearing two storey construction. However, a majority of these structures suffer from the drawback of the formation of cracks few years after the construction. A majority of these cracks are due to thermal movement, creep and shrinkage of brick walls. Generally, these cracks are of small crack width. Nevertheless, those impair the serviceability of the structure since any cracks in brick walls cast doubt in the minds of the occupants about the safety of the structure. This is specially true for loadbearing two storey houses. It is possible to use reinforced brick work to minimise these cracks. It is shown that reinforced brickwork can be effectively used to take flexure and direct tension to minimise the occurrence of cracks. Extra cost involved with such use of reinforced brickwork is not appreciable.

INTRODUCTION

Brickwork is a very good material for carrying compressive forces. It is also useful in carrying inplane forces and hence used to brace reinforced concrete frame structures. However, brickwork has certain weaknesses such as:

1. low tensile strength
2. low flexural strength
3. low bond shear strength between bricks and mortar
4. inability to resist differential settlements of foundations without cracking.

These weaknesses often lead to various types of defects in brick wall structures. When defects occur, considerable amount of money has to be spent on the rectification of those. If the cost due to the loss of utility during the repair is then added to the actual cost of repair, it becomes clear that the elimination of defects would give valuable financial benefits.

Very often, the structural significance of cracks tend to be exaggerated. This is a natural reaction of the owners or occupants of a building. Although, some cracks will be an indication of instability of the structure, but many others which look quite serious may have little or no effect on the stability; this is primarily because the brick wall buildings have a high factor of safety or because the affected area does not contribute to the stability of the structure.

Loadbearing brickwork buildings are constructed in Sri Lanka by adopting normal construction practices such as supporting a reinforced concrete slab directly on unreinforced brick walls. The door and window openings are provided with reinforced concrete lintels. The foundation often consist of random rubble work and generally a reinforced concrete plinth beam is used to tie the foundation. The buildings constructed with this normal method of construction often develop various types of cracks within one

year of construction. This has often led to consider that loadbearing brickwork is not desirable for Sri Lanka due to low strength of bricks. The bricks manufactured in many areas of Sri Lanka are of low compressive strength and high water absorption type with extremely low tensile strength.

Reinforced brickwork is often used to replace the concrete lintels or reduce the size of those, thus achieving economy. Brick work can be reinforced in a number of ways. It is possible to improve the performance of brick work by embedding reinforcement in the bed joints or by using tie beams of small cross section to act in conjunction with the brickwork. The use of tie beams of small cross section is considered more appropriate in loadbearing construction due to superior durability and the possibility of using normal reinforcement with out galvanising. It was shown by Chandrakeerthy (1986) that low strength high water absorption bricks available in Sri Lanka can be successfully used for reinforced brickwork. In this paper, another application of reinforced brickwork is presented. That is its ability to resist tensile forces. It is shown that reinforced masonry can be very effectively used to minimise cracks in brickwork while performing its usual task of providing the flexural strength.

REASONS FOR DEFECTS

Defects in buildings can occur due to several reasons such as when the original design is inadequate, the building was not constructed in accordance with structural design, the workmanship is below standard, or the building has been subjected to forces and agents not allowed for in the design.

Major defects result from (Eldridge, 1976):

a. the application of forces, either externally or internally, greater than those which the building materials can withstand:- For example, excessive settlement of foundation or poor strength resulting from bad workmanship.

b. The changes of materials that take place with time:- As an example, the size of most porous building materials increase with an increase in their water content and vice versa. Often these changes will not be noticeable, but sometimes may result in defects of appreciable magnitude. The decrease in size when wet materials dry out leads to shrinkage cracks particularly noticeable in the early life of the building. On the other hand, the absorption of water or moisture may lead to expansion in ceramic products like bricks and tiles.

c. Changes in temperature of various parts of the building:- This is a common feature due to diurnal and seasonal changes of temperature. For a country like Sri Lanka, located close to the equator, the brick walls facing either north or south can be exposed to about 10-12 hours of direct sun light per day during certain parts of the year. Thus, considerable amount of precautions should be taken to keep the walls free of thermally induced cracks.

DEFECTS IN WALLS

Any defect either due to bad workmanship, thermal stresses or moisture movement of materials, would result in cracks especially in external walls. The cracks that occur in walls can be classified according to the direction as vertical, horizontal or diagonal. The direction of crack can be coupled with either straight or toothed for further information. These cracks are shown in Figure 1.

The construction of crack free brick work structures should start with good quality bricks. The bricks available in Sri Lanka vary from one manufacturing site to another. Therefore, certain precautions should be taken in selecting suitable bricks for construction. It has been suggested by Jayasinghe (1998) that physical testing of bricks can serve as an important indicator for the selection of good quality hand moulded bricks. It is based on a detailed testing programme carried out for locally available bricks. The most important physical test has been the ability of a brick laid on ground to withstand an impact caused by another brick falling from a height of 1.2 m without breaking. Such bricks have given a characteristic compressive strength in excess of 1.5 N/mm^2 when constructed with 1:6 cement sand mortar.

The other physical testing can be the checking for ringing sound by tapping two bricks together or inspecting a broken face of a brick for the uniform colour to evaluate the degree of burning and excessive pores.

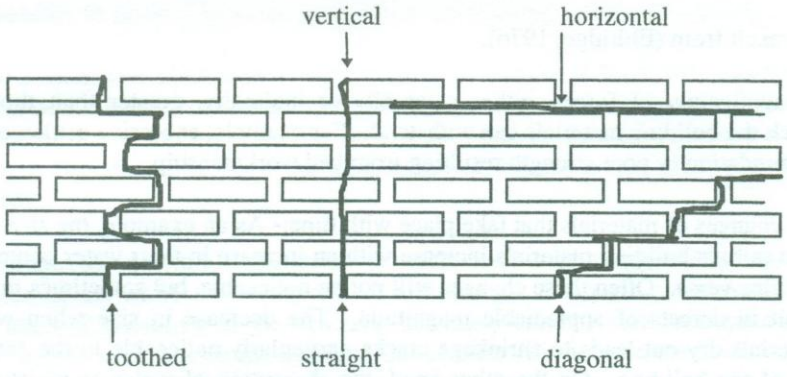

Figure 1: Forms of cracks in a brickwork

Vertical Cracks on External Walls due to Temperature Variation

Since Sri Lanka is a tropical country with long hours of sunshine, temperature induced cracks are a common feature on walls that are exposed to the direct sunlight. For a house of approximately rectangular shape with front facing south, the following exposure conditions will occur during an year. The front face will be exposed to the sun from

October to March everyday from the sun rise to the sun set. The amount of sunlight received by the wall depends on the length of the eaves and the shading offered by nearby trees. The rear face will be exposed to sun from May to September everyday from the sun rise to the sun set. The side facing east will receive sunlight from the sun rise until noon throughout the year. The side facing west will receive sunlight from noon until the sun set.

Out of these faces, the worst affected are those facing north and south since they receive direct sunlight for about *10-12* hours for at least five months of the year. The most common location for the occurrence of a thermal crack is the wall portion below a window as shown in Figure 2.

These cracks will generally appear at the end of the first five month spell of direct sunlight after the construction of a house build with normal practice in Sri Lanka. Initially, they appear as hairline *through cracks*. *Through cracks* are those that penetrate the full width of the wall, thus appear on both inside and outside face. Those cracks will gradually widen up to about *0.3-0.5 mm*. The crack is almost vertical and extends from the window sill level towards the foundation level. The crack width close to foundation level would be smaller.

It is possible to verify that these cracks are due to temperature variation by using the following simple technique. When a crack below the window is repaired with a non-flexible repair material like plaster of Paris at the end of a season of direct sunlight, the crack will not reappear until the next season. If the crack is due to any other reason, this type of seasonal variation would not be possible.

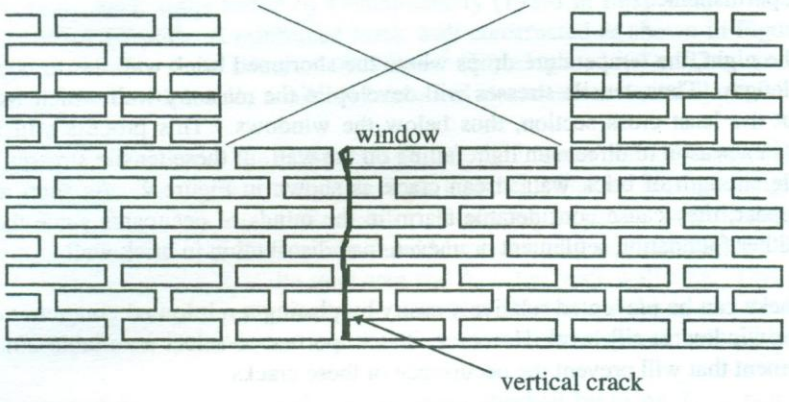

Figure 2: Thermal cracks below the window in the brick wall

The reason for these vertical cracks can be found by considering the cause for early thermal cracks in water retaining structures such as ground water reservoirs (Anchor, 1992). The concrete walls of ground water reservoirs can develop early thermal cracks

which are almost vertical. These cracks occur in the following manner. A few hours after the concrete has been poured, the temperature of concrete can rise by about *30-50 °C* above the ambient temperature. However, the concrete that has been poured to the shutters would not be able to respond to the temperature rise by expanding freely. Any restraint to thermal expansion of concrete will give rise to compressive stresses in concrete, which will be relieved to a certain extent due to the creep of concrete resulting in shortening of concrete. Creep of concrete at these initial stages can be relatively high due to low strength of concrete.

When the temperature drops to the ambient after about three days of casting the concrete, the length of concrete available is less than the original length. Therefore, a smaller length than required would have to occupy the available length, thus giving rise to tensile stresses in concrete. If these tensile stresses are large enough, vertical tensile cracks will develop in the concrete. These cracks will appear as through cracks. In water retaining structures, these thermally induced cracks are controlled by providing sufficient amount of reinforcement.

The cracks that occur in brick walls can also be explained with reasoning similar to those given for early thermal cracking in water retaining structures. When brick walls receive a considerable amount of sun light over long hours, the temperature of the brick walls would rise by a few degrees. However, this expansion is generally restrained by cross walls, foundations, lintels or concrete floor slabs. Thus, compressive stresses of small magnitude can develop in brick walls. These compressive stresses would be highest at sections where the masonry wall area is minimum; generally below the windows. When subjected to compressive stresses, masonry shortens due to creep. It is reported by Hendry (1981) that about 50% of stresses in brick walls can be relieved by creep if the loads are permanent.

During the night, the temperature drops where the shortened brick wall has to occupy its original length. Thus, tensile stresses will develop in the masonry wall which would be highest at the least cross section, thus below the windows. This process will happen everyday in a season of direct sun light falling on the wall. If these tensile stresses exceed the tensile strength of brick wall, it can crack as shown in Figure 2. As soon as these cracks appear, they cause considerable alarm in the minds of occupants since they may suspect either foundation settlement or uneven load distribution in brick wall.

These cracks can be prevented relatively easily by placing a reinforced concrete tie beam below the window at sill level. However, it is important to select a suitable amount of reinforcement that will prevent the occurrence of these cracks.

The concrete beam placed below the window at sill level will function as a strut which relieves the compressive stresses in the masonry wall below the window. It can also resist tensile stresses that occur in the wall. The beam should have been sufficiently embedded into the wall on either side of the window.

Unfortunately, it is not possible to determine the exact reinforcement requirement since it depends on the temperature variation, orientation and creep characteristics of the wall. However, the minimum amount of reinforcement required can be calculated on the assumption that when the wall cracks, the tensile stresses in the masonry will be transferred to steel reinforcement. This is very similar to the assumption made in water retaining structures to determine the minimum amount of reinforcement (ρ_{crit}).

One of the problems faced here is finding the tensile stress carrying capacity of brickwork. The tensile strength of brickwork can be found by testing a brick wall supported on a concrete lintel in two point loading by using an arrangement as shown in Figure 3.

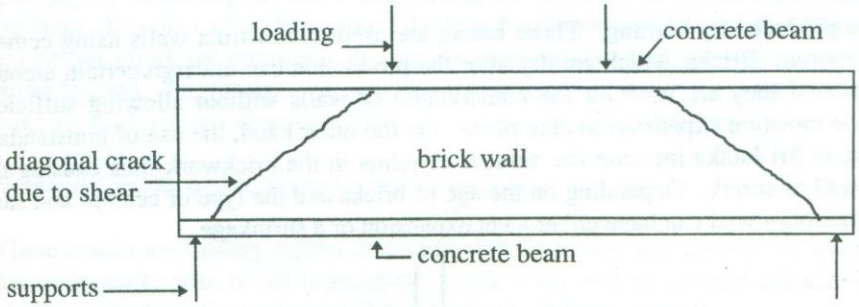

Figure 3: Testing of a reinforced brick wall in two point loading

The failure occurs due to principal tensile stresses induced due to shear stresses. The magnitude of the principal tensile stress is equal to the magnitude of the shear stress. Reinforced brick walls tested by Chandrakeerty (1989) in flexure have failed at a shear stress of 0.2 N/mm^2. A reinforced brick wall constructed as shown in Figure 3 also has given an ultimate shear stress of 0.2 N/mm^2 (Jayasinghe, 1997). Thus, it can be stated that brickwork with locally available bricks fail at a tensile stress of about 0.2 N/mm^2.

If a factor of safety of *1.5* is assumed, a value of *0.3 N/mm^2* should be used for the tensile strength of masonry; it should be noted that a higher value for tensile strength will give a larger steel area. The argument used for calculating minimum steel is that after tensile failure of brickwork, all the tension should be carried by reinforcements. Thus, A_s/A_b = *0.3/(0.87x460)*, where A_s is the steel area and A_b is the brick wall area. This gives an area of *126 mm^2* for high tensile steel with a wall of thickness *0.21 m* and the height below window of *0.8 m*. If mild steel is used, the reinforcement requirement will be *231 mm^2*.

The applicability of this calculation has been checked by using *2T10* bars that give an area of *157 mm^2* in several two storey loadbearing wall houses. These reinforcement were provided using *75 mm* x *210 mm* tie beams provided below the window. Not a single thermal crack has been observed in these houses three years after construction. However, such cracks have appeared within one year of construction in other houses without the tie beams when similar climatic conditions prevailed.

Thus, the use of tie beams with *2T10* high yield steel reinforcement below the windows is recommended. The size of the tie beam can be *75 mm* x *210 mm* for one brick walls. The thickness of *75 mm* is sufficient to give adequate cover for the reinforcement. It is reported by Chandrakeerthy (1989) that for reinforcement embedded in concrete, a cover of 30 mm can offer sufficient durability when used in reinforced brickwork. It is shown later that the reinforced brick wall formed due to this tie beam can be used to enhance the flexural strength so that brick wall will be able to resist cracking due to foundation settlements.

Vertical Cracks due to Moisture Movement

Bricks are produced by burning. These bricks are used to construct walls using cement and sand mortar. Bricks, which are dry after the production can undergo certain amount of expansion if they are used for the construction of walls without allowing sufficient time for the moisture expansion to take place. On the other hand, the use of nonstandard size bricks in Sri Lanka increase the number of joints in the brickwork thus causing the masonry wall to shrink. Depending on the age of bricks and the type of cement and sand used, the masonry wall can have either a net expansion or a shrinkage.

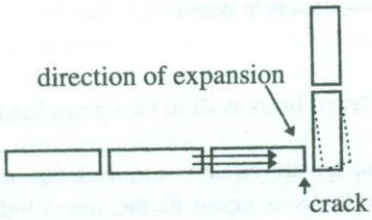

Figure 4: Cracking at the corners due to moisture or thermal expansion

The vertical cracks due to moisture expansion generally occur at the external corners. The same crack can also be caused due to thermal expansion as well. The nature of the crack is shown in Figure 4.

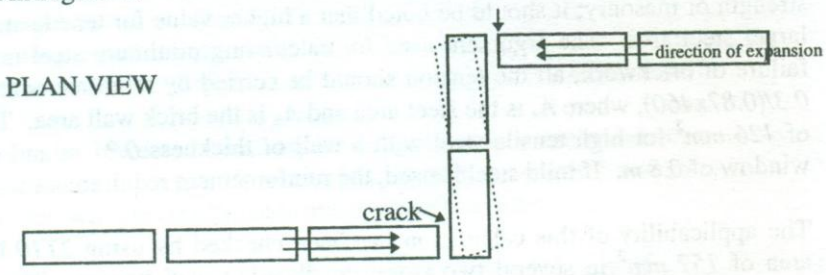

Figure 5: Cracking due to moisture or thermal expansion when two long walls are connected by a short wall.

When two parallel walls are connected by a short return wall on an external wall as shown in Figure 5, similar cracks can occur. These cracks are also a result of moisture expansion or thermal movement of two elevations of brickwork joined by the short return. When each section of brickwork on either side of the short return expands rotating the short return, the tensile cracks are caused on both sides. The expansion is generally accommodated without cracking by brick returns of the form shown in Figure 5 when those are generally more than *1.0m* in length. These cracks are not of any structural significance.

The shrinkage of brickwork due to shrinkage of mortar can not be prevented, but it is possible to distribute the shrinkage by connecting the brick walls together by a tie beam possibly by extending the beam provided at the sill level of the window right round the building. It is also advisable to limit the length of brick wall to less than *10.0 m*, when no expansion joints are provided. In this situation too, the reinforced brickwork is used to resist tension, not flexure. It can be seen that provision of a continuous tie beam at window sill level is a departure from the normal practice in Sri Lanka.

Vertical Cracks due to Foundation Expansion

These cracks are usually widest at the top of the building and diminishes downwards to a hair line crack close to the foundation. Often there will be a single crack in each of the two opposite elevations of the building as shown in Figure 6.

The defect, which is not quite common in regions where the rainfall is high, occurs when the foundations are laid on shrinkable clayey sub soils that is drier than normal due to either abnormal climatic dry conditions or to the ground having cleared of large trees immediately prior to the start of the construction of the building. The trees could have made the ground exceptionally dry and sufficient time has not been allowed for between the felling of trees and the start of construction (Eldridge, 1976).

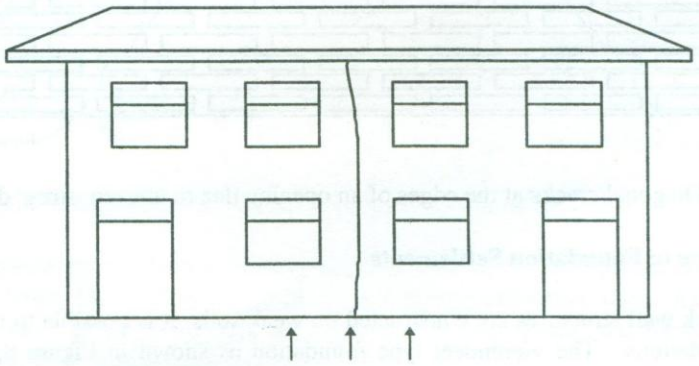

Figure 6: Swelling of clay under the centre of the building

The subsequent wetting of the clay sub-soil is accompanied by an expansion and the ground exerts an upward pressure on the foundation. This force may be considerable and can cause the vertical cracks of above nature. This type of cracks can be a possibility in masonry buildings constructed in the dry zone of Sri Lanka as soils with high clay content can shrink during the long dry spells and swell during the rainy season.

It is a good practice to do the site clearing well in advance so that a time lapse of about one year can be allowed before the construction commences. The provision of a continuous tie beam around the building at the window sill level may improve the flexural strength of brick wall building against heaving of soil. In this situation, reinforced brickwork is used in flexure.

Diagonal Cracks at the Edges of an Opening due to Uneven Stress Distribution

In loadbearing structures, it is quite common to observe diagonal cracks at the edges of an opening as shown in Figure 7. These cracks occur due to uneven stress distribution since the brickwork below the opening is stressed to a lesser degree. These diagonal cracks generally appear as hairline cracks.

In order to prevent these cracks, it would be necessary to ensure that the stresses in the brickwork is more or less uniform. This could be achieved to a certain degree by providing a concrete tie beam below the windows at the sill level which will provide the flexural strength required for the distribution of stresses. In this case reinforced brick wall acts in flexure.

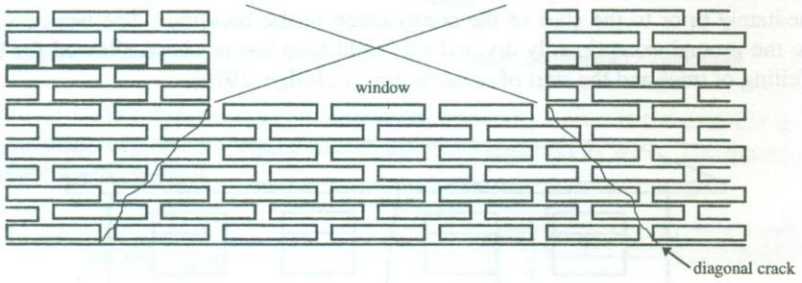

Figure 7: Diagonal cracks at the edges of an opening due to uneven stress distribution

Cracks due to Foundation Settlements

When brick wall structures are constructed on weak soils. It is possible to use Vierendeel type foundations. The vierendeel type foundation as shown in Figure 8, consists of a reinforced concrete inverted T - beam where the webs are filled with rubble instead of concrete, thus reducing the cost. However, in order to ensure composite action of top and

bottom flanges, stub columns should be provided at an appropriate interval, generally considered as equal to the lever arm depth of the foundation.

Since this type of foundation is selected for soil where differential settlements are expected, the foundation design criterion can be based on the possible differential settlement forms (Tennekoon & Raviskanthan, 1989). For reinforced concrete frame structures, the *angular distortion* β is important whereas for loadbearing structures, the limiting deformation criterion defined in terms of *deflection ratio* is more important. The deflection ratio means the deflection at the centre of the wall to the length of the wall.

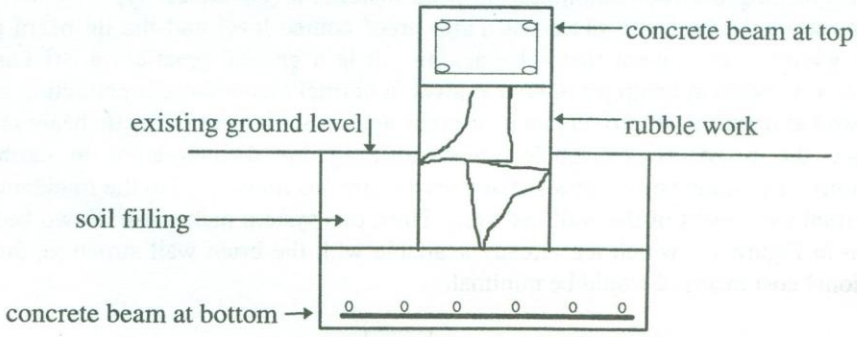

Figure 8: Vierendeel type foundation

For structures constructed with locally available bricks, the limiting deflection ratio for a load bearing structure is estimated as *1/2750* on the basis of a considerable number of actual measurements made on existing structures (Tennekoon & Raviskanthan, 1989). This compares well with the value given by Hendry et. al. (1981) for clayey soils, which is equal to *1/2500*.

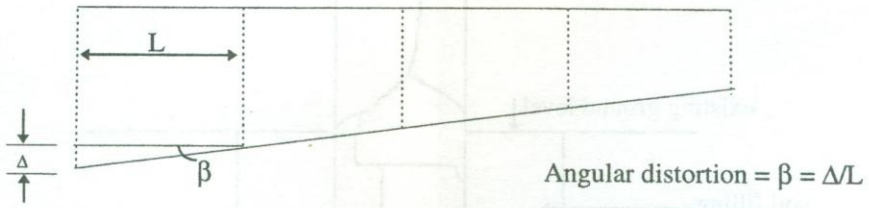

Figure 9: Definition of angular distortion for framed structures

The function of the Vierendeel type foundation is to stiffen the foundation so that it can resist the loads that would arise due to a limiting deflection ratio. As a result, the deflection ratio of the brick wall would be within the limits, and hence it would be possible to prevent cracking of the brickwork.

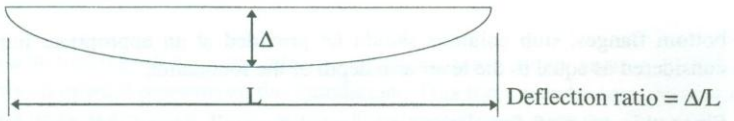

Figure 10: Definition of deflection ratio for loadbearing wall structures

The cost of Vierendeel type foundations can be much more than the normal rubble foundations. It is shown (Jayasinghe, 1997) that a composite reinforced brickwork and rubble foundation system where the brick wall has been given a flexural capacity instead of strengthening the foundation can be used instead of Vierendeel type. This system makes use of the tie beam placed at damp proof course level and the tie beam placed below windows to prevent thermal cracking. It is a general practice in Sri Lanka to provide a tie beam at damp proof course level in normal loadbearing construction since it is viewed as means of improving the resistance against settlement. This tie beam also can enhance the resistance of rubble foundations against disintegration in earthquake situations. The same beam can resist any tensile stresses transferred to the foundation due to thermal movement of the walls as well. Thus, this system makes use of two beams as shown in Figure 11, which are already available with the brick wall structure, thus, the additional cost incurred would be minimal.

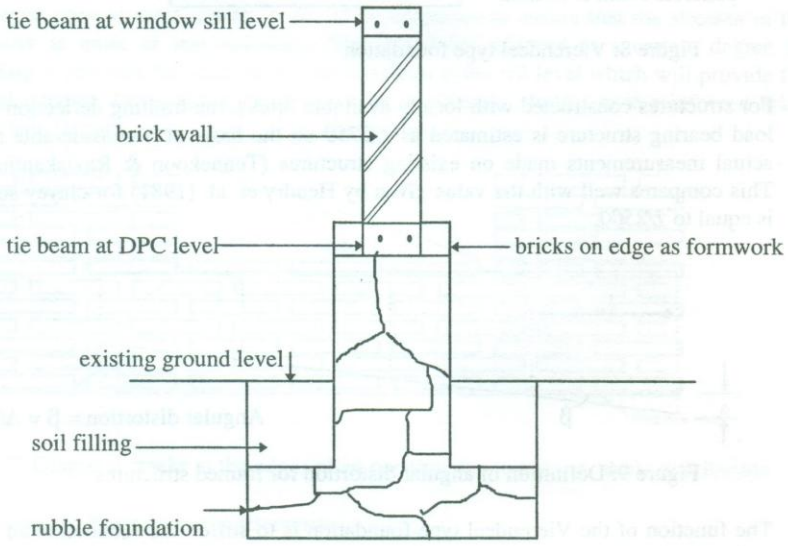

Figure 11: Rubble foundation with tie beams at DPC and window sill levels

In this composite system, it is important to prevent the flexural and shear failures. The calculation technique is presented with a case study in Jayasinghe (1997). In this case, the reinforced brickwork is used to resist flexure.

COST INCREASES DUE TO EXTRA TIE BEAMS

One of the key factors that discourage the owners of buildings in adopting robust building construction techniques is the high cost associated with such techniques. The tie beam introduced at window sill level is a departure from the normal construction practice in Sri Lanka and hence its adoption will depend on the extra cost involved. Thus, a cost calculation has been performed for a typical case where the cost of constructing a brick wall of length 3.0 m and height 2.7 m have been evaluated with a tie beam at lintel level and without it.

The cost comparison was carried out on the basis of the following information.

a. Cost of $1m^2$ of one brick thick brickwork = *Rs 550/=*
b. Cost of $1m^3$ of concrete = *Rs 4300/=*
c. Cost of $1m^2$ of shuttering = *Rs 300/=*
d. Cost of *1 Tonne* of reinforcement = *Rs 48,000/=*

These rates include the cost of labour and materials.

Case 1:	Cost of brick wall of size *3.0m* x *2.7m*	= Rs *4455/=*
Case 2:	Cost of $0.04730m^3$ of concrete	= Rs *203/=*
	Cost of *0.0018* Tonnes of reinforcement	= Rs 86/=
	Cost of $0.45\ m^2$ of shuttering	= Rs *135/=*
	Cost of *3.0 m x 2.625 m* of brick work	= Rs *4331/=*
	Total cost of Case 2	= Rs *4755=*
	Cost increase is Case 2	= Rs *300/=*

If there is a length of about 60.0 m in an average house (about 100 m^2 at ground floor), the cost increase will be Rs 6000/=. With the present day costs, a house of 200 m^2 will at least cost Rupees one million and hence the cost increase due to providing an additional tie beam at window sill level will be in the range of 0.6% of the total cost.

CONCLUSIONS

It is practically possible to construct loadbearing brick wall structures which would not show any signs of defects in the form of cracking, by taking adequate precautions. These precautions should be considered prior to starting the construction of the structure since some of them are applicable to site preparation, construction of foundations, walls, floor slabs, balcony slabs, roofs and finishes. Therefore, the builder has to be aware of these

cracks and should take appropriate actions to prevent the occurrence of undesirable cracking which often impair the serviceability of the brick wall structures.

The precautions that have been explained in detail in this paper can be summarised as follows:

1. The construction of crack free structures should be started at the site clearing stage. The site should be cleared of all large trees about one year prior to the construction of the structure so that the soil will be able to regain its natural moisture content during the rainy season.

2. A thorough soil investigation should be carried out at the site to identify the suitability of the soil. This can be done easily by using a trial pit where the soil samples are inspected to identify the type of soil at every *0.3m* depth up to a depth of about *1.5 m - 2.0 m*, depending on the type of soil. If undesirable soil types like peaty soil or clayey materials, which can shrink during dry spells are encountered, special precautions should be taken.

3. The foundation should be adequately tied so that it will be able to resist earthquake loads without disintegrating. Thus, the provision of a continuous tie beam which will connect all the internal and external wall are highly recommended.

4. The brick walls should be constructed with bricks of length *200 mm*, width *100 mm*, and a height of *50 mm*, since the use of smaller bricks will give higher number of mortar joints, thus increasing the tendency for shrinkage cracking. The bricks selected should satisfy all the physical tests and should be constructed with adequate quality controlling measures.

5. It is advisable to provide a tie beam at the window sill level to prevent the occurrence of vertical thermal cracking close to the middle of windows. These tie beams can also act in composite with the tie beam provided at the foundation level to resist settlement cracks.

6. A concrete beam similar to the one provided at the ground floor window sill level should be provided below the upper floor windows as well. However, this beam need not be continuous. It may be possible to precast these beams to reduce the cost.

7. The lintel provided over the upper floor windows may be made continuous to enhance the resistance of the structure to withstand accidental loads like trees falling on the roof during high winds.

The loadbearing brick wall structures constructed by taking all these precautions have performed quite satisfactorily in Sri Lanka, without showing any cracks or distress.

REFERENCES

ANCHOR, R. D. 1992, *Design of liquid retaining concrete structures*, Edward Arnold, London, 2nd Ed, 185 p.

BS 5628: Part 1: 1978, "Code of practice for structural use of masonry - Unreinforced masonry", B.S.I., London.

BS 8007, 1987, "Design of concrete structures for retaining aqueous liquids", British Standards Institution.

CHANDRAKEERTHY, S. R. De. S., JAYAWARDANE, D. S. & PANILA, S. D. 1986, "Feasibility of reinforced brickwork beams using low strength high water absorption bricks", Masonry International, No: 8, pp 1-7.

CHANDRAKEERTHY, S. R. De. S, 1989, "Durability of reinforcement in reinforced brickwork made with local materials", Transactions of the Institute of Engineers, pp 15-30.

ELDRIDGE, H. J. 1976, *Common defects in buildings*, Her Majesty's Stationary Office, London.

HENDRY, A.W., SINHA, B.P., DAVIES, S.R. 1981, *An introduction to loadbearing design*, Ellis Horwood, England, p184.

HENDRY, A. W. 1981, *Structural Brickwork*, MacMillan Press, London, p 209, 1981.

JAYASINGHE, M. T. R., "Monograph on Suitability of Sri Lankan bricks for loadbearing construction", Department of Civil Engineering, University of Moratuwa, Sri Lanka, 1996.

JAYASINGHE, M. T. R., "Monograph on improvements to foundations of load bearing brickwork buildings", Department of Civil Engineering, University of Moratuwa, Sri Lanka, 25 p, 1997.

JAYASINGHE, M. T. R. (1998), "Loadbearing construction with local bricks", Engineer, Vol xxvii, No 1, pp 49-57.

TENNEKOON, B. L., RAVISKANTHAN, A., " Design of foundations based on limiting deformation criteria", Engineer, December. 1989, pp 8-26.

A DESIGN METHOD FOR PRISMATIC PRESTRESSED CONTINUOUS BOX GIRDER BRIDGES

W M D N Ranasinghe*. MTR Jayasinghe**.
* Buildings Department, Western Province
** Department of Civil Engineering, University of Moratuwa.

A DESIGN METHOD FOR PRISMATIC PRESTRESSED CONTINUOUS BOX GIRDER BRIDGES

W M D N Ranasinghe*, M T R Jayasinghe**.
* Buildings Department, Western Province
** Department of Civil Engineering, University of Moratuwa.

ABSTRACT: Prestressed concrete is one of the most difficult building materials to design due to many reasons such as number of different solutions available for the same problem and the time dependent changes that take place. When used for continuous box girder bridges, there are added problems associated with secondary moments. In this paper, a straight forward design method has been presented that localises the iterations involved in the design process as much as possible so that the calculations involved can be minimised. The guidelines to determine the cross sectional dimensions has also been discussed. A complete design example has been presented for a three span continuous bridge. A simple method for modelling a box girder as a grillage of beams also has been presented.

INTRODUCTION

Box girder bridges are often used in the span range of 30 to 200 m. They are quite popular due to inherent torsional rigidity that gives very good load sharing characteristics. The box girder consists of single or multiple cells with cantilever overhangs on either side at the top flange. Since these structures are generally constructed as continuous over the supports, the design process becomes a complicated task. This is especially true with prestressed concrete box girders due to the secondary moments induced due to prestressing effects.

The secondary moments are induced because there is a tendency for the continuous prestressed bridge to lift up at the supports which is prevented by the bearings. This uplift and as a consequence, the secondary moments depend on the prestressing forces applied and the tendon profile selected. In the normal design process for prestressed concrete, the prestressing forces and the tendon profile is selected on the basis of the bending moment envelope due to loads. However, for continuous bridges, the secondary moments alter the bending moment envelope, but these secondary moments are not known until the tendon profile and the prestressing forces are known. This leads to an iterative process which could be quite cumbersome since the amount of calculations involved is large.

A design method has been developed by Jayasinghe (1992) that minimises the amount of iteration and also allows the designer full control of the structural design process. In this method, the analysis was carried out by considering that the bridge can be modelled as a continuous beam. In this paper, it is shown that the same method can be extended to the grillage analysis thus allowing the designer to use grillage analysis for the structural design process. The main advantages of this method include the ability of the design engineer to select the secondary moments at the beginning of the design process and to achieve exactly those assumed without going through an iterative process, ability of the design engineer to optimise the section dimensions by altering the secondary moments

appropriately, and the section of a prestressing force which is close to minimum throughout the length of the bridge thus achieving savings in cost. The tendon profile and the prestressing forces so selected can be further validated using a detailed design taking all the effects into account.

SELECTION OF CROSS SECTIONAL DIMENSIONS

The cross section of a box girder can be idealised as shown in Figure 1 for the preliminary design. The important parameters can be selected as given below.

Overall Depth of the Section

This is determined by the design engineer in general. It may be specified in the client's brief or it may be governed by vertical alignment considerations. If it is not given, the designer is free to select a reasonable value for the span/depth ratio; values between 14 and 25 are typical. It has been stated by Gee (1987) that it is economical to use larger depths and a reduced prestress if it is allowable. Greater depths allow a reduction of the bottom flange area, but carry the penalty of increased weight due to increased depth of web, which may outweigh the benefit from the improved flexural behaviour. The most economical solution can be obtained by using few alternative designs, that can easily be achieved with the design method described in this paper.

The Width of the Top Flange

When the top flange is used for the roadway in highway structures, the width is controlled by the number of traffic lanes, cycle lanes etc. Hence, the selection of top flange width can be easily selected by the design engineer.

The Web Spacing

The web spacing is governed by local bending of the top slab. Increasing the web spacing increases the thickness required for the top slab, but reduces the number of webs. Thus, there is a trade-off between additional material in the top slab and in the webs. However, extra material in the flanges contribute to global bending resistance and stiffness, whereas the extra web material simply add to the weight. The practical maximum web spacing for a reinforced concrete top slab is about 6.0 m and for a prestressed concrete top slab is about 7.5 m.

The Cantilever Overhang

In box girder bridges, cantilever overhangs are used which is a convenient way of minimising the number of webs while achieving the required width for the top flange. Generally the length of the cantilever overhang is kept around 0.5 times the spacing between the webs.

The Thickness of the Webs

The primary purpose of the webs is to resist the shear stresses due to torsional moments and shear forces. However, for constructable thicknesses of the webs, adequate shear resistance can be obtained by adding shear reinforcement, except possibly near the supports, when it becomes economic to increase the thickness of the webs locally. Thick webs carry a double penalty (Gee, 1987), since they add not only to the dead weight without resisting additional resistance, but also the area that has to be prestressed. Thus, the most logical criterion for selecting web thicknesses becomes one of constructability. The following guidelines have been suggested by Podolny & Muller (1982).

Table 1: Web Thicknesses Required Depending on the Type of Ducts

Type of ducts	Web thickness (m)
No prestressing ducts in webs	0.200
Small ducts for vertical prestressing	0.250
Ducts for the prestressing cables	0.300
Anchors for the prestressing cables	0.350

The Thickness of the Top Flange

The top flange thickness is generally governed by local bending considerations and the form of construction. The thicknesses for the top flange have been obtained from the survey by Swann (1972), where the thickness depends on the clear spacing between webs. Once these thicknesses are adopted, the top flange area would be large enough to meet the area required by the global bending criteria.

Table 2: Minimum Thicknesses Required for the Top Flange

Clear spacing between webs (m)	Thickness for transversely reinforced web (m)	Thickness for transversely prestressed web (m)
up to 3.00	0.250	0.200
3.00 - 4.50	0.300	0.225
4.50 - 6.00	0.350	0.275
6.00 - 7.50	-	0.300

The Width of the Bottom Flange

The designer turns out to have surprisingly little control over the bottom flange width. It depends on the cantilever overhang, inclination and number of webs, the clear spacing between webs and the thickness of webs. At this stage of the design process, the only decision that the designer needs to make is the inclination of the webs, which may be governed by the aesthetic considerations.

The Thickness of the Bottom Flange

In prismatic box girder bridges, the bottom flange provides the compressive resistance over the supports. Away from the supports, the function of the bottom flange is primarily non structural such as supporting the services etc. Therefore, it is advantageous to minimise the thickness of the bottom flange as much as possible. The minimum constructable thickness of the bottom flange is 125 mm, but this minimum value is not adopted due to difficulties of preventing cracks caused by horizontal shear. The recommended minimum thickness is 175 mm. However, this must be checked with the thickness required over the supports.

OPTIMISATION OF SECTION DIMENSIONS

In box girder bridges, it is useful to minimise the cross sectional area, thus minimising the dead load moments. The top flange dimensions are generally governed by the flexural behaviour in the transverse direction. These dimensions will generally be much larger than the dimensions required for longitudinal flexural behaviour and hence minimum should be selected by considering the transverse behaviour. The dimensions and number of webs must be minimised, since the shear is critical only close to the supports. However, the minimum thickness of webs is generally governed by the constructability hence cannot be minimised beyond that can be constructed. The bottom flange width depends on the inclination of webs, which may depend on aesthetics and ease of construction.

The thickness of the bottom flange is governed by the flexural behaviour in the longitudinal direction. In prismatic box girder bridges, the thickness of bottom flange over the support is governed by the hogging moments induced there. It is possible to change the magnitude of the hogging moments by using the secondary moments since they are generally of sagging nature. The advantage is that it is possible to use the minimum serviceable thickness of 175 mm by selecting an appropriate set of secondary moments thus minimising the moment due to dead load.

USE OF SECONDARY MOMENTS TO MINIMISE THE BOTTOM FLANGE THICKNESS

This can be achieved in the following manner:

1. Select the section dimensions using the guide lines given in Section 2.
2. Determine the dead load bending moment envelope. The dead load moments will form an envelope due to this reason. In continuous bridges, it is not possible to carry out the construction in one step. A large number of different construction techniques such as span by span, incremental launching, segmental construction with balance cantilever etc have often been used. Span by span construction is quite common for medium scale bridges where the prismatic box girders are used. In this method, one span and about 5 m length of the next span are constructed in one operation. The

difference in moments between as built and monolithic construction are called the trapped moments. Once the bridge is constructed this way, the creep and shrinkage of concrete will gradually relieve the trapped moments thus a long time after the construction, the magnitude of trapped moments can be reduced to about 20-25% of the original trapped moments (Neville et al., 1983). This can be clearly seen with the detailed analysis carried out for Kylesku bridge in Edinburgh, United Kingdom (Nissen et al., 1985). When this effect is taken into account, there will be a bending moment envelope for the dead loads as well.

3. Determine the bending moments due to imposed and other loads and produce the bending moment envelope.
4. Select a suitable magnitude for the secondary moment at each support and alter the origin of the bending moment envelope. The magnitude of the secondary moments can be any value between 0% and about 70% of the as built dead load bending moment values since secondary moments are generally used to counteract the permanent loads.
5. Draw Magnel diagrams at each support section and check whether the feasible region is sufficient to have the tendons installed. If insufficient, increase the secondary moments further. If this cannot give a suitable feasible region, the bottom flange thickness selected may be too thin, thus would have to be increased.

The dimensions used for a prismatic prestressed concrete box girders can be optimised using this simple technique.

SELECTION OF THE CABLE PROFILE

Once the secondary moments are selected over the supports, the design engineer has to select a cable profile that will generate exactly the same as those assumed. This is not a trivial task and usually the design engineer may resort to iterative process. A design technique is presented that will almost eliminate the need for iterations. This is a combination of two design techniques available for the design of continuous bridges.

Line of Thrust Design

In line of thrust design, the secondary moments are treated as prestressing effects. This means that the secondary moments are unknown until the cable forces and profile are found. Therefore, secondary moments are not directly considered in the design. There are a number of stress conditions which need to be satisfied by the cable forces and eccentricities. If the horizontal component of the cable force is P, the area of concrete is A_c, the section modulus is Z, the permissible stress of concrete is compression is f_c, and the permissible stress of concrete in tension is f_t, then the stress conditions can all be presented in the following form using the bounds on the line of thrust, e_p.

$$f_c \leq -P/A_c - P\, e_p /Z + M/Z \leq f_t$$

This equation can be rearranged to give the bounds of e_p. Since there are two bounds at each cross section, it can form a line of thrust zone when the full length of the beam is considered. The designer has to find a profile which not only fits within the bounds of the line of thrust zone throughout the length of the beam, but is also concordant, which means that this profile does not generate any secondary moments. Then, this profile can be linearly transformed to fit within the bounds imposed by the concrete cover required for prestressing cables. The designer may have to resort to trial and error process if he finds that linearly transformed profile does not satisfy the physical bounds imposed by the concrete cover at all locations along the beam.

Actual Cable Profile Design

In actual cable profile design, the secondary moments (M_2) are assumed initially and treated as loads. Therefore, they appear in the eccentricity equation, which is now written in the terms of the actual cable profile.

$$-Z/A_c - f_c\, Z/P + (M+M_2)/P \geq e_s \geq -Z/A_c - f_t\, Z/P + (M+M_2)/P$$

Since there are two bounds at each cross section, this will result in a cable profile zone. A cable profile has to be found which not only satisfies the limits set on e_s, but also causes the assumed values of the secondary moments. In this method too, the designer has to resort to iteration when he finds that the cable profile selected does not generate the assumed secondary moments.

Proposed Design Method

The design method proposed to find the cable profile combines both these methods. The steps involved are as follows:

1. Find the cable profile zone using the Magnel diagram so that there is sufficient space to fit the prestressing cables at the critical sections, primarily over the supports and at the mid span sections. For this purpose, a set of prestressing forces also have to be selected, which can be done as explained in Section 5.4. Generally at critical sections, the bounds on the cable profile will not be governed by e_s, but by the physical limits imposed by the cover requirements.
2. Transform this cable profile with the actual limits (either e_s or physical limits due to cover) using the relationship which exist between the cable profile and the line of thrust, which is given by $e_s - e_p = M_2/P$. Since the secondary moments and prestressing forces have already been selected to determine the cross section, this transformation is possible.
3. Fit a concordant profile into the line of thrust zone, which means this profile does not generate any secondary moments. For the existence of a concordant profile, certain conditions should be satisfied by the upper and lower bounds of the line of thrust zone as explained in Section 5.4. The concordant profile can easily be found by fitting a bending moment diagram that correspond to some notional loads applied to the box

girder beam, since any bending moment diagram representing zero deflections at supports can be scaled down to form a concordant profile.

4. Transform the concordant profile back to the cable profile zone by using the assumed secondary moments and the prestressing forces selected. The resulting cable profile will generate secondary moments which are exactly the same as those assumed, thus eliminating the need for any iterations.

Selection of Cable Forces

The selection of the cable forces for a determinate prestressed concrete beam is straight forward task because the cable forces can be found directly from the Magnel diagram. However, this is not the case with continuous beams due to the existence of secondary moments. The cable force is additionally constrained because it has to ensure that the assumed secondary moment distribution is obtainable.

When the cable forces are selected, it is possible to obtain the bounds of cable profile zone and then transform those linearly to obtain the bounds of line of thrust zone. There is a unique criterion for the existence of a concordant profile within the line of thrust zone (Burgoyne, 1987 a). That is if a cable is fitted along the upper boundaries of the line of thrust zone, it should generate hogging secondary moments. If a cable is fitted along the lower boundaries of the line of thrust zone, it should generate sagging secondary moments. Then only a profile can exist that will generate zero secondary moments, thus concordant. Therefore, the designer can determine whether the magnitude of prestressing forces selected are sufficient by determining the magnitude of secondary moments with profiles fitted along the upper and lower boundaries of the line of thrust zone before trying to fit a scaled down bending moment diagram. If a concordant profile is not available, the designer will never fit a bending moment diagram within the line of thrust zone.

The condition for the existence of a line of thrust (a concordant profile) can be presented as follows. When a cable profile and the prestressing forces are known, it is possible to find the secondary moments by using the generalised Clark Maxwell's theorem or principle of virtual work (Burgoyne, 1987a). The main advantage is that the analysis can be performed symbolically. The associated equations are given in Appendix A. If the cable is concordant, the reactant moment at each support is zero. It is both a necessary and sufficient condition for this that the terms in the right hand side of Eq. A.3 are all separately zero. Thus a cable profile is concordant if:

$$\int \frac{\beta_i RPdx}{EI} = 0 \qquad \text{for all } i.$$

It is shown by Jayasinghe (1992) that it is more effective to increase the prestressing forces over the support regions than increasing them in the span regions for the existence of a concordant profile when different cable forces are used over the supports and span regions. This is because, the function β is close to 1.0 over the supports whereas it is a

much lower value in the span regions. Therefore, the following strategy can be adopted for the selection of prestressing forces.

1. Select a minimum prestressing force in the span regions so that there is sufficient feasible region to fit the prestressing cable. For this purpose, the Magnel diagram should be drawn using the moments resulting from loading and secondary moments, thus $M + M_2$.
2. Select a suitable force over the support regions, but this can be larger than the minimum required. Select the relevant cable profile and then transform it to form the line of thrust zone. Check whether a concordant profile exist within this zone by calculating the secondary moments over the supports with the cable fitted at upper and lower boundaries of the line of thrust zone. This is further explained in the design example. If not, increase the prestressing force over the support further. This check will ensure if there is any iteration in the design process, it is only localized.
3. Select a concordant profile using a set of notional loads. Even this can be automated as described by Burgoyne (1987b) and Jayasinghe (1992).

USE OF GRILLAGE METHOD FOR ANALYSIS OF BOX GIRDERS

Grillage analogy is extensively used for the analysis of bridges due to reasons such as:

a. the grillage analogy can be used even in cases where the bridge exhibits complicated features like heavy skew, edge stiffening, deep haunches over supports, etc.
b. the representation of a bridge as a grillage ideally suited to carryout the necessary calculations associated with analysis and design on a digital computer,
c. the grillage representation is conducive to give the designer a feel for the structural behaviour of the bridge and the manner in which bridge loading is distributed and eventually taken to the supports.

In cellular bridges, longitudinal grillage beams are usually placed coincident with webs of the actual structure. The transverse medium, which consists of both the top and bottom flanges, is represented by equally spaced transverse grillage beams. The properties of the longitudinal beams are calculated by considering I sections as shown in Figure 2.

The structural action of the transverse medium of a cellular structure can be explained using Figure 3a, which shows the transverse slice of the structure being subjected to a vertical load at one end and an equlibrating moment at the other. If the plane sections remain plane thus there is negligible shear deformation, the transverse slice will deform as shown in Figure 3.b. However in cellular structures without frequent transverse diaphragms, the flanges and webs do flex significantly about their individual axes and this causes the cross section to distort as shown in Figure 3.c. Plane sections do not remain plane and the flexibility of the slices increases. The increase in flexibility cannot be accounted for by reducing the flexural rigidity of the equivalent beam because the additional deflections of the slice respond to shear in the slice rather than moments.

In the grillage analogy, this deformations of the cells in transverse direction can be taken into account by assigning an equivalent shear area for the transverse beams. The equivalent area can be found by using the Equation 1 (Jaeger & Bakht, 1982).

$$A_y = \frac{12L_x}{P_y}\frac{E_c}{G_c} \times \left[\frac{I_3(12I_1I_2 + L_xI_1I_3 + L_xI_2I_3)}{4P_yI_1I_2 + 4P_yI_2I_3 + 12H^2I_1I_2 + P_y^2I_3^2} \right] \quad \text{Eq. 1}$$

The following notations have been used:

L_x = distance between transverse grillage members
P_y = distance between webs
I_1 = second moment of area of top flange per unit length in longitudinal direction
I_2 = second moment of area of bottom flange per unit length in longitudinal direction
I_3 = second moment of area of a web per unit length in longitudinal direction
H = height of the section as shown in Figure 4.

The second moment of area of the transverse members, I_y, can be found by using Equation 2 where the notations are as given in Figure 4.

$$I_y = L_x(t_1h_1^2 + t_2h_2^2) \quad \text{Eq. 2}$$

The torsional inertia in the longitudinal direction, J_x, can be found by using Equation 3 where the notations are given in Figure 5.a.

$$J_x = L_y \frac{A_1^2}{b\oint \frac{ds}{n_s t}} \quad \text{Eq. 3}$$

The torsional inertia in the transverse direction, J_y, can be found by using Equation 4 where the notations are given in Figure 5.b.

$$J_y = L_x \frac{2A_2^2}{L\oint \frac{ds}{n_s t}} \quad \text{Eq. 4}$$

DESIGN EXAMPLE

In order to illustrate the design method a complete design example has been presented. The box girder bridge consist of three spans of 30m, 40 m and 30 m. This bridge will carry a two lane highway of lane width 3.0 m, also having two cycle paths of width 1.5 m each on either side and two walkways of width 1.0 m on either side. Thus the total top flange width is 11.0 m. The webs are selected at a spacing of 5.5 m, thus the overhang is 2.75 m. The thickness of the top flange selected is 0.35 m in average. The thickness of

the webs selected is 0.35 m. The depth of the bridge is selected as 2.0 m thus giving a rather shallow bridge with span/depth ratio of 20 for the mid span. The average thickness of the bottom flange is selected as 0.175 m. It is also assumed that the large diameter cable used will necessitate the centroid of the cable to be at least 150 mm away from the top and bottom fibres. A cross section of the selected section is given in Figure 6.

This bridge is analysed for HA loading and 30 units of HB loading as given in BS 5400/2 using the grillage analogy. The grillage consists of two longitudinal beams, each representing a web and the two flanges connected to it. The transverse beams are arranged at 5.0 m spacing. The diaphragms over the supports are ignored since those are likely to have large openings for service runs and inspection purposes. The section properties used for each grillage member for the analysis are given in Table 3.

Table 2: Section Properties Used for the Analysis

	Longitudinal	transvers
Area (m^2)	2.922	0.0052
Second moment of area (m^4)	1.41	1.754
Torsional inertia (m^4)	0.741	0.508

The concrete used for the analysis is grade 40 with elastic modulus of 30 kN/mm^2. The Poisson's ratio, ν, is considered as 0.15. The allowable compressive stress is taken as -14 N/mm^2 and the allowable tensile stress is taken as $-2N/mm^2$. The reasons for these values can be explained as follows. If the structure is designed as a class 1 structure, the allowable working stress is $-16N/mm^2$ for grade 40 concrete and the allowable tensile stress is 0.0 (BS 5400/4). Since there can be temperature induced stresses and other secondary stresses of magnitude of about 2 N/mm^2, the above values have been used so that once the final stresses are checked, no adjustment will be required for the prestressing forces or cable locations.

Table 4a: Moments Used for Structural Design

Chainage	0	5	10	15	20	25	30	35	40	45	50
M as-built	0	3069	4455	4085	1961	-1919	-7552	-757	3739	6718	7942
M_2	0	503	1006	1509	2012	2515	3020	2879	2738	2597	2456
M_{min}	0	3317	3827	2932	-787	-6854	-17006	-5467	793	4447	5751
M_{max}	0	7116	10734	10783	6537	-1275	-12656	-1625	7109	12630	14702

Table 4b: Moments Used for Structural Design.

Chainage	55	60	65	70	75	80	85	90	95	100
M as-built	7411	5125	1084	-4713	460	3878	5541	5449	3602	0
M_2	2315	2174	2033	1885	1570	1256	942	628	314	0
M_{min}	4704	1307	-4512	-15398	-6378	-403	3223	4499	3424	0
M_{max}	13323	8495	573	-6846	1150	8070	11415	11186	7380	0

Bridge is considered as constructed with span by span construction technique with 5.0 m cantilevering to the next span. The dead load bending moment envelope is obtained by considering that 80% of the trapped moments will be relieved by the creep of concrete. The superimposed dead load is calculated for an asphalt concrete filling of 150 mm thickness. The imposed load envelope calculated consisted of a sagging and a hogging bending moment at each section. The bending moment envelope used for the design is given in Tables 4a & 4b. The secondary moments are assumed as 40% of the as built bending moments at the supports. For clarity, the as-built bending moments are also given. The bending moment envelope for the determination of cable profile zone can be calculated by adding the secondary moments to the bending moments due to dead and live loads.

Since the design calculations are of repetitive nature, those are carried out using a spread sheet program as given in Data sheet 1. In this example, a constant prestressing force of 38,000 kN has been used. The prestressing force effective after losses is 0.7 x 38,000. The prestressing force has been adjusted until the secondary moments due to a cable placed at the upper boundary of the line of thrust zone will produce hogging secondary moments at each support. At the same time, the cable placed at the lower boundary of the line of thrust zone should produce sagging secondary moments. The secondary moments obtained for a cable force 0.7 x 38000 kN are given in Table 5.

Table 5: Secondary Moments When the Cable is at Upper and Lower Bounds of Line of Thrust

Location	M_2 at first internal support	M_2 at second internal support
Cable at upper bound of line of thrust	-3779	-1356
Cable at lower bound of line of thrust	3315	1236

These secondary moments are calculated as given in Appendix A. The right hand side of Equation A.3 is obtained by using the Simpson rule. The calculations performed are given in Data sheet 1. The secondary moments produced by the actual cable profile selected is also calculated as a check. Those are given in Table 6.

Table 6: Secondary Moments Assumed and Those Actually Occur

Location	first internal support	Second internal support
Assumed secondary moment (kNm)	3020	1885
Actual secondary moment (kNm)	3032	1897

The concordant profile that fits within the line of thrust zone is calculated in the following manner. First the boundaries of the line of thrust zone has been converted to a force-eccentricity zone where the eccentricity has been multiplied by the prestressing force selected. A set of notional loads have been selected that produces a bending moment diagram that fits within the force-eccentricity zone. The notional loads

considered consist of uniformly distributed element loads of the magnitudes given in Table 7. Negative sign indicates that the loads are acting downwards.

Table 7: Notional Loads Applied to the Beam to Obtain the Line of Thrust.

Chainage	0-5	5-10	10-15	15-20	20-25	25-30	30-35	35-40	40-45	45-50	50-55
Notional load (kN/m)	-120	-120	-120	-120	-120	220	220	-135	-135	-135	-105

Chainage	55-60	60-65	65-70	70-75	75-80	80-85	85-90	90-95	95-100
Notional load (kN/m)	-105	-105	170	170	-105	-105	-95	-95	-95

The concordant profile is obtained by dividing the bending moments due to notional loads by the prestressing force of 0.7 x 38000. This concordant profile is transferred back to the cable profile zone by using the relationship, $e_s = e_p + M_2/(R.P)$, where R.P is the effective prestressing force. The actual stresses resulting from the cable profile selected also can be calculated. In this case, the stresses will satisfy the stress limits since the cable is within the boundaries of the cable profile.

CONCLUSIONS

A design method, that guides the designer as a logically evolving process has been presented. The main advantage of this design method is that the designer has the opportunity to select the section dimensions of the box section by considering the governing criterion for each component such as top flange, webs and bottom flange. It is shown that the secondary moments can be used to minimise the thickness of the bottom flange to minimum constructable thickness. This helps the designer to achieve the minimum cross section for the prestressed concrete section, thus allowing him to develop a solution quite close to the optimum that can be achieved. It should be noted that with this technique, the secondary moments have already been assumed at the end of the selection of section dimensions.

It is shown that there is a unique criterion to satisfy the existence of a concordant profile within the line of thrust zone. This condition can be used by the designer to check the existence of a concordant profile within the line of thrust zone that is obtained corresponding to the prestressing forces selected. This helps the designer to eliminate any iterations involved by carrying out this simple check and to alter the prestressing force if the need arises. The application of this technique is illustrated using a design example.

Since the secondary moments have already been assumed, it is necessary to ensure that the cable profile selected will generate those assumed moments. The steps that should be followed to fulfil this objective is also presented.

With this straight forward design technique, the design process has been considerably simplified and also it offers an engineer without much experience in the design of continuous bridges to obtain a close to optimum solution.

REFERENCES

BS 5400/2, 1978, Code of practice for Design of Concrete Bridge, British Standards Institution, BS 5400, Part 2, London.

BS 5400/4, 1984, Code of practice for Design of Concrete Bridge, British Standards Institution, BS 5400, Part 2, London.

BURGOYNE, C.J. 1987a, "Cable design for continuous prestressed concrete bridges", Proc. Instn. Civ. Engrs., Part 2, Vol 85, pp. 161-184.

BURGOYNE, C.J. 1987b, "Automated determination of concordant profiles", Proc. Instn. Civ. Engrs., Part 2, Vol 85, pp. 333-352.

GEE, A.F. 1987, "Bridge winners and losers", The Structural Engineer, Vol 65A, No. 4, pp 141-145.

JAEGER, L.G. & BAKHT, B. 1982, "The grillage analogy in bridge analysis", Canadian Journal of Civil Engineering, Vol 9, No. 2, June, pp 224-235.

JAYASINGHE, M.T.R. 1992, "Rationalisation of prestressed concrete spine beam design philosophy for expert systems", Ph.D. Thesis, Department of Engineering, University of Cambridge, United Kingdom, p 234.

NEVILLE, A.M., DILGER, W.H., BROOKS, J.J. 1983, *Creep of plain and structural concrete*, Construction press, London.

NISSEN, J., FALBE-HANSEN, K., STEARS, H.S., 1985, "The design of Kylesku Bridge", The Structural Engineer, Vol. 63A, No. 3, pp. 69-76.

PODOLNY, W. & MULLER, J.M. 1982, *Construction and design of prestressed concrete segmental bridges*, John Wiley & Sons, New York.

SWANN, R.A. 1972, "A feature survey of concrete box spine-beam bridges", Technical Report 469, Cement and Concrete Association, London.

Appendix A:

It is possible to determine the secondary moments in a beam once the cable profile and the cable forces are known by using the generalised Clark Maxwell's theorem which states that when two force systems act on a linear elastic structure, the work done by the

forces of first system on the displacements of second system is equal to the work done by the forces of the second system on the displacements of the first system ($\Sigma P_i \Delta_{ii} = \Sigma P_{ii} \Delta_I$).

The first system consist of a set of fictitious moment system and associated reactions as shown in Figure A.1 with one system at each internal support. The reactions R'_{ik} are unknown, but need not be determined since they do not appear in the equations. The second system consist of the cable forces, corresponding secondary moments and associated reactions at the internal supports. Due to cable forces and secondary moments, there is a curvature at each section given by $(\Sigma(\beta M_2)_j$ - RPe)/EI. The support reactions resulting from cable forces are R_{jk}, but those need not be calculated since they appear at the supports where the displacements are zero in the first system. The application of the generalised Clark Maxwell's theorem results in Equation A.1from which $(M'_2)_i$ can be cancelled from the equation without loosing the generality, thus resulting in Equation A.2.

$$\int \beta_i (M_2')_i \left(\sum_j \beta_i (M_2)_j - Pe\right) \frac{1}{EI} dx = 0 \qquad \text{for } i = 2, 3, \ldots\ldots, n\text{-}1 \qquad \text{Eq. A.1}$$

$$\sum_j (M_2)_j \int \frac{\beta_i \beta_j}{EI} dx = \int \frac{\beta_i Pe}{EI} dx = \int \frac{\beta_i Pe}{EI} dx \quad \text{for } i = 2, 3, \ldots\ldots, n\text{-}1 \qquad \text{Eq. A.2}$$

The equations form a set of linear equations consisting of unknown secondary moments $(M_2)_j$. The cable profile, e, appears on the right hand side of the equations, and the coefficients of the $(M_2)_j$ terms are integrals of products of the β functions, many of which are zero since β_i is non zero only on either side of the support under consideration. The integration $\int \beta_i \beta_j dx$ results in simple expressions as indicated in the left hand side of the matrix notation given in equation A.3. The integral $\int \beta_i$ RP.e.dx/EI can be determined using numerical integration, preferably using the Simpson's rule, since the cable profile is known as a set of eccentricities with parabolic segments in between. In Data sheet 1, the values of β factors and the Simpson's rule coefficients (s) have been indicated. For each of the β coefficients, a row of β.RP e_s.s, have been prepared and then summed to give the totals shown at the end of the row. These values should be multiplied by h/3 as generally done in Simpson's rule summations where h is the interval considered for the cable eccentricities. The matrix can now be inverted to obtain the unknown secondary moments.

$$\frac{1}{6}\begin{bmatrix} 2(L_1+L_2) & L_2 & 0 & - \\ L_2 & 2(L_2+L_3) & L_3 & - \\ 0 & L_3 & 2(L_3+L_4) & - \\ - & - & - & - \end{bmatrix} \begin{bmatrix} (M_2)_2 \\ M_2)_3 \\ M_2)_4 \\ - \end{bmatrix} = \begin{bmatrix} \int \frac{\beta_2 RPe}{EI} \\ \int \frac{\beta_3 RPe}{EI} \\ \int \frac{\beta_4 RPe}{EI} \\ - \end{bmatrix} \qquad \text{Eq. A.3}$$

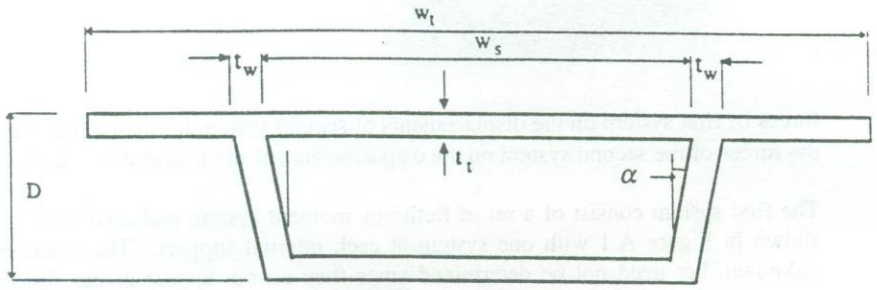

Figure 1: Idealization of a box girder for design

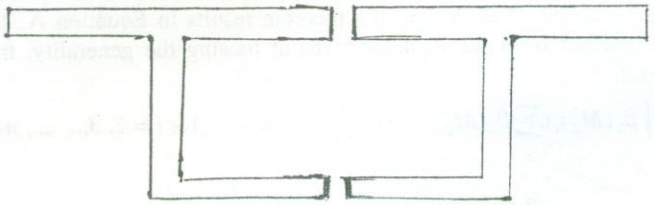

Figure 2: Box girder divided into I-girders

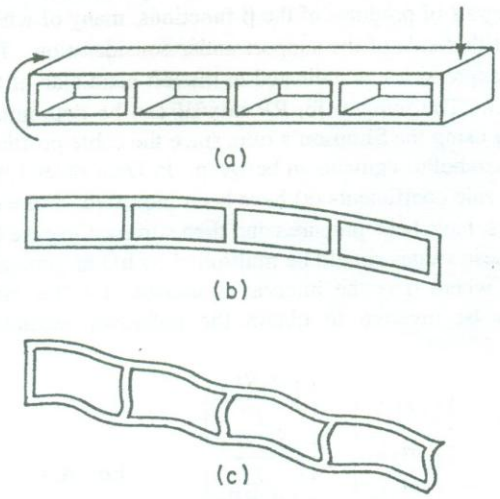

Figure 3: Transverse deformation of a cellular structure

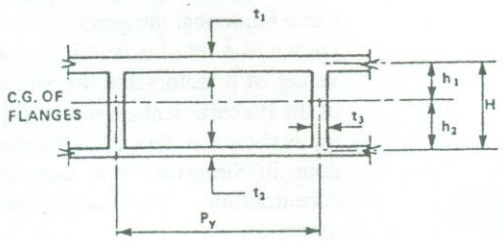

Figure 4: Partial cross-section of a cellular structure

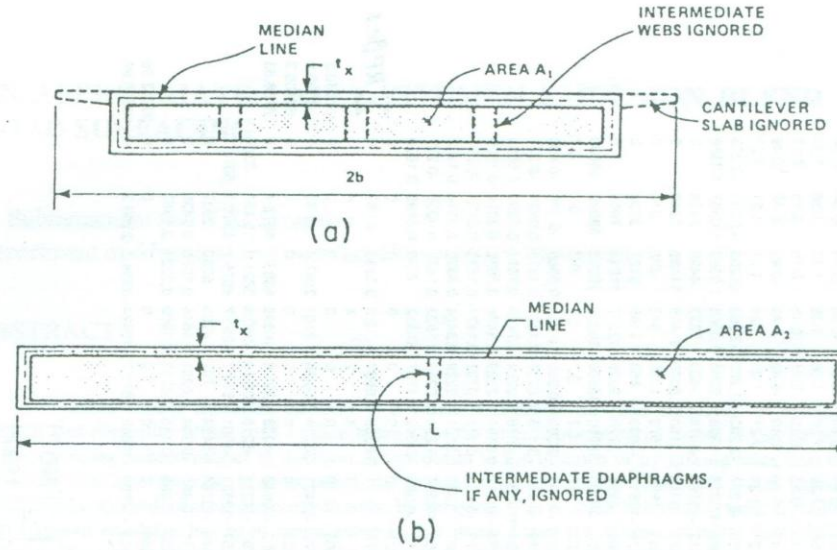

Figure 5: Areas considered in the calculation of torsional properties: (a) Cross section, (b) Longitudinal section

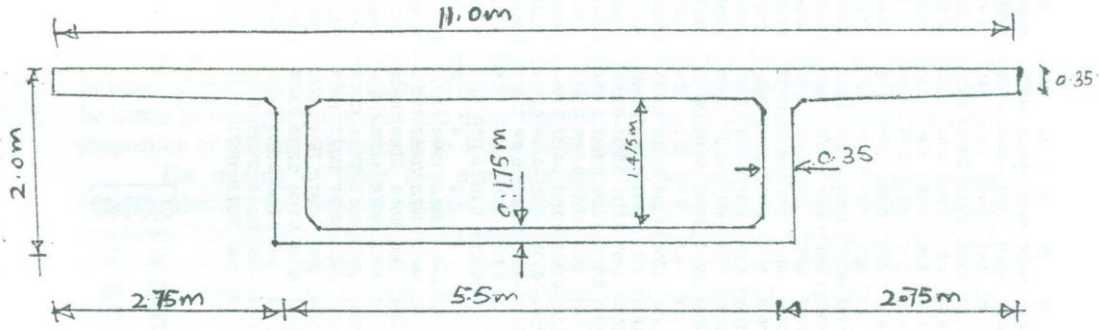

Figure 6: Section used for design

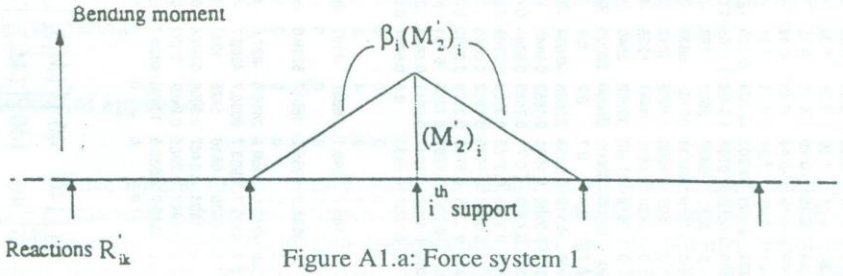

Figure A1.a: Force system 1

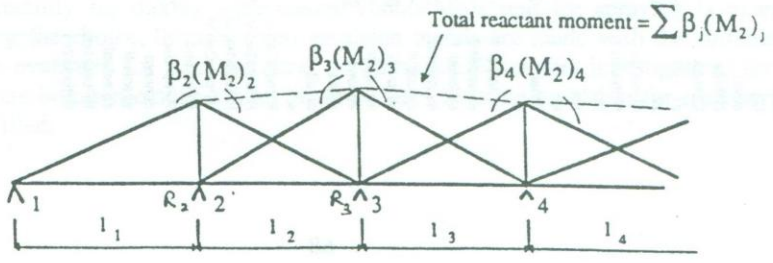

Figure A1.b: Reactant moment at the j^{th} support is $(M_2)_j$: Force system 2

chainage	0	5	10	15	20	25	30	35	40	45	50	55	60	65	70	75	80	85	90	95	100	
fcw	-14000	-14000	-14000	-14000	-14000	-14000	-14000	-14000	-14000	-14000	-14000	-14000	-14000	-14000	-14000	-14000	-14000	-14000	-14000	-14000	-14000	
ftw	-2000	-2000	-2000	-2000	-2000	-2000	-2000	-2000	-2000	-2000	-2000	-2000	-2000	-2000	-2000	-2000	-2000	-2000	-2000	-2000	-2000	
Ic	1.41	1.41	1.41	1.41	1.41	1.41	1.41	1.41	1.41	1.41	1.41	1.41	1.41	1.41	1.41	1.41	1.41	1.41	1.41	1.41	1.41	
Ac	2.922	2.922	2.922	2.922	2.922	2.922	2.922	2.922	2.922	2.922	2.922	2.922	2.922	2.922	2.922	2.922	2.922	2.922	2.922	2.922	2.922	
C1	-0.64	-0.64	-0.64	-0.64	-0.64	-0.64	-0.64	-0.64	-0.64	-0.64	-0.64	-0.64	-0.64	-0.64	-0.64	-0.64	-0.64	-0.64	-0.64	-0.64	-0.64	
C2	1.36	1.36	1.36	1.36	1.36	1.36	1.36	1.36	1.36	1.36	1.36	1.36	1.36	1.36	1.36	1.36	1.36	1.36	1.36	1.36	1.36	
cover	0.15	0.15	0.15	0.15	0.15	0.15	0.15	0.15	0.15	0.15	0.15	0.15	0.15	0.15	0.15	0.15	0.15	0.15	0.15	0.15	0.15	
C1MIN	-0.49	-0.49	-0.49	-0.49	-0.49	-0.49	-0.49	-0.49	-0.49	-0.49	-0.49	-0.49	-0.49	-0.49	-0.49	-0.49	-0.49	-0.49	-0.49	-0.49	-0.49	
C2MAX	1.21	1.21	1.21	1.21	1.21	1.21	1.21	1.21	1.21	1.21	1.21	1.21	1.21	1.21	1.21	1.21	1.21	1.21	1.21	1.21	1.21	
z1	-2.203	-2.203	-2.203	-2.203	-2.203	-2.203	-2.203	-2.203	-2.203	-2.203	-2.203	-2.203	-2.203	-2.203	-2.203	-2.203	-2.203	-2.203	-2.203	-2.203	-2.203	
z2	1.0368	1.0368	1.0368	1.0368	1.0368	1.0368	1.0368	1.0368	1.0368	1.0368	1.0368	1.0368	1.0368	1.0368	1.0368	1.0368	1.0368	1.0368	1.0368	1.0368	1.0368	
Ma(actu)	0	3317	3827	2932	-787	-6854	-17006	-5467	793	4447	5751	4704	1307	-4512	-15398	-6378	-403	3223	4499	3424	0	
Mb(actu)	0	7116	10734	10783	6537	-1275	-12656	-1625	7109	12630	14702	13323	8495	573	-6846	1150	8070	11415	11186	7380	0	
M2	0	503	1006	1509	2012	2515	3020	2879	2738	2597	2456	2315	2174	2033	1885	1570	1256	942	628	314	0	
Ma	0	3820	4833	4441	1225	-4339	-13986	-2588	3531	7044	8207	7019	3481	-2479	-13513	-4808	853	4165	5127	3738	0	
Mb	0	7619	11740	12292	8549	1240	-9636	1254	9847	15227	17158	15638	10669	2606	-4961	2720	9326	12357	11814	7694	0	
Ptrial	38000	38000	38000	38000	38000	38000	38000	38000	38000	38000	38000	38000	38000	38000	38000	38000	38000	38000	38000	38000	38000	
R	0.7	0.7	0.7	0.7	0.7	0.7	0.7	0.7	0.7	0.7	0.7	0.7	0.7	0.7	0.7	0.7	0.7	0.7	0.7	0.7	0.7	
es upper 1	-0.406	-0.119	0.0358	0.0565	-0.084	-0.359	-0.768	-0.358	-0.035	0.1669	0.2395	0.1823	-0.004	-0.308	-0.592	-0.303	-0.055	0.059	0.0386	-0.116	-0.406	
es upper 2	-0.277	0.0096	0.1645	0.1852	0.0445	-0.23	-0.639	-0.23	0.0933	0.2956	0.3682	0.311	0.1242	-0.179	-0.463	-0.175	0.0737	0.1877	0.1673	0.0124	-0.277	
es lower 1	0.5883	0.7319	0.77	0.7553	0.6344	0.4252	0.0625	0.491	0.7211	0.8531	0.8969	0.8522	0.7192	0.4951	0.0803	0.4076	0.6204	0.7449	0.7811	0.7289	0.5883	
es lower 2	0.1909	0.3345	0.3725	0.3578	0.2369	0.0277	-0.335	0.0936	0.3236	0.4557	0.4994	0.4547	0.3217	0.0977	-0.317	0.0101	0.2229	0.3474	0.3836	0.3314	0.1909	
es upper	-0.277	0.0096	0.1645	0.1852	0.0445	-0.23	-0.49	-0.23	0.0933	0.2956	0.3682	0.311	0.1242	-0.179	-0.463	-0.175	0.0737	0.1877	0.1673	0.0124	-0.277	
es lower	0.1909	0.3345	0.3725	0.3578	0.2369	0.0277	-0.335	0.0936	0.3236	0.4557	0.4994	0.4547	0.3217	0.0977	-0.317	0.0101	0.2229	0.3474	0.3836	0.3314	0.1909	
ep upper	-0.277	-0.009	0.1267	0.1285	-0.031	-0.325	-0.604	-0.338	-0.01	0.198	0.2758	0.224	0.0425	-0.255	-0.534	-0.234	0.0265	0.1523	0.1437	0.0006	-0.277	
ep lower	0.1909	0.3156	0.3347	0.3011	0.1613	-0.067	-0.448	-0.015	0.2207	0.358	0.4071	0.3677	0.24	0.0212	-0.388	-0.049	0.1757	0.312	0.36	0.3196	0.1909	
beta1	0	0.1667	0.3333	0.5	0.6667	0.8333	1	0.875	0.75	0.625	0.5	0.375	0.25	0.125	0	0	0	0	0	0	0	
beta2	0	0	0	0	0	0	0	0.125	0.25	0.375	0.5	0.625	0.75	0.875	1	0.8333	0.6667	0.5	0.3333	0.167	0	$\sum RP\beta e.s$
s	1	4	2	4	2	4	2	4	2	4	2	4	2	4	2	4	2	4	2	4	1	
RPbeta1ep u	0	-165.7	2246.1	6837	-1103	-28798	-32108	-31463	-383.3	13164	7337.5	8937.7	565.25	-3396	0	0	0	0	0	0	0	-58330.2
RPbeta2ep u	0	0	0	0	0	0	0	-4495	-127.8	7898.2	7337.5	14896	1695.7	-23770	-28421	-20714	940.66	8101	2547.4	10.35	0	-34100.9
RPbeta1ep lo	0	5595.9	5935.2	16017	5719.6	-5924	-23859	-1366	8804.5	23809	10828	14671	3191.8	282.33	0	0	0	0	0	0	0	63705.3
RPbeta2ep lo	0	0	0	0	0	0	0	-195.2	2934.8	14286	10828	24452	9575.5	1976.3	-20643	-4338	6231.6	16599	6383.1	5678.4	0	73768.63
RPep upp	-7365	-248.5	3369.5	3418.5	-827.5	-8640	-16054	-8990	-255.5	5265.5	7337.5	5958.5	1130.5	-6792	-14211	-6215	705.49	4050.5	3821.5	15.493	-7365	
RPep low	5076.7	8393.7	8903.7	8008.7	4289.7	-1777	-11929	-390.3	5869.7	9523.7	10828	9780.7	6383.7	564.67	-10321	-1301	4673.7	8299.7	9575.7	8500.7	5076.7	
concord	0	4808	6616	5425	1233	-5957	-11899	-5010	2941	7518	8720	6922	2499	-4548	-10784	-5424	747	4295	5280	3827	0	
epactual	0	0.1808	0.2487	0.2039	0.0464	-0.224	-0.447	-0.188	0.1106	0.2826	0.3278	0.2602	0.0939	-0.171	-0.405	-0.204	0.0281	0.1615	0.1985	0.1439	0	
es actual	0	0.1997	0.2865	0.2607	0.122	-0.129	-0.334	-0.08	0.2135	0.3803	0.4202	0.3473	0.1757	-0.095	-0.335	-0.145	0.0753	0.1969	0.2221	0.1557	0	
RPbeta1es	0	3540.7	5080.8	13868	4326.7	-11473	-17758	-7459	8518.5	25288	11176	13856	2336.5	-1258	0	0	0	0	0	0	0	50042.96
RPbeta2es	0	0	0	0	0	0	0	-1066	2839.5	15173	11176	23093	7009.5	-8803	-17798	-12846	2670.7	10474	3938.3	2766.2	0	38626.99

$$\frac{1}{6}\begin{bmatrix}140 & 40\\ 40 & 140\end{bmatrix}\begin{bmatrix}(M_2)_2\\ (M_2)_2\end{bmatrix}=\begin{bmatrix}50042.96\times 5/3\\ 38626.99\times 5/3\end{bmatrix}$$

$$\begin{bmatrix}(M_2)_2\\ (M_2)_2\end{bmatrix}=\begin{bmatrix}3032\\ 1897\end{bmatrix}$$

DATA SHEET 1

AN APPROPRIATE LATEX-BITUMEN EMULSION BLEND FOR ROAD SURFACING

K. Subramaniam and T.K. Sivarajan
Department of Chemical Engineering, University of Moratuwa.

AN APPROPRIATE LATEX-BITUMEN EMULSION BLEND FOR ROAD SURFACING

K. Subramaniam and T.K. Sivarajan
Department of Chemical Engineering, University of Moratuwa.

ABSTRACT

Natural rubber modified bitumen is a valuable material for road surfacing. It enhances the strength and durability of the road surface better than the bituminous material alone. It can be produced by incorporating natural rubber in the form of powder in to hot bitumen or by mixing latex into bitumen emulsion. The latter process is most beneficial to road engineers as the blend is a water based liquid which can be applied on road surfaces directly, by spraying. The process of blending natural rubber latex with bitumen emulsion has been investigated in this work. From the studies, suitable formulations for preparing bitumen emulsion and blend of latex bitumen emulsion for road surfacing have been identified.

Introduction

It is widely recognized that natural rubber blended bitumen is superior to bitumen alone, for road surfacing. The roads surfaced with the blend have been found to be better in strength properties and more durable. For its production, generally a small proportion of natural rubber ca. 2 to 4 w/w %, is incorporated into bitumen.

The mixing of these two materials may be accomplished by incorporating natural rubber in the form of powder into hot bitumen melt or latex with cold bitumen emulsion. The latter process is more advantageous as the blend is a water based liquid, which requires no heating prior to its application and can be used directly for road surfacing. However the process has not hitherto been successfully carried out locally, due to problems of producing latex-compatible bitumen emulsion.

Thus the objective of this work is to identify a suitable bitumen emulsion for mixing with natural rubber latex and to investigate the quality of the resulting blend for road surfacing.

Method of approach

Since natural rubber latex is locally available as an anionic latex, attempts are made in this work to produce bitumen also, in the form of anionic emulsion, with a view to enhance the miscibility of two components. Thus anionic bitumen emulsions of various formulations having different proportions of their contents are prepared and their suitability for mixing with natural rubber latex and for spraying is examined. Following the choice, latex-bitumen emulsion blends are made with the suitable ones and then evaluated for their technical performance. From this investigation, the most appropriate bitumen emulsion and blend of latex-bitumen emulsion for road surfacing are identified.

Materials Used

Bitumen : 80/100 penetration grade bitumen is chosen, as the grade is commonly used for road surfacing in this country.

Emulsifier: Emulsifier based on locally available vegetable oil is considered for low cost production. For the production of the emulsifier, rubber seed oil is saponified with potassium hydroxide. The choice of the oil is made, because of its higher proportion of unsaturated fatty acid components (Table 1). These components are believed to give more stable lathers in emulsifying system, in comparison to saturated fatty acid components.

For saponification, potassium hydroxide is preferred to other alkalis because of its higher solubility.

Stabilizer: Casein is chosen, to enhance the stability and bonding property of the bitumen emulsion.

Latex: Ammoniated 60% centrifuged natural rubber latex is selected as it is accessible in adequate quantity in the plantation industries of the country.

Table 1
Fatty acid composition of rubber seed oil

	Weight %
Plamitic acid $C_{15}H_{31}COOH$	10.6
Stearic acid $C_{17}H_{35}COOH$ Saturated acids	11.5
Arachidic acid $C_{19}H_{39}COOH$	1.0
Oleic acid $[CH_3(CH_2)_7CH=CH(CH_2)_7COOH]$	17.2
Linoleic acid $[CH_3(CH_2)_4CH=CHCH_2CH=CH(CH_2)_7]$	35.8
Linolenic acid $[CH_3CH_2CH=CHCH_2CH=CH(CH_2)_7COOH]$	23.9

Experimental

Preparation of the components of bitumen emulsifying system

The following formulations were used to prepare the components, emulsifier and stabilizer of the emulsifying system.

Emulsifier (30%)

	Pwt
Rubber seed oil	250
Potassium Hydroxide	50
Water	560

Stabilizer (5%)

	Pwt
Casein	5
Borax	10
Water	85

Preparation of bitumen Emulsions

Bitumen emulsions according to formulations as shown in the table 2, were prepared by means of a laboratory colloid mill. Bitumen content in the mix formulations were varied from 50 % to 60 % (w/w) in the emulsions with a view to produce stable emulsions.

For the preparation of emulsion, a mix containing the emulsifier, stabilizer and water at temperature ca. 40°C and kerosene added bitumen at temperature ca. 130-140 °C were fed separately, in required proportions, into the chamber of the colloid mill, and the mixing temperature was maintained around 85°C-95°C.

Blending Latex with Bitumen Emulsions

Required quantity of ammoniated centrifuged natural rubber latex (60%) was added into each of the most suitable ones of the above emulsions, to about 3-4 % w/w rubber in bitumen.(see Table 3)

Characterisation tests for bitumen emulsions

The following tests were carried out to characterise the bitumen emulsions prepared in this work.
Viscosity test (ASTM D88-79)
Storage Stability test (ASTM D244 -77)
Sieve test (ASTM D244 – 77)
pH determination

The test results are presented in table 2

Characterisation and Technical performance Tests for Blends of Latex-bitumen emulsions

In addition to above characterisation tests, the following tests were carried out to evaluate the quality of the blends.

(a) Tests on residue of the blend after distillation
Penetration (ASTM D5-78)
Softening point (ASTM D36-76)

(b) Performance tests (see appendix 1)
Sand sealing
Cold mixing
Coating and Stripping

The test results are presented in table 3

Results

Table 2
Anionic Bitumen Emulsions

Formulations

	A	B	C	D	E	F
Components	Pwt.	Pwt.	Pwt.	Pwt.	pwt	pwt
Bitumen	50	55	55	55	55	60
Kerosene	2	2	2	2	2	2
Emulsifier (k-soap Of Rubber seed oil)-30%	20	20	20	20	10	5
Stabiliser (5%)	-	10	7.5	5	2.5	1
Water	28	13	15.5	18	30.5	32

Characterisation test results

	A	B	C	D	E	F
Viscosity (Saybolt Furol at 25°C, S)	15	102	94	38	35	34
Storage stability (24 hrs) %	0.0	0.1	0.1	0.0	0.0	0.1
Sieve test %	0.0	0.02	0.01	0.0	0.0	0.0
pH	11	10.5	10.5	10.5	11	10.5

Table 3
Latex – Bitumen emulsion Blends

Formulation

Components	Formulation I Pwt	Formulation I pwt	Formulation I pwt
Ammoniated NR-Latex (60%)	3	3	3
Bitumen Emulsion D	100	-	-
Bitumen Emulsion E	-	100	-
Bitumen Emulsion F	-	-	100

Characterization test results:

Viscosity (Saybolt, Furol at 25oC,S	31	33	32
Storage Stability (24 Hours, %	0.0	0.0	0.1
Sieve test %	0.0	0.02	0.04
pH	10.5	10	10

Performance test results

Sand Sealing	Good	Good	Good

Cold mixing:

a) Metal aggregate	Not Satisfactory	Not Satisfactory	Not Satisfactory
b) Lime stone aggregates	Not Satisfactory	Good	Good
c) Metal aggregates + 5% w/w lime	Not Satisfactory	Good	Good

Coating and stripping:

a) Metal aggregates	<95%	<95%	<95%
b) Lime stone aggregates	<95%	>95%	>95%
Metal aggregates + 5% w/w lime	<95%	>95%	>95%

Test results on residue, after distillation

a) Softening point oC	56	60	61
b) Penetration (ASTM D5-78)	55	52	50

Discussion And Conclusion

Choice of Bitumen Mix for Blending with Latex

The results of the study reveal that among all mixes (A, B, D, E & F) used for the preparation of bitumen emulsions, the mixes D, E & F have been found to be most suitable (Table 2). The emulsions produced from these mixes have desirable viscosity values, in addition to other favorable characteristics such as storage stability and sieve test results, that required for road emulsions. Mix A is unsuitable for it gives too low viscosity emulsion (15 Saybolt, Furol, S), which if used, may drain off road, during spraying. Mixes B & C could not also be considered befitting, because the emulsions produced have shown very high viscosity values (>90 Saybolt, Furol, S.) The spraying this emulsion may cause problems through the conventional jets.

Choice of Latex – Bitumen Emulsion Blend

The test results of the latex – bitumen emulsion blends (table 3) indicate that all these blends I, II & II have required values of viscosity, storage stability and sieve test results, for them to be used as road surfacing bituminous emulsions .The blends have also proved to be suitable ones for sand sealing, and for producing rubberized bitumen with higher softening point (= 60°C) and better resistance for deformation (penetration = 52). However, on investigating, the performance test results of cold mixing and coating and stripping, it has been found that, **a)** All three blends I, II & III have failed to give satisfactory results with normal aggregates (metal aggregate) and, **b)** the blends II & III (compared to blend I) show promising results if only the normal aggregates are replaced with lime stone aggregates or the aggregates are partially mixed (5% w/w) with lime powder.

The failure of obtaining good results with blend I, with all type of aggregates (Normal, aggregates) could be attributed to its higher content of emulsifier (20 pwt).

Thus the following conclusions can be made from this work:

a). Bitumen emulsions, similar in contents and compositions to mix E or Mix F could be successfully used to produce natural rubber latex – bitumen emulsion blend for road surfacing , and

b). For better performance of such blend, the roads must be constructed with either lime stone aggregates or 5% w/w lime mixed normal (metal) aggregates.

References

1. Ministry of transport , Road Research Laboratory, Middlesex ,Bituminous Material in Road Construction, 1962.
2 Road Development Authority, Sri Lanka, Seminar on Modified Bitumen for Improved Performance on Road Works, 1993.
3 M.R.N.Fernando , Manufacture of Dark Factice from Rubber Seed Oil, RRIC , Quarterly Journal Vol.47 , April- June 1971 , pp. 59-64.

Acknowledgements

The authors wish to thank the Road Construction and Development Company, Ratmalana, Sri Lanka, for funding the work described in this paper. They are also grateful to the Director , research and Development, Road Development Authority, Ratmalana, for granting his permission to carryout the experimental and testing work in RDA laboratory. Thanks are also due to RDA laboratory staff and Mr. S.H.Waidyasekara, Dept. of Mining & Mineral Eng., University of Moratuwa for their assistance given to us during the experimental and testing work.

Appendix 1

Sand Sealing test

In this test, the latex-bitumen emulsion blend is applied on a sand surface and visually inspected for its bonding property.

Cold mixing test

The road surfacing aggregates are spreaded on a surface and wet with water spray. Then the latex-bitumen emulsion blend (6% w/w on the aggregates) is applied on the aggregates and visually inspected for its coating property.

Coating and Stripping

100g of the surfacing aggregates of size 9.5mm is mixed with 8g of the latex-bitumen emulsion blend and the resulting mix is kept under water for 24 hours. Following this treatment, the surface area coated with the bitumen is determined and expressed as a percentage of the total surface area of the aggregates.

THE USE OF SALTERN BITTERNS FOR MANUFACTURING MAGNESIA REFRACTORIES.

W.L.W.Fernando
Dept. of Mining and Minerals Engineering
University of Moratuwa
Moratuwa.

THE USE OF SALTERN BITTERNS FOR MANUFACTURING MAGNESIA REFRACTORIES.

W.L.W.Fernando
Dept. of Mining and Minerals Engineering
University of Moratuwa
Moratuwa.

ABSTRACT

In Srilanka there are salterns where bitterns are produced as potential magnesia compounds , from which magnesia can be precipitated , consolidated and heat treated under certain conditions to produce high quality magnesia pellets which are of similar quality to that produced in the U.K. This is confirmed by the microscopical , chemical and X-ray diffraction studies. This research describes the recovery of magnesia in the lab scale using the sea water bitterns ,from Hambantota salterns , which is presently discarded.

Introduction

The term basic refractories is used to describe refractory materials that react as chemical basic materials at high temperatures and therefore resist attack by alkali , and lime rich fluxing materials. Magnesia is one such material which can be recovered from the bitterns. The major application of basic refractories is in the steel industry as a lining material for basic steelmaking processes including the steel refining. Furthermore , significant basic refractory consumptions are taking place in lime kilns , cement kilns , glass tank regenerators and the refining of nonferrous metals.

Sources of High grade Magnesia for Refractory Manufacture

Salterns are the potential magnesia sources in Srilanka. Refractory grade magnesia could be produced from these salterns. This research deals with the production of such high grade magnesia pellets from the discarded bitterns.

Salterns

There are four major salterns available in Srilanka as sources of magnesia raw materials for the manufacture of basic refractories. At the present moment this valuable raw material (Bittern) is discarded into the sea. The approximate tonnage of bitterns produced in Srilanka is about 100,000 tons per year with the production

Precipitation and Drying

Magnesium salts from the bitterns were precipitated by the addition of (1: 1) ammonia solution into a 1000 cc bittern sample. A thick gelatinous precipitate was formed almost immediately. Alternative methods such as slaked dolomitic lime water could be used but the yield was not as good as that obtained with ammonia. The precipitate was filtered using BCRA vertical filter press. The filter cake was air dried in a fume cupboard for about 4 hours and subsequently oven dried at 110 ^{0} C for 2 hours using a Gallenkamp oven. A sharp volume reduction of the precipitate took place during the drying process.

Calcination of Magnesia

The above product was calcined in a gas fired furnace at 1000^{0} C (fig. 3). Thereafter it was ground in a ceramic lined mortar followed by sieving through 300 mesh B.S sieve. Immediately after sieving , the powder sample was stored in a desiccator as it was hygroscopic.

Powder Pressing

The powder specimens prepared were subjected to washing with acetone for several times and the dry product was finally pressed uniaxially using a hand operated hydraulic press (Fig.4). A specially fabricated 15 mm diameter die was used for powder pressing. The load on the plunger was increased gradually from zero to 8000 kg , and maintained at this maximum load for 10 sec. before it was released. The powder compact sample was thereafter removed from the die in the normal way.

Sintering of Magnesia

The sintering of the Magnesia pellets was carried out using the induction furnace as shown in (Fig. 5 & 6). The sample of magnesia approximately 15 mm diameter and 3 mm thickness was carefully inserted via the feed system into the Alumina working tube coupled with a graphite succeptor. Power was supplied through the coil via a R.F generator while the optical pyrometer was used to measure the temperature inside the furnace. The current through the coil was gradually increased until the required temperature was attained (1900 ^{0} C) , thereafter this maximum temperature was maintained for 10 seconds before cooling.

points located at Palavi , Elephant pass , Puttalam & Hambantota. The analysis of the bittern from Hambantota is as follows :

Bittern Analysis (Hambantota)

Constitutent	Percentage
NaCl	16
$MgCl_2$	6
$MgSO_4$	4
KCl	1
NaBr	0
Water	72
Total	99

Sample Collection

The Bittern samples were collected from Hambantota salterns. The particular location was Mahalevaya (Fig. 1) , where the bittern was pumped out and discarded from the salting out yard into the discharge pond. The sampling was done during a dry season when the harvest of common salt was taking place
(Fig. 2).

Experimental procedure

The samples of bittern collected were subjected to the following :-

(i) Precipitation of Magnesia in the form of Magnesium hydroxide from the liquor using ammonium hydroxide (1:1) .

(ii) Calcination and Powder preparation.

(iii) Uniaxial pressing into tablets.

(iv) Sintering using an Induction Furnace.

(v) Microstructure determination.

(vi) X-ray analysis.

Microstructure Examination

After cooling , the samples of sintered Magnesia pellets were mounted in araldite in the usual way. The vacuum technique was adopted while mounting the specimens into specimens holders. The polishing of the specimens for microstructural determination was carried out using the silicon-carbide powder of various grades starting with the coarsest grade initially. The final polishing was done using 6-micron and 1-micron diamond paste in that order using the laps.

The microstructure examination was done using Vickers microscope with a photographic camera attachment , and thereafter the two specimens , viz : Srilankan magnesia and Steetley (U.K) magnesia pellets were compared.

X-Ray Analysis

The samples of magnesia sintered at 1800^0 C , 1850^0 C and 1900^0 C respectively, using the induction furnace were examined using pinhole transmission camera using Copper K_α radiation . The variation of grain sizes at different sintering temperatures was studied from the spot sizes and the X-ray diffraction pattern was obtained corresponding to the maximum spot size.

Results

The chemical analysis of the magnesia pellet using the classical chemical analysis shows the following :

Composition	Percentage
MgO	98.75
Fe_2O_3	0.75
$Na_2O + K_2O$	0.25
Total	100.00

The microstructural examination reveals that the magnesia produced from Srilanka bittern and Steetley (U.K) magnesia are almost identical (fig. 7 , 8) .

The X-ray diffraction pattern shows the presence of Periclase (MgO) lines as shown in the fig. 9 . It is also clear that there is a change in spot size of the magnesia grains as sintering progresses , with the maximum spot size occuring at 1900^0 C (fig. 10).(Compare this with the spot size of Steetly magnesia fig. 11).

Conclusion

The preliminary research into the recovery of magnesia from sea water bittern clearly shows that high grade magnesia refractories could be manufactured in Srilanka. The microstructure , X-ray analysis , and chemical analysis show that the properties of Srilankan magnesia are similar to Steetley Magnesia in the U.K.

Suggestion For Further Work

I suggest that this research should be continued on a pilot scale..At the moment such facilities are not available in the University. Instead of using ammonia which is rather expensive , the possibility of using an other alkaline solution such as calcined dolomitic limestone in water should be investigated. Such a solution may impart impurities into the magnesia grains , causing physical and chemical property variations. The effects of these impurities on magnesia have to be studied. Further research should be conducted on magnesia brick specimens prepared from a pilot plant pellets , for its mechanical and high temperature properties, particularly Refractoriness Under Load, and Spalling tests.

Acknowledgement

I wish to thank .Steetly Refractories of Great Britian for providing a sample of high grade dead-burnt magnesia for this research work.Thanks are also due to the Heads of Departments of Ceramics and Metallurgy in Leeds University for providing laboratory facilities to complete this research work.Finally, thanks are due to Lanka Salt Ltd for permitting me to collect bittern samples from Hambantota Salterns and also providing other technical information.

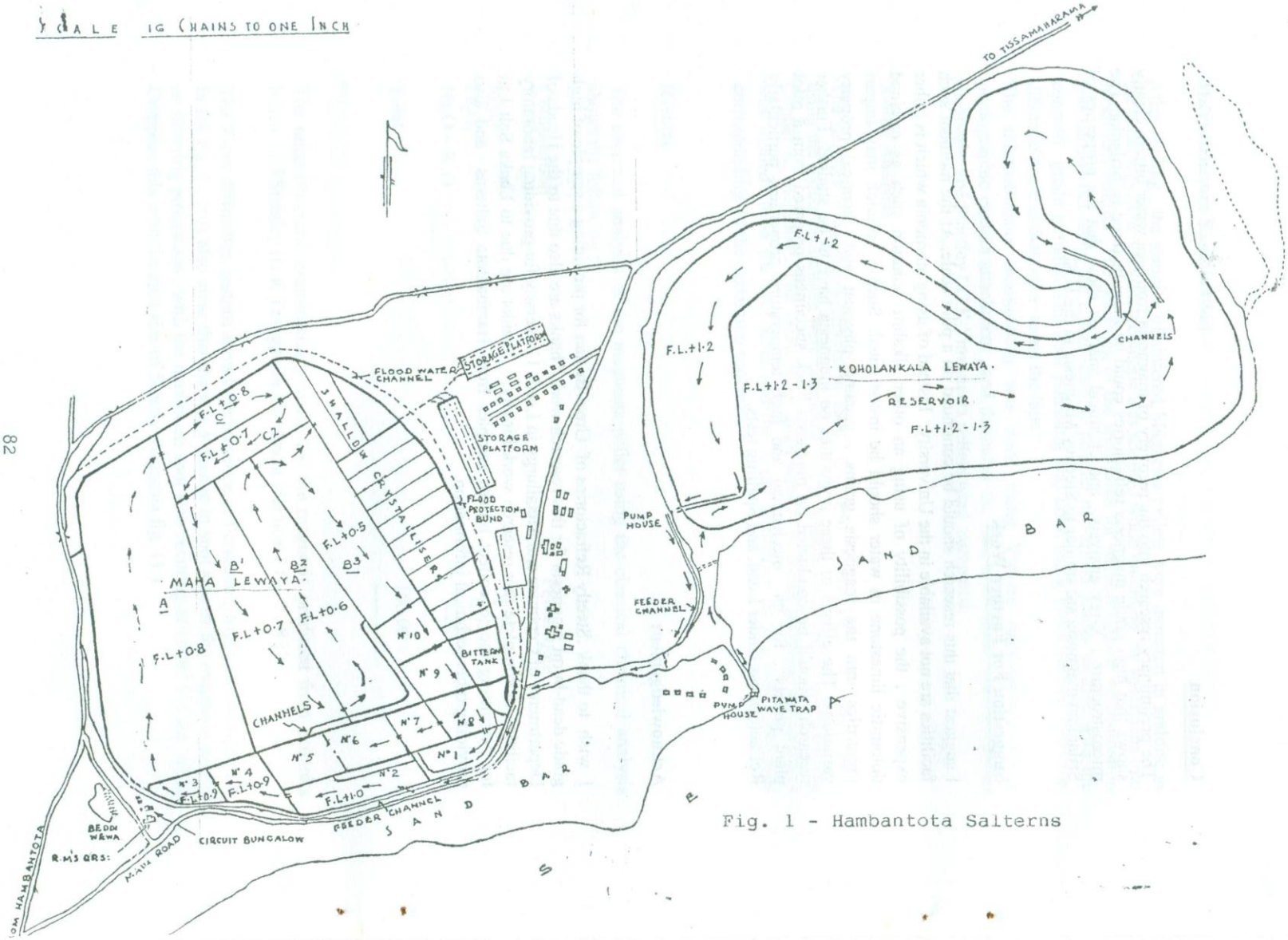

Fig. 1 - Hambantota Salterns

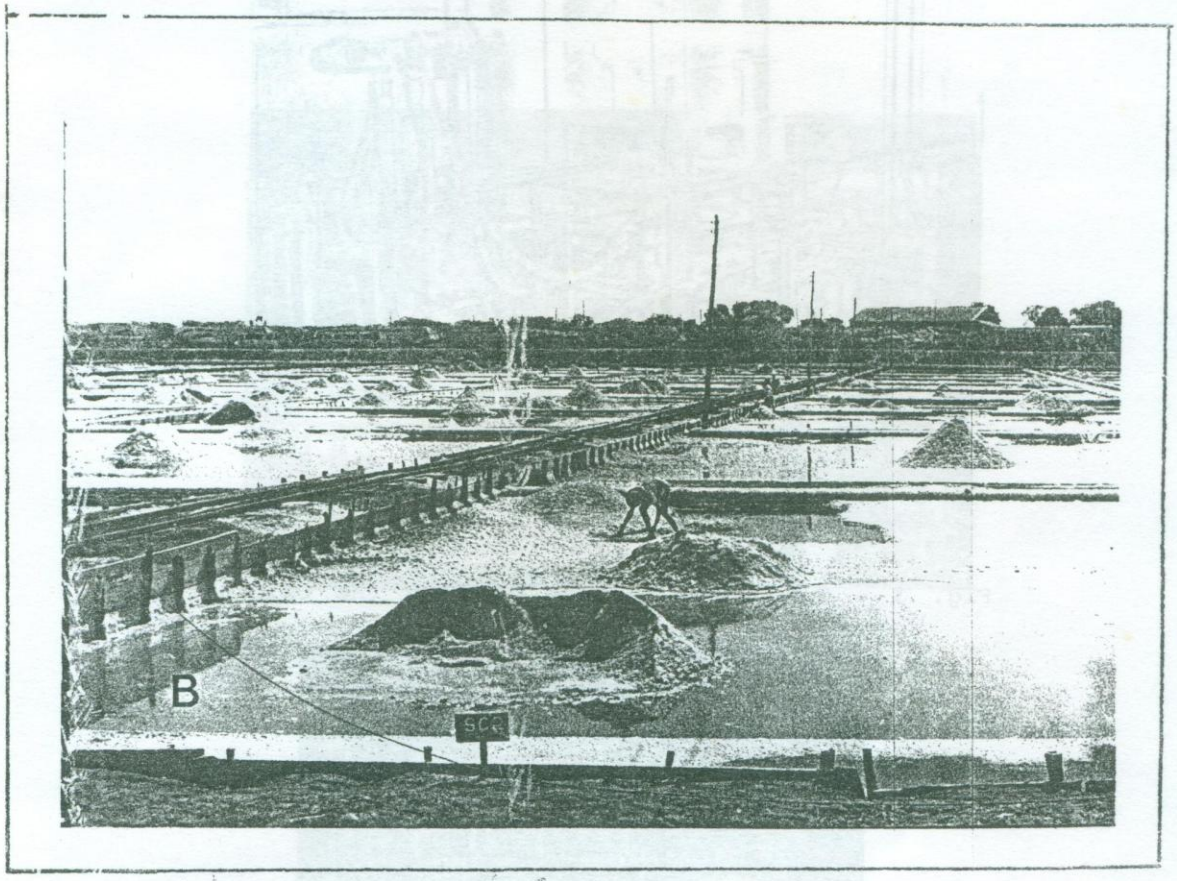

Fig. 2 - Harvesting Common Salt
Note: B is the sample location.

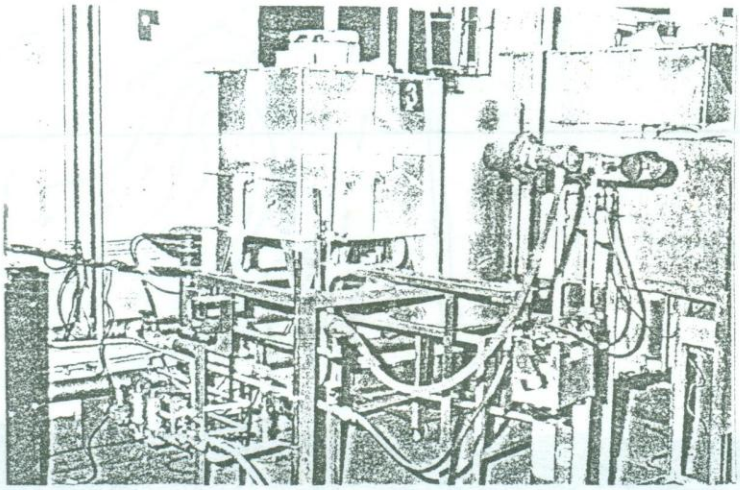

Fig. 3 - Gas fired furnace used in the calcination of Sri Lanka Magnesia Pellets

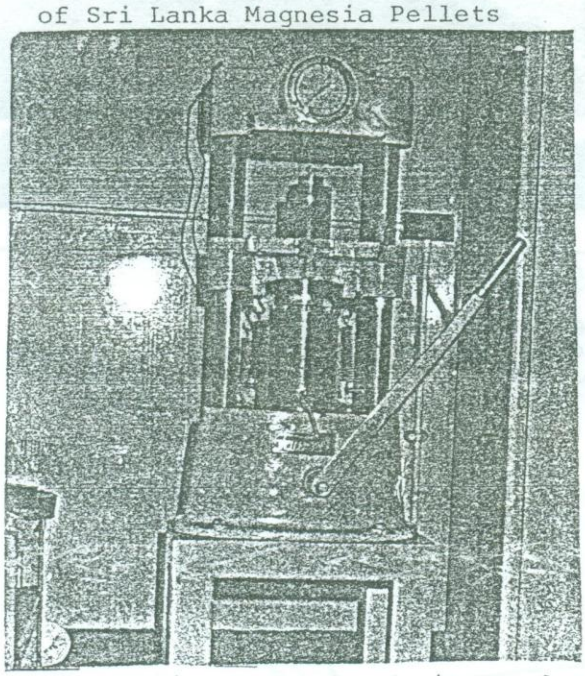

Fig. 4 - Hydraulic Press used in powder pressing

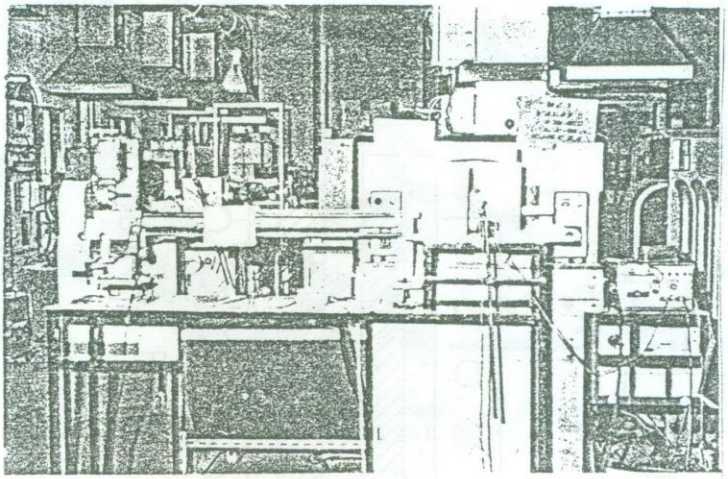

Fig. 5 - Induction Furnace used in the sintering of Magnesia Pellets.

NOTE - THE FEED SYSTEM ON THE LEFT HAND SIDE

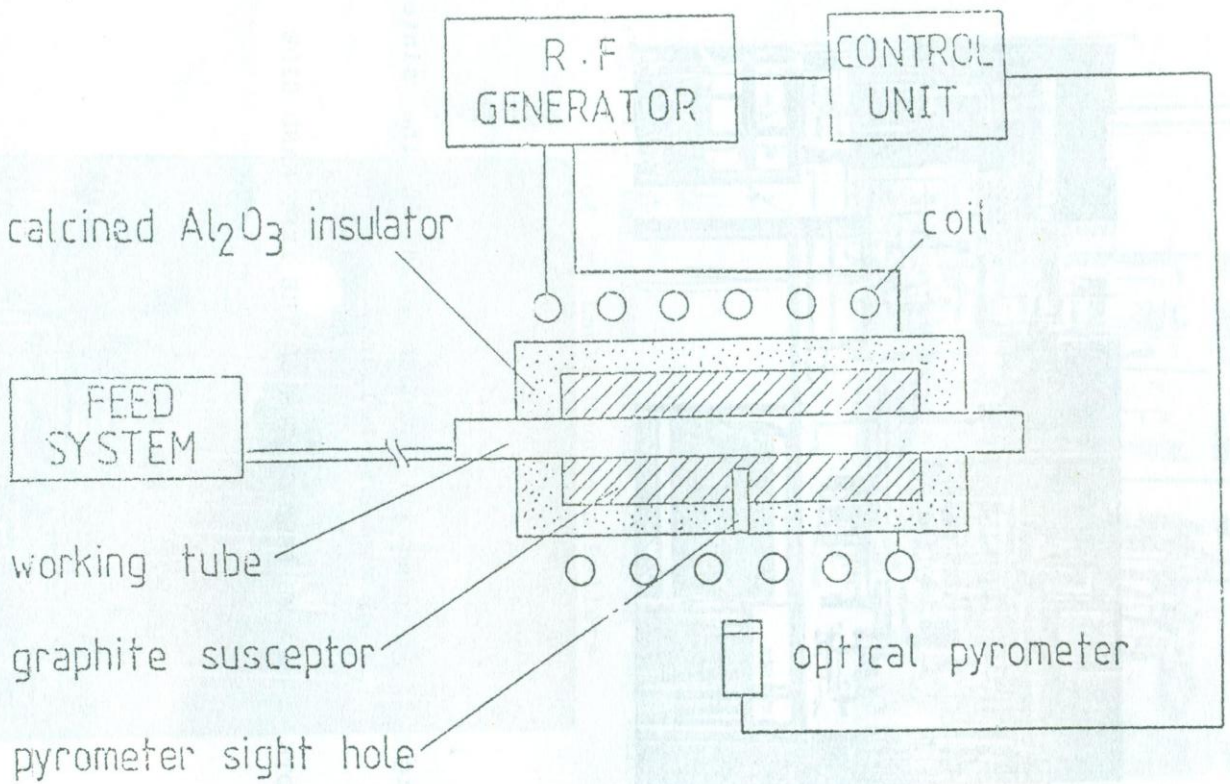

Fig. 6 - Induction Furnace (Layout)

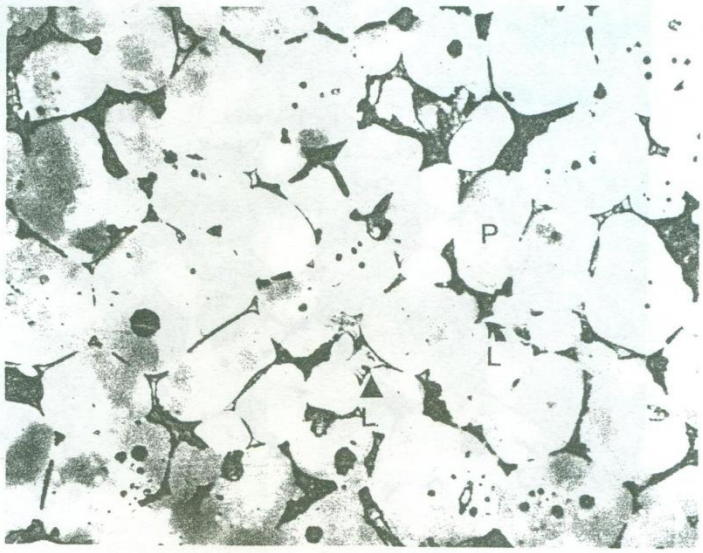

Fig. 7 (a) Optical Micrograph of Srilankan Magnesia Pellet. Mag. X 400 (Fired at 1900°C)

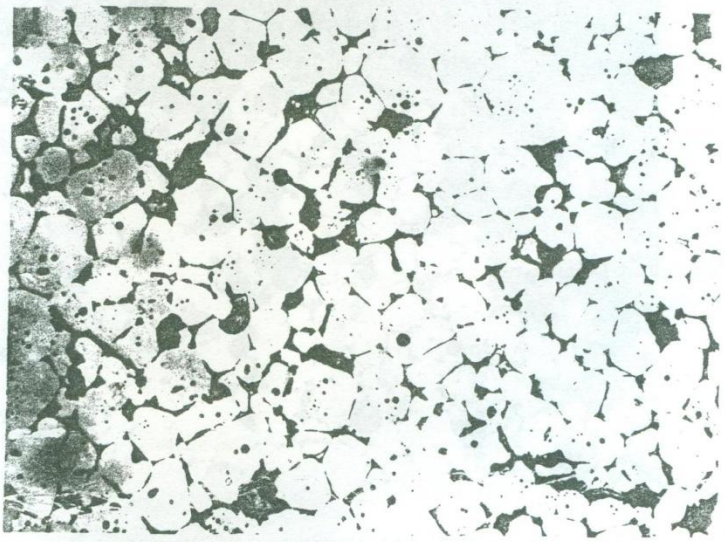

Fir. 7 (b) Optical Micrograph of Sri Lankan Magnesia Pellet. Mag. X 200 (Fired at 1900°C)

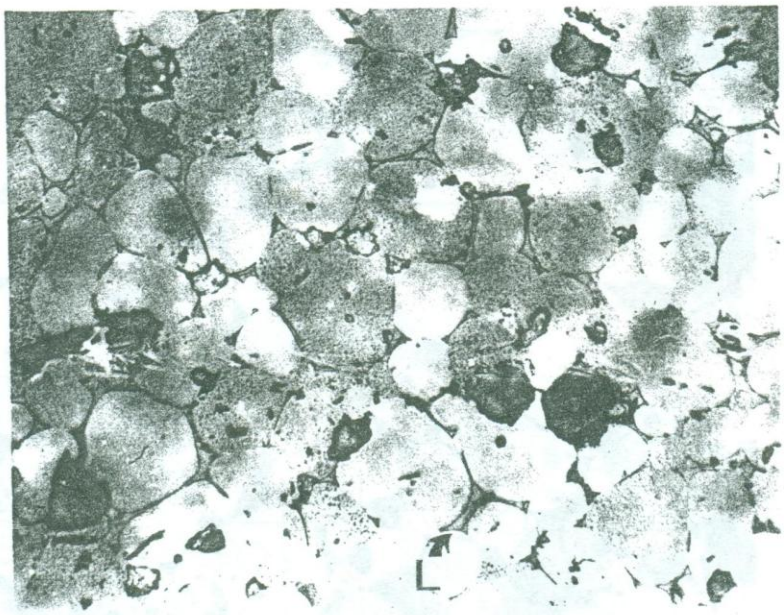

Fig. 8 (a) Optical Micrograph of Steetly Magnesia Pellet. Mag. X 400

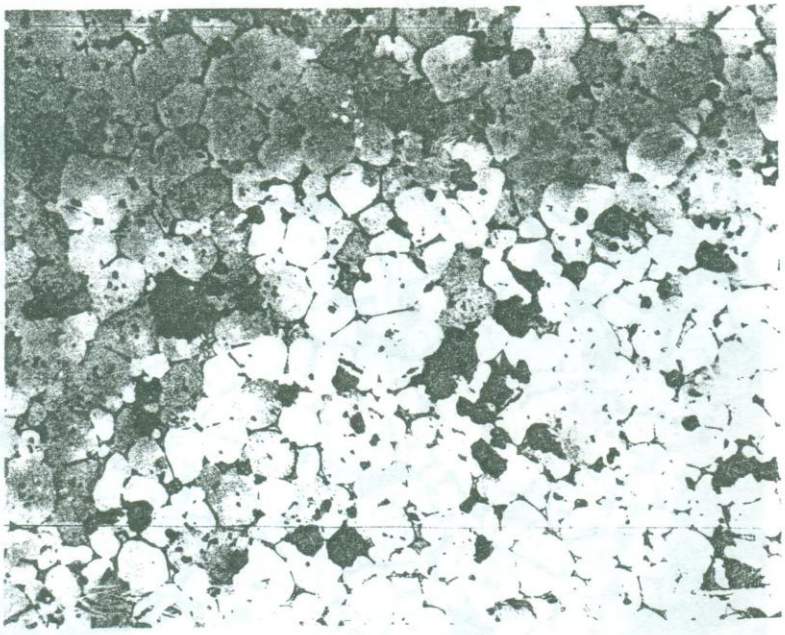

Fig. 8 (b) - Optical Micrograph of Steetly Magnesia Pellet. Mag. X 200

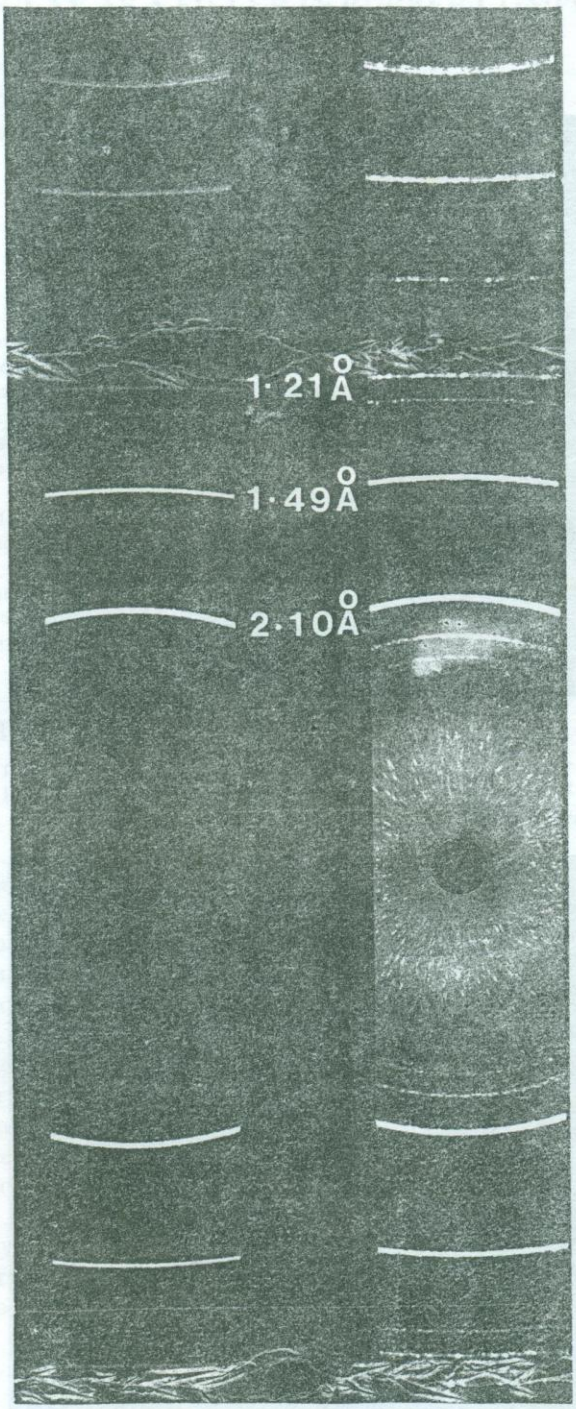

Fig. 9 X-ray Diffraction Patterns
R.H.S. - Sri Lankan Magnesia
L.H.S. - Steetly Magnesia
Note : The sharp Periclase (MgO) lines

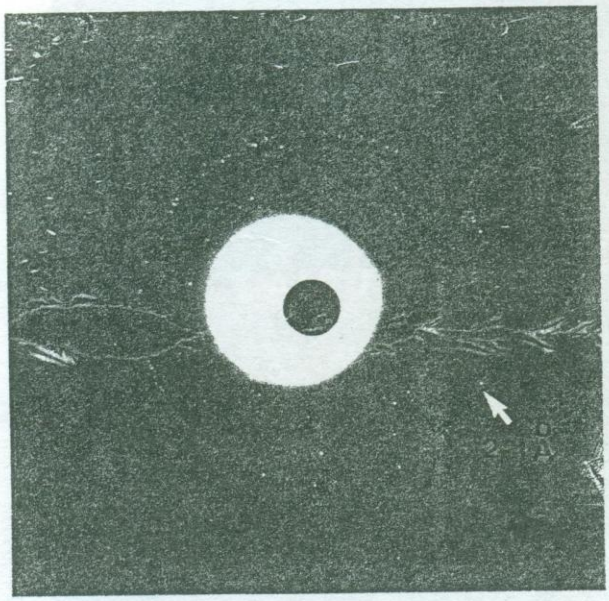

Fig. 10 - X-ray Pinhole transmission, Srilankan Magnesia

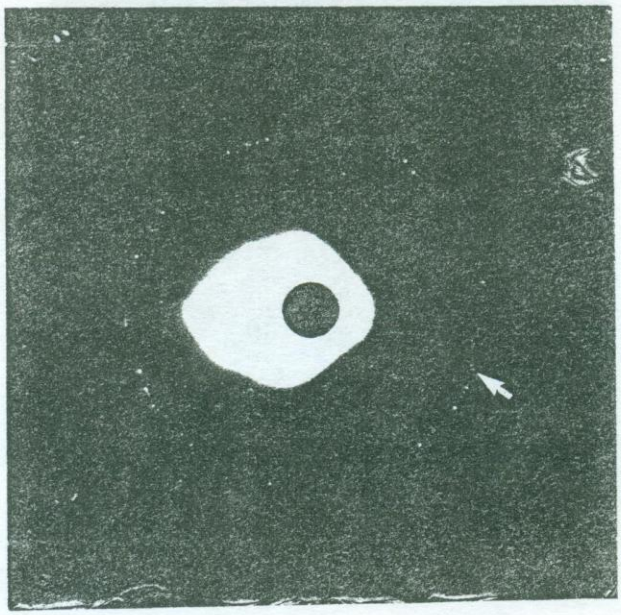

Fig. 11 - X-ray Pinnole transmission, Streetly Magnesia

MODIFIED CLAY AS A FILLER IN RUBBER COMPOUNDING

P.Y. Gunapala , and M. Sivasundaram
Dept. of Materials Engineering. University of Moratuwa

MODIFIED CLAY AS A FILLER IN RUBBER COMPOUNDING

P.Y. Gunapala , and M. Sivasundaram
Dept. of Materials Engineering, University of Moratuwa

ABSTRACT

Elastomer formulations have changed continuously in order to achieve optimum cost-performance characteristics. The surface modification of low cost mineral fillers had an impact on the rubber industry, because it made possible to convert non reinforcing mineral fillers into reinforcing ones and displace expensive carbon black fillers from rubber compound. Therefore low cost mineral filler such as china clay has been upgraded by surface modification to obtain creditable performance as reinforcing filler in rubber industry.

Also this modified filler has improved the quality of rubber compound through better dispersion of ingredients added to the mix.

But primary advantage of the modification has been related to the interfacial adhesion between rubber and filler, since the modificator, acting as a surfactant provides the bond formation across modificator-clay interface as well as rubber-modificator interface.

INTRODUCTION

Mineral fillers today mainly fulfil the same purpose as they did at the start of this century, mainly to lower rubber compound cost due to its diluent effect.

Surface modification of clay minerals has recently experienced significant interest from rubber technologists. A result of this renewed interest is associated with the real perspective of partial or complete displacement of expensive carbon black fillers from rubber compounds with much cheaper mineral ones without any deteriorating in the performance/properties.

Surface modification techniques generally consist of surface treatment, where the composition or mechanical properties of the existing surfaces are altered or the deposition of coatings where a different material is deposited to create a new surface Surface treatment is regarded as a chemical treatment, if the composition changes by chemical reactions, that can be originated by ion implantation or deposition. [1]

Major intensity in the development of modification technologies is focused on the production of low cost fillers with improved reinforcing properties similar to properties of traditional carbon black fillers.

The relative positions of rubber fillers in terms of filler usage are shown below;

Filler	Usage %
Carbon black	44
Whiting	17
Clay	15
ZnO	4.4
TiO_2 + and Baryta	2.3
Talc	1.2
Miscellaneous }	
Non-Black fillers }	8.3
	48.2% Non-Black fillers

In order to convert a mineral filler in to reinforcing one, a filler must comply with two main following requirements;

1. Develop a large interface between the filler particles and polymeric substance.
2. Posses a surface with high degree of activity.

Therefore the main aim of our investigation was to fulfil the above mentioned requirements with regard to clay.

EXPERIMENTAL

The high grade china clay selected for our investigation was obtained from Borelesgamuwa
Initially clay was calcinated for 8 hours at 900°C to remove the organic substances present in the clay. After the calcination the clay was ball milled for 8 hours to convert the two-layer structure to a booklet structure. Then 0.1 M ammonium acetate solution was added to china clay. The last was wetted well and two components were intermixed thoroughly. The mixture was allowed to stand 12 hours and filtered. The filter cake was washed with a small amount of ethyl alcohol at ambient temperature.

To ensure absorption of ammonium ions by the clay and to control required amount of ammonium ions, Nessler's solution was used. The series of complex investigations were conducted using a number of physico-chemical analyses. The amount of bound rubber was calculated on the basis of solubility of the rubber compound in toluene. The formulation used is given in Table 1

The Natural Rubber, filler (modified and unmodified) and other additives were mixed in two stages. Primary mixing was done by using a laboratory internal mixture. Secondary mixing was done on a laboratory size two -roll mill (16"x18").To find out the effect of bound rubber, master batches were prepared and tested after 24 hours of preparation. It was reported by several authors that after keeping the specimen of compounded rubber at ambient temperature for a long time, the content of the bond rubber increased.

All experiments on uncured compounds were performed with a simple mixture of filler and rubber.
The bound rubber was measured by extracting rubber with toluene at ambient temperature for four days, weighing the residue and calculating the percentage of insoluble polymer.

All curing characteristics were measured using a Moony viscometer and a Monsanto Rheometer. Vulcanised samples for physical and mechanical testing were prepared by compression moulding in an electric press.

RESULTS AND DISCUSSION

The curing characteristics of the rubber compounds filled with modified and unmodified china clay are given in Table 2. Obtained results showed that effect of modification manifested in decreasing the cure time and consequently in increasing the cure rate. Compound B, filled with modified china clay required shorter period to become fully vulcanized as compared to compound A, filled with unmodified china clay, while other curing parameters were fairly similar.

Such effect of modification is considered as a positive one, in terms of capital investments and can be explained as follows.

In clay minerals, the oxygen and hydroxyl valencies at the planer surfaces of the structure are completely satisfied. However, there are aluminium, silicon, oxygen and hydroxyl ions at the edges that are not so satisfied, because the lattice is capable of extension indefinitely in the "ab" plane [Fig 1] .These unsatisfied valencies or "broken bonds", are satisfied in practice by external ions that do not form part of the structure, but merely act as counter -ions, preserving electrical neutrality. These counter-ions, particularly the cations, are capable of being exchanged for other ions. However in disordered kaolinites, additional balancing cations are present because of the lattice substitutions. These additional cations probably account for greater part of the action exchange that occurs with disordered kaolinites [3]

Organic electrolyte (i.e. ammonium acetate), that is ionised in aqueous solution, may also replace other cations on clay surfaces, as shown below;

$$R.\ NH_3 + Ca\text{ - clay} \rightarrow R.\ NH_3\ Clay + Ca^{+2}.$$

Since the amine is absorbed with NH_3^+ group close to the surface, the alkyl group R projecting outwards the surface presented to the suspending medium is effectively an "Organic" surface that is hydrophobic one.[Fig 2] Thus, association energy of the composite clay particles is drastically reduced.while solvation energy of clay particles by organic medium increases in other words amine clay having now organophobic surface properties is highly compatible with organic rubber matrix.

The concept of surface activity refers to inter reaction between filler particles and polymer leading to formation of various type of adhesion bonds across their interface. Partial insolubility of polymer in a filled elastomer is due to adsorption

of the macromolecules on to the surface of reinforcing fillers.[4] But we presume, that effect of amine modification on physical and mechanical properties due to ;

(1) Increasing in the adhesion between rubber and filler by improvement their interfacial interaction. [Fig.2]
(2) Improvement of quality of the rubber compound by better dispersion of filler particles in rubber matrix.

Fundamental thermodynamic equation of the adhesion work shows, that

$W = \gamma_{filler\text{-}air} + \gamma_{Rubber\text{-}air} - \gamma_{Rubber\text{-}filler}$

Where	W	=	Adhesion work
	$\gamma_{Fill\text{-}Air}$	=	Surface energy of filler - air interface
	$\gamma_{Rubber\text{-}Air}$	=	Surface energy of rubber -air interface
	$\gamma_{Rubber\text{-}Fill}$	=	Surface energy between rubber -filler interface

the adhesion can be increased by minimising (decreasing) surface energy at rubber-filler interface.

Therefore any treatment of filler with an agent, which can act as surfactant, decreasing interfacial energy, will improve its adhesion to rubber [5]

After modification the inorganic surface of the filler is transformed into "organic" hydrophobic or "rubber philic" one. So the closer nature of contact surfaces, lower their interfacial energy ($\gamma_{Rubber\ -\ filler} \rightarrow 0$) and higher adhesion values are to be expected.

The adhesion of macromolecules to filler surface proceeds through adhesion of structural units on the filler surface where attractions are formed and these attractions are sufficiently permanent to resist the swelling action of a solvent [3].
Our experimental data on swelling test confirmed this assumption.

Practical results namely in bound rubber content, tensile strength, abrasion resistance, swelling test and fatigue resistance quite clearly indicated that part of the rubber molecule was strongly adhered to the surface of the filler. [Table3] The larger the surface area of the filler, the larger the number of structural units which are strongly adhered to the surface in this way. The content of bound rubber was higher for the new product than the content of bound rubber for the unmodified clay mineral again indicating a high interaction.

Discussion of dispersion quality would be incomplete without evidence from microscopy analysis. Fig. 3 and Fig. 4 indicate typical micrographs of both compounds. From these, it appears that the particle distribution of new product was more uniform than that of the unmodified clay.

Also we assumed, cation exchange is not a one to one replacement. Therefore neutrality of the clay particle is disturbed [2]. This result is present of a net charge. Due to this the particles are repelled and the dispersion is increased.

Also maximum reinforcing effect is realised by complete wetting of all clay particles with rubber that can be considered as a high viscosity liquid phase. So no agglomeration of filler particles must be in rubber matrix. After the modification of clay mineral by ammonium acetate, the solvating energy of hydrophobic filler particles in organic medium is increased, while association energy is drastically reduced. [5]. Therefore created conditions induce deflocculation of filler particles that provides their better dispersion in rubber matrix.

The next important point is the rate of cure. [Table.2] We can not also ignore the possibility of chemical interaction of alkyl amine groups with elementary sulphur or with mercapto benzo-thiazole accelerator or with both. Most likely product of this reaction was responsible for the acceleration of vulcanization.

Also amine liberated from the modified clay mineral and present in the reaction system is capable of further reaction with sulphur compounds as well as the sulphur molecules. Some papers report that both alkyl and aryl amines accelerate the reaction of hydrocarbon with sulphur [6].

CONCLUSION

The active development of modification of the functions of clay was devoted to match carbon black /silica fillers in its reinforcing capability.

However, new development promises to improve physico-mechnical properties of clay more closer to reinforcing properties of carbon black/silica. Also, the. properties contributed by low-cost extended filler (clay) can be modified and compound is given greater control over all performance properties. It provides a desirable balance between dynamic and mechanical properties too.

ACKNOWLEDGEMENT

The authors would like to acknowledge the help and support of Mr. Sarath Chandrapala and Mr.Ananda Suraweera for the dynamic measurements and optical micrography.

REFERENCES

(1) A.R. Payne The physics of reinforcement
1st European Conference of Technology of Reinforcement of Elastomers. Brussels, April 1975

(2) W.E. Worrall, Clays and Ceramic Raw Materials, Applied Science Publishers Ltd., London, 1975.

(3) Susy Varughese and D.K. Tripathy, Rubber to filler interaction
Studies, Plastic, Rubber and Composites processing and applications, p. 219 - 223, Vol. 17, No: 4, 1992.

(4) Claude Hepburm, Filler Reinforcement of Rubber, Plastic and Rubber International, p.11-15, Vol.9, No: 2, April 1984

(5) I.S. Miles, S. Rostami, Multicomponent Polymer Systems, Longman Scientific and Technical, UK. 1972

(6) Haruko Fukuda, Jitsuo Tsurugi the Chemistry of Vulcanisation,
Accelerating mechanism of sulphonamide type accelerators.
Rubber Chemistry and Technology, p.491-497, Vol.35, 1962

Curing Characteristics

A - compound with unmodified china clay
B -. Compound with modified china clay

Table 1

	compound A	compound B
Minimum Torque N/m	28	24
Minimum Torque N/m	3.5	3.5
Scorch Time Min	3.5	3.5
Curing Time Min	12.0	7.0
Cure rate Min^{-1}	11.8	28.8

Physical and Mechanical Properties

Table 2

Properties	Units	Compound A	Compound B
Hardness	IRHD	53-54	54-55
50% Modulus	mPa	3.67	3.00
300% Modulus	mPa	7.45	8.00
Tensile Strength	mPa	17.15	25.93
Elongation at Break	%	600	750
Resilience (Lupke)	%	58-60	62-64
Fatigue Resistance	cycles	29829	181487
Abrasion Resistance(DIN)	g	.19	0.013
Swelling in Toluene	%	287	194
Bound Rubber	%	1.98	12.56

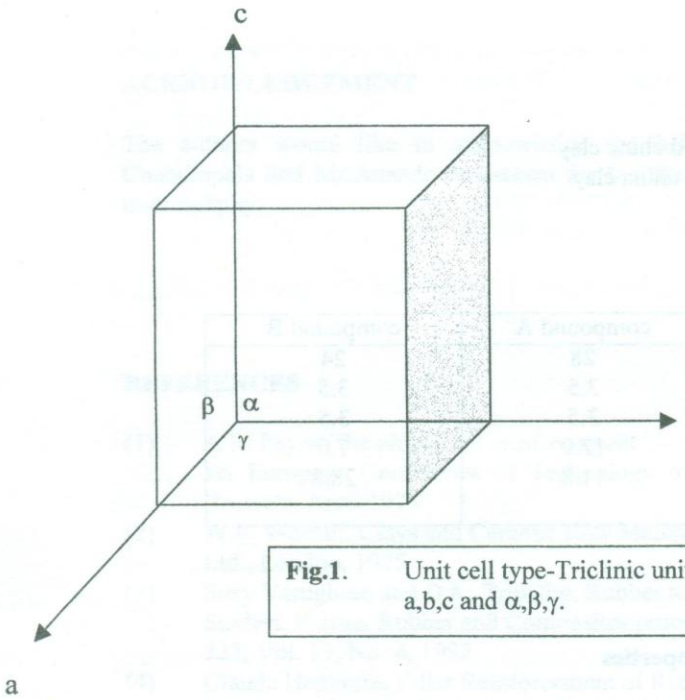

Fig.1. Unit cell type-Triclinic unit cell dimensions a,b,c and α,β,γ.

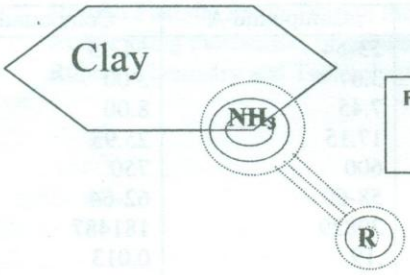

Fig. 2 A schematic diagram of the possible interaction between rubber and modified filler.

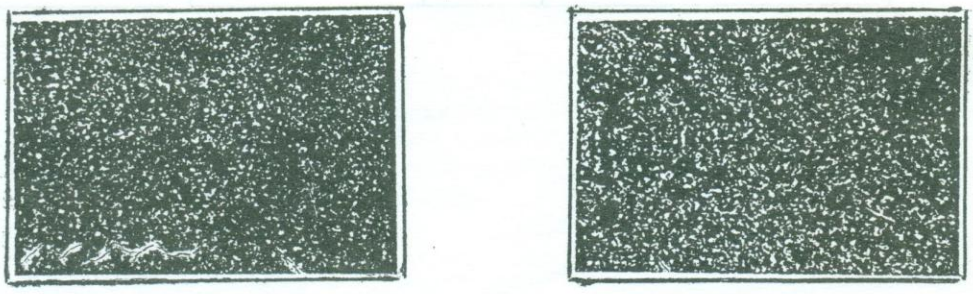

Fig3-Micrograph of polymer-filler blends consisting of (a) modified (b) unmodified fillers

INVESTIGATION OF WAVE REFLECTION FROM COASTAL STRUCTURES.

S.S.L.Hettiarachchi and P.D.Mirihagalla
Department of Civil Engineering, University of Moratuwa.

INVESTIGATION OF WAVE REFLECTION FROM COASTAL STRUCTURES.

S.S.L.Hettiarachchi and P.D.Mirihagalla
Department of Civil Engineering, University of Moratuwa.

ABSTRACT

Wave reflections at and within a coastal harbour may make a significant contribution to wave disturbance in the harbour. Reflected waves may lead to danger to vessels navigating close to structures and may cause mooring problems. Wave reflections may also increase local scour or general reduction in sea bed levels. In the design of breakwaters, seawalls and coastal revetments it is very important to estimate and compare the reflection performance of alternative structural types with respect to wave energy dissipation characteristics. This paper presents the results from a study of the reflection performance of a wide range of structures used in harbour and coastal engineering.

1. Objective of the paper

This paper presents selected results of a detailed study the objectives of which were to assess the hydraulic performance of coastal structures with respect to energy transformation processes. The study investigated various aspects of wave/structure interaction of a wide range of coastal structures used in practice. This paper focuses attention on wave reflection an important design parameter which is a quantitative measure of the hydraulic performance with respect to wave energy dissipation. The reflection performance of different configurations are discussed based on research data obtained as part of this investigations and analysis of data from previous investigations conducted at leading research laboratories. Types of prediction methods are identified and empirical equations are presented as design guidelines.

2. Wave absorbing structures for coastal and flood defence

Coastal structures are used to dissipate and/or reflect wave energy to protect land or water behind them from the effects of waves. Although tide or surge-induced water movements may influence the water levels at the structure giving rise to local currents, it is the action of wind waves and swell which constitute the principal forces acting on the structure. These structures may be broadly classified into five main categories.

a) Non-porous slopes
b) Armoured porous slopes
c) Non-porous vertical walls
d) Porous vertical walls
e) Porous sloping protection to vertical walls

Each of these structure types will dissipate some proportion of the incident wave energy and will generally reflect the greatest part of the remainder. In the extremes the reflection performance of such structures may be compared either with that of a solid vertical wall for which the proportion reflected approaches unity, or with a gently sloping yet porous beach for which the energy reflected approaches zero.

Wave action on a coastal structure results in a number of processes of interest to the designer. Wave energy arriving at a structure will experience three main transformations, namely,

a) dissipation
b) transmission, by overtopping and due to the permeability of the structure, where applicable
c) and reflection

The conservation of energy will be satisfied by an energy sum;

$$E_i = E_r + E_t + E_d \qquad (1)$$

where E_i = total incident energy
E_r = energy reflected
E_t = energy transmitted
E_d = energy dissipated at the structure

In effect the purpose of the structure is to alter the balance of these three processes to reduce the amount of wave action reaching the land or water behind and/or to reduce reflections. The conservation of energy shows that in order to decrease the significance of a particular process it is necessary to increase the significance of the others or to reduce the amount of energy reaching the structure.

The wave reflection coefficient (Cr), the transmission coefficient (Ct) and the dissipation coefficient (Cd) are correlated by the relationship.

$$Cr^2 + Ct^2 + Cd^2 = 1 \qquad (2)$$

where

$$Cr = (E_r / E_i)^{½} \qquad (3a)$$

$$Ct = (E_t / E_i)^{½} \qquad (3b)$$

$$Cd = (E_d / E_i)^{½} \qquad (3c)$$

Each of these energy components is considered to be expressed by the corresponding square of the wave height ($E \propto H^2$) and measured over the same frequency range.

The total energy dissipated E_d may be divided into the dissipated energy components on and in the armour layer (E_{da}), in the underlayer (E_{du}) and in the core (E_{dc}).

Therefore $$E_d = E_{da} + E_{du} + E_{dc} \quad (4)$$

so that the following relationship for the corresponding local dissipation coefficients will result.

$$C^2_{da} + C^2_{du} + C^2_{dc} = 1 \quad (5)$$

where $$C_{da} = (E_{da} / E_d)^{1/2} \quad (6a)$$

$$C_{du} = (E_{du} / E_d)^{1/2} \quad (6b)$$

$$C_{dc} = (E_{dc} / E_d)^{1/2} \quad (6c)$$

Most wave energy absorbing structures possess a significant degree of porosity. Armoured slopes are constructed with voids between and sometimes within the armour units. In this context the term 'porous' in general refers to the presence of voids of a sufficient size as to allow a significant quantity of water to pass and hence pressure gradients to remain low, over the time of a typical wave period. Conversely 'non-porous' implies that the slope or wall would not allow significant flows under wave action. Hence it is evident that 'non-porous' does not imply that the structure is necessarily impermeable to the quasi-hydrostatic flows induced by water level changes of tides and surges. Similarly the terms 'smooth' or 'rough' are measures of relative hydraulic friction of the slope or wall in relation to wave-induced flows.

Wave reflections from coastal structures are of considerable importance both in relation to coastal harbours and the open coast.

The interaction of incident and reflected waves will often lead to a confused sea state in front of the structure, giving rise to occasional steep and unstable waves of considerable hazard to small boats. Reflected waves can also propagate into areas of a harbour previously sheltered from wave action.

Reflection of wave energy at a coastal structure leads to increased peak orbital velocities, increasing the likelihood of movement of beach material. The reflection of obliquely incident waves will tend to excite littoral currents, which taken together with the increased bed velocities, will further enhance the tendency for sediment to be transported away from the area immediately seaward of the structure. Such conditions will lead to potentially greater local scour or sea bed erosion. This aspect is of particular significance to the performance of seawalls used for coastal and flood defense. Although a seawall will protect land behind it, it may not necessarily protect the coastline on its own. If, for example, such a wall is sited on a naturally eroding coastline it may not prevent the overall erosion process and in instances may aggravate the situation. The exact effect of a seawall on the erosion/accretion process is difficult to assess and in the case of seawalls whose main function is to prevent or alleviate flooding it is extremely important that the design takes full account of the relevant coastal processes. Therefore, all seawalls reflect a certain proportion of the incident

wave energy, thereby modifying the near-shore wave field and the sediment transport potential. It is now established that significant wave reflection can increase local scour, reduce foreshore levels and undermine the wall itself.

An important element of the design process for coastal structures is to identify the possible failure modes and to design against them. Table 1 from CIRIA guidelines on Maintenance of Coastal Revetments illustrates the more common causes of seawall failure based on a survey in the United Kingdom. It identifies the marked dominance of toe failure normally caused by scour and beach lowering. Thomas and Hall(1992) in analysing fault trees in relation to seawalls identified that a common initial failure is associated with low beach level which can lead to toe failure and also permit higher waves to reach the seawall.

3. Types of prediction methods for wave reflection

The importance of wave reflection has led to several investigations on the prediction of the level of reflected wave energy using both theoretical and experimental studies. Measurements of wave reflection have been made in model studies of the structural categories identified earlier and methods which allow prediction of reflection performance of similar structures have been identified using three main approaches:

a) graphical presentation of model test results
b) empirical equations based on model test results
c) mathematical modelling

In developing empirical equations which have wider applications, attention should be focused on the following criteria,

1. The equations should be consistent with the current understanding of the physical processes.
2. The equations should approach logical limiting values.
3. The equations should be relatively simple and not include variables of questionable or marginal influence.
4. The equations should be consistent with data from a wide range of wave and structure conditions, but not at the expense of criteria (1) or (2).

Most predictive equations have been based on the Iribarren number, Ir, sometimes known as the 'surf similarity' parameter, as introduced by Battjes (1974).

The Iribarren number is defined as

$$Ir = \tan\alpha / (H/L)^{1/2} \qquad (7)$$

where

tanα is the slope of structure
H is the wave height and
L is the wave length.

The slope of the structure, the wave height and the wave length (wave steepness) have a direct influence on wave reflection and wave transmission through the structure. In this context it is a valid variable to be incorporated in empirical equations.

The following general empirical equations have been used.

$$Cr = a.\ Ir^b \quad (8)$$

$$Cr = a(1-\exp(-b.Ir)) \quad (9)$$

$$Cr = a.Ir^2/\ (Ir^2+b) \quad (10)$$

where Cr is the reflection coefficient; Ir is the Iribarren number; *a* and *b* are empirical coefficients.

The reflection coefficient, Cr is defined in terms of the total reflected and incident energies, E_r and E_i respectively. The empirical calibration coefficients account for effects such as porosity, surface roughness, wave breaking offshore of the structure and multiple layers of armour.

Of the above equations, researchers have preferred the use of Equation 10 which primarily satisfies the first, second and third criteria. The continued use of the equation has proved that it is consistent with data from a wide range of wave and structure conditions and as such it can be used with confidence in the design procedure.

The value of the Iribarren number will depend on the relevant parameters used for the definition of wave height and wave length.

For random waves the significant wave height, H_s is usually used as the wave height parameter. In the case of wave length there are several options available depending on which value of wave period and wave length is used for the definition of wave steepness. The mean wave period, T_m , or the period corresponding to the period of peak energy density, T_p , can be used to compute the wave length which could either be the deep water value (L_{om} or L_{op}) or that corresponding to the water depth local to the structure (L_{sm} or L_{sp}). The latter may seem to represent the local wave breaking in a more realistic form, although it is less easy to calculate and complicates the use of any prediction formulae. Thus, in the case of random waves, four possible definitions can be used for Iribarren number depending on wave length and wave period. Using the same notations these will be denoted by: Ir_{om}, Ir_{op}, Ir_{sm} and Ir_{sp}.

For regular waves the Iribarren number is usually based upon the incident wave height and the wave length corresponding to deep or local water depth at the structure and are denoted here as Ir_o and Ir_s, respectively.

Both analytical and numerical techniques have been used to model wave action on porous coastal structures. In most cases the greater emphasis has been on predicting internal wave height decay and external wave transmission through the structure. The available models are subject to a number of simplifying assumptions and also require information on the porosity and on hydraulic parameters relating to the permeability characteristics of the structure. At present such information is primarily available for rock structures. A summary of the numerical modelling techniques was presented by Hall and Hettiarachchi (1991).

4. Discussion of results

4.1 Presentation of results

The hydraulic performance of a range of coastal structures were assessed via review and re-analysis of data from previous investigations covering both experimental and field studies. These include recent investigations conducted by the authors. Table 2 describes the structural configurations of which reflection performance were examined. Wave transmission characteristics were also investigated for rock armoured trapezoidal structures.

Tables 3 and 4 present the empirical equations and relevant description of wave reflection for the different types of structures investigated. These two tables refer to results from experimental and field investigations respectively. In the tables provided a differentiation is made between empirical equations which have been quoted directly from references and those equations which have been derived by re-analysis of data by the authors. The equations and information can be used in the design of such structures which have to accommodate the impacts of wave reflection.

4.2 Non porous slopes

Non porous slopes can be broadly classified into simple smooth slopes and simple rough slopes. For simple smooth slopes the results of several investigators are presented in Table 3 and it is observed that Equation 10 provides consistent results with a=1.0 and b varying over a small band of 4.8 to 6.2, covering slopes of 1:1.33 to 1:2.5.

Simple rough slopes will reflect less wave energy than the equivalent smooth slope due to the additional energy dissipation resulting from the protrusion of the roughness elements. Any reduction measured in model tests has proved to be small and there are no reliable general data available on the reflection performance of such slopes. It is therefore recommended that if the roughness of the slope does not generate a sufficiently porous slope which could contribute to the energy dissipation process, the value of Cr used should be that corresponding to a smooth slope.

4.3 Armoured porous slopes

Armoured porous slopes can be broadly classified into rock armoured and concrete armoured rough slopes. Porous trapezoidal structures and porous sloping protection to vertical walls also have a similar configuration.

4.3.1 Rock armoured slopes

Allsop and Channel (1989) conducted detailed tests on a range of rock armoured slopes including that for a single layer of armour. Usually armoured rock is laid in two layer thickness for which design methods have been developed. However there are instances where only a single layer of armour has been used. Although such a form of design and construction is not recommended it has been considered useful to have an assessment made of the reflection performance of such structures. The results of Allsop and Channel (1989) using Equation 10 are presented in Table 3. The table also presents the results of Postma (1989) who analysed the data measured by Van der Meer (1988) on simple armoured slopes as well as the data measured by Allsop and Channel (1989) on rock armoured slopes. Postma observed that a simple curve as given by Equation 8 gave a good fit to the data.

4.3.2 Concrete armoured slopes

Concrete armoured structures will exhibit reflection characteristics similar to that of the equivalent rock armoured slope. Breakwater designers have developed various shapes of concrete armour units in order to obtain high hydraulic stability and performance at a relatively small armour block weight.

The different types of artificial armour units used in practice can be broadly classified into four types,

1) Double layer bulky units
2) Double layer interlocking units
3) Single layer interlocking units
4) Single layer hollow block units

Armour units belonging to the bulky type and the interlocking type are normally placed in two layers and at random although there are instances when these units are placed in a predetermined layout. Therefore the void dimensions and shapes which influence the dissipation of wave energy are generated between the armour units in a random manner and for all practical purposes, this is also valid when slender interlocking type of armour units are placed in a predetermined manner. The same applies to single layer armour units of the interlocking type.

The single layer hollow block type of armour units are somewhat different to the other two types in that the voids are built into the individual units in the required form. Armour units

belonging to this type are always placed in a pre-determined manner and the resulting voids matrix of the primary armour is geometrically well-defined and not generated randomly. Thus the geometry of the voids within the confined boundaries of an individual armour or a group of armour units is controlled to produce a cost-effective primary armour layer which has a high overall porosity and is very efficient with respect to wave energy dissipation.

From the above discussion it is evident that some types of concrete armour units are more open and permeable to wave action than rock armouring and that it is also possible to incorporate a pre-determined voids matrix for greater wave energy dissipation. Therefore reduced reflections may be expected under these conditions. Conversely, on certain occasions bulky armour units such as concrete cubes have been placed in a tight packing, generating an armour layer of low porosity leading to higher reflections than might be predicted.

Table 3 presents the empirical equations for the reflection performance of a range of concrete armour units. It is noted that the investigations of Oumeraci and Partenscky (1990) and Murray, Oumeraci, Zimmerman and Partenscky (1992) have been conducted on trapezoidal breakwater cross-sections as opposed to simple armoured slopes.

Comparison of different investigations provided important information on the use of prediction equations. Allsop and Hettiarachchi (1989) analysed the reflection studies of Stickland (1969) on Cob armour units using regular waves. Stickland used units of side length 5.9 cm on slopes of 1:1.33 to 1:2.5 for wave periods 1.2 to 1.8 secs using a constant water depth of 38.1 cm. Equation 10 provided a good fit for the data, which exceeded 50 values, with the coefficients being a=0.50 and b=6.54 for the range $4.5 \geq Ir_o \geq 1.5$. Hettiarachchi and Holmes (1988) conducted investigations on a range of single layer hollow block armour units, including Cobs, Sheds and Seabees using regular waves. All armour units were approximately of the same external size of 4.2 cm on a slope 1:1.33 for wave periods 1.0 to 2.0 secs using a constant water depth of 25 cm. Equation 10 provided a good fit for the data, which exceeded 50 values, with the coefficients being a=0.41 and b=22.2 for the range $16 \geq Ir_s \geq 4$.

The above comparison clearly shows that the expressions given by the two equations should only be used to predict the reflection coefficients for values of Ir which lie within the range used to determine empirical constants in the respective equations. This discussion also recognises in general the importance of obtaining experimental data over a wide range so that more generalised formulae can be obtained. Some of the differences observed in the two expressions for the reflection coefficient, may be due to scale effects, the model armour units being of different sizes. This appears to be the major difference in the two experimental studies and clearly implies that Equation 10 is inadequate in representing scale effects.

4.4 Porous sloping protection to vertical walls

From previous studies on vertical or steep seawalls it has been noted that a step or berm placed at, or close to, the design water level will often improve the hydraulic performance considerably. There are many instances where seawalls have been built into or at the back of a sloping beach resulting in energy dissipation due to breaking of waves before reaching the wall. Increased wave activity due to reflection at the wall will contribute to local scour, lowering the beach level and allowing waves of greater height to reach the wall. This will in turn increase wave reflection resulting in higher velocities at the sea bed leading to greater scour and sediment transport. It is in this context that sloping protection in front of vertical non-porous seawalls can be used effectively to improve its overall hydraulic performance and stability. Similarly a step or berm placed in the region of the design water level will contribute to an improvement in the hydraulic performance.

An example of protection to an existing seawall by the use of rock armour placed against it was presented by Henton (1986). The results of this study were analysed by Allsop and Hettiarachchi (1989). The reflection performance of three sections, namely, the existing section and the alternatives are presented in Figure 1, measurements having taken for three water levels.

The existing seawall (section 1) has high reflections approaching 0.9 at the higher water levels. At lower water levels the reflections are reduced to around 0.65 due to wave breaking in front of the seawall, illustrating the influence of the smooth slope. For alternative sections 2 and 3, the reflection performance varies with the water level, and in particular with the relative position of the berm formed by the crest level of the rock protection. For these water levels close to the crest level reflections are very low within the range 0.2 -0.3, illustrating clearly the influence of a berm type of structure. The reflection coefficients increase to around 0.4 when waves reflect from the armour slope.

From investigations on berm structures it is observed that Iribarren Number is not the best parameter to study the influence of berm slopes. The berm length to wave length (B/L) is found to be an appropriate parameter for such structures. The slope angle of the berm and its length are two parameters which influence the reflection performance. Influence of these parameters has to be investigated by conducting a well formulated series of experiments with the variables being the berm length, slope angle, the water level and the incident wave climate.

4.5 Armoured porous trapezoidal structures

Most investigations of wave reflection on porous sloping structures have concentrated on two dimensional cross-sections which simulate revetment type of structural forms. Very few investigations have been conducted on porous trapezoidal cross sections which not only reflect waves but also transmit waves through their porous bodies. In addition to the principal use as breakwaters in harbours, this type of structure is used as offshore breakwaters in coast

protection and in the construction of nearshore causeways. In analysing wave action on these structures it is important to consider both wave reflection and transmission performance in order to assess the wave energy dissipation.

Results from investigations on rock armoured porous trapezoidal structures conducted by Sollitt and Cross (1972), Sulisz (1985) were analysed by Hettiarachchi and Mirihagalla 1997). In both studies reflection and transmission have been measured for at least five wave periods varying from 0.7 to 2.5 secs. Although there is a certain scatter in the data, it is clearly possible to identify the general trend of the variation of the respective coefficients with the Iribarren number and the wave period. In general the wave reflection increased with increasing period and in particular for wave period of the order of 2 secs the reflection coefficients were comparatively high. The transmission coefficients too increased with wave period. Comparison of results indicate the influence of the material used in reducing permeability characteristics of the structure and the possible influence of air entrainment in the porous media which will contribute towards a decrease in transmission and increase in reflection.

As part of this investigation the experimental results of Gunbak (1979), Sollitt and Cross (1972) and Sulisz (1986) were further analysed and prediction equations were derived. All these rock armoured structures consisted of primary armour, secondary armour and the core. The seaward face of the structures covered slopes of 1:1.5 and 1:2.5. In addition the results of an investigation on a porous trapezoidal structure assembled with hollow square blocks (model COB armour units) having a front slope of 1:1 was analysed. This structural configuration had a high volumetric porosity of the order of 60%. Although wave reflections for this structure is lower it will exhibit significant transmission coefficients due to the high porosity of the structure. The respective empirical coefficients for Equation 10 which gave a good fit for the data are given in Table 3.

4.6 Field investigations on wave reflection

In comparison with laboratory investigations very few field studies have been conducted on prototype structures. Thornton and Calhoun (1972) conducted a pioneering study on wave reflection and transmission for a rubble mound breakwater in California. It was observed that reflection and transmission coefficients displayed a dependence on wave frequency, tidal stage and the incident wave amplitude.

Davidson, Bird Bullock and Huntley (1994) presented the results of an extensive field investigation on wave reflection on an offshore breakwater and a berm breakwater on the south coast of England. Results of the investigations are presented in Table 4.

The raw data showed a general trend of a decrease in wave reflection with an increase in frequency. Wave breaking on the natural beach resulted in almost negligible reflected wave energy, of the order of 4%, with no clear trend with frequency. There was a trend for wave reflection to increase with the gradient of the shoreface.

In the case of the offshore breakwater, the considerably higher values of the Iribarren Number than those reported in most laboratory experiments are mainly due to low amplitude waves acting on a relatively steep gradient of the structure (1:1.1). The results do illustrate well the trend of the data at the extreme range with the upper saturation value of the order of 0.6 to 0.65. In view of the scatter of data due to the possible influence of local water depth (tidal variations), the equations have been fitted for different depth bands.

The variation of the reflection coefficient versus the Iribarren Number for the berm breakwater displayed a similar trend to that of the offshore breakwater. The Iribarren numbers were lower due to the high energy of the incident waves and the shallower sloping shoreface. The reflection performance were dependent on the water depth over the berm. For low water depths over the berm the reflection coefficient was low and could not be related to the Iribarren number. The reflection estimates for the berm breakwater were consistently less than those obtained for the steeper offshore breakwater. More dissipative nature of the structure including the shallower shoreface slope, the dissipating effect of the berm, the positioning of concrete blocks on the berm and the influence of wave transmission over the structure near high tide would have contributed to lower reflection.

5. Conclusions and Recommendations

This study has examined the hydraulic performance of a range of coastal structures with respect to energy transformation processes. In particular attention is focused on wave reflection performance mainly due to the fact that the structures examined refer to coast protection works of the revetment/seawall type for which external transmission is not very relevant. Since low crest structures were not considered in detail, wave overtopping was not included in the analysis.

This study has reviewed the reflection performance of a wide range of structures. Types of prediction methods for wave reflection are discussed and an assessment is made of the predictive equations. The Iribarren Number is identified as a relevant variable in quantifying wave reflection on simple sloping structures. The predictive equation $Cr=a.Ir^2/(b+Ir^2)$ was found to be acceptable to describe the variation of Cr with Ir for a range of coastal structures and the degree of fitness was very satisfactory. Where possible all results have been presented within a uniform framework in which the Iribarren Number was the principal variable. However it was observed that this number was not the best parameter to study the influence of berm slopes and sloping protection to vertical walls.

From the study of the performance of porous armoured trapezoidal structures it was evident that Iribarren Number could also be used to describe the external transmission coefficients. It is recommended that further investigations be carried out in this respect.

The analysis of results from field studies have strengthened the findings of the hydraulic model studies. The recent work of Davidson, Bird, Bullock and Huntley (1994) has contributed to improved understanding of reflection performance of prototype structures and established a positive link between experimental and field results.

This study has presented reliable predictive equations for wave reflection for a range of structures used in practice. The relevance of scale effects and the influence of extrapolation outside the experimentally measured range of Ir are clearly identified. These observations recognised the importance of conducting large scale experiments in order to obtain reliable experimental data covering a wide range leading to the development of generalized formulae. Such formulae will be representative over a wide range of input parameters.

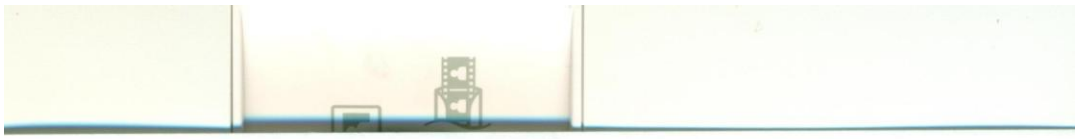

References

Allsop,N.W.H. and **Channell,A.R.** (1989) *Wave reflection in harbours : Reflection performance in rock armoured slopes in random waves*. Report OD 102, March 1989, HR Wallingford.

Allsop,N.W.H. and **Hettiarachchi S.S.L.** (1989) *Wave reflection in harbours : Design, Construction and Performance of wave absorbing structures.* Report OD 89, February 1989, HR Wallingford.

Allsop,N.W.H., McBride,M.W. and **Colombo,D** (1994) *The reflection performance of vertical walls and low reflection alternatives : Results of wave flume tests*. Paper presented to the MCS Project Workshop, Delft Hydraulics,Emmeloord, Nov.1994.

Battjes,J.A. (1974) *Surf similarity*. Proc. of the 14th Conference on Coastal Engineering, Copenhagen. Denmark.

Davidson,M.A., Bird,P., Bullock,G.N. and **Huntley,D.A.** (1994) *Wave reflection : Field measurements, analysis and theoretical developments.* Proc. Conf. Coastal Dynamics 94, ASCE, Barcelona, Spain.

Gotschenberg,A. and **Scheffer,H.J.** (1984) *Three dimensional investigations on wave reflection including irregular waves.* Paper presented at the Fourth Congress - Asian and Pacific Division, IAHR, Thailand.

Gunbak,A.R. (1979) *Rubble Mound Breakwaters*. Research Report No.1, Civil Engineering Department, University of Trondheim, Norway.

Hall,K.R. and **Hettiarachchi,S.S.L.** (1991) *Mathematical modelling of wave interaction with rubble mound breakwaters*. Proc. Conf. On Coastal Structures and Breakwaters organized by the ICE, London.Thomas Telford, London.

Henton,F.J. (1986) *Rehabilitation of a seawall using large rock.* Proc. Seminar on the Use of rock in coastal structures. HR Wallingford.

Hettiarachchi,S.S.L. (1987) *The influence of geometry on the performance of breakwater armour units.* PhD Thesis, Imperial College, University of London, May 1987.

Hettiarachchi,S.S.L. and **Holmes,P.** (1988) *Performance of single layer hollow block armour units*. Proc. Conf. Design of Breakwaters organized by the ICE, London. Thomas Telford, London.

Hettiarachchi,S.S.L. and **Mirihagalla,P.D.** (1997) *Hydraulics of wave structure interaction- Wave reflection from coast protection structures.* Research Report. University of Moratuwa.

Hettiarachchi,S.S.L. and **Mirihagalla,P.D.** (1998) *Hydraulic model investigations of rock armoured trapezoidal breakwaters.* Internal Research Report. University of Moratuwa.

Mattson,A. (1963) *Reflections of gravity waves.* Proc. of the IAHR Congress, London.

Muttray,M., **Oumeraci,H.**, **Zimmermann,C.**, and **Partenscky,H.W.** (1992) *Wave energy dissipation on and in rubble mound structures.* Chapter 110, Proc. Int. Conf. on Coastal Engineering, ASCE.

Oumeraci,H. and **Partenscky,H.W.** (1990) *Wave-induced pore pressures in rubble mound breakwaters.* Chapter 100, Proc. Int. Conf. on Coastal Engineering, ASCE.

Postma,G.M. (1989) *Wave reflection from rock slopes under random wave attack.* MSc Thesis, Delft University of Technology, Delft.

Scheffer,H.J. and **Kohlhase,S.** (1986) *Reflection of irregular waves at partially reflecting structures including oblique wave approach.* Proc. 20th Int. Conf. on Coastal Engineering, ASCE, Taiwan.

Seelig,W.N. (1983) *Wave reflection from coastal structures.* Proc. Coastal Structures-83, pp 961-973.

Seelig,W.N. and **Ahrens,J.C.** (1981) *Estimation of wave Reflection and Energy Dissipation Coefficients for Beaches, Revetments and Breakwaters.* US Army Corps of Engineers. Coastal Engineering Research Center, Fort Belvour Va.Feb.81.

Sollitt,C.K. and **Cross,R.H.** (1972) *Wave transmission through permeable breakwaters.* Proc. 13th Conference on Coastal Engineering, Canada, Ch 103, pp 1827-1846.

Stickland,I.W. (1969) *Cob Units.* Report on Hydraulic Model Research Wimpey Laboratory Reference No. H/334.

Sulisz,W. (1985) *Wave reflection and transmission at permeable breakwaters of arbitrary cross-section.* Jr. of Coastal Engineering 9 pp 371-386.

Thomas,R.S. and **Hall,B.** (1992) *Seawall Design.* CIRIA, Butterworth and Heinemann.

Thornton,E.B. and **Calhoun,H.J.** (1972) *Spectral resolution of breakwater reflected waves.* Jr. of the Waterways, Harbours and Coastal Engineering Division. Proc. of the ASCE Vol. 98.WW4 pp 443-460.

Van Der Meer,J.W. (1988) *Rock slopes and gravel beaches under wave attack.* Delft Hydraulics Communication No.396.

Wens,F., De Rouck,J. and **Van Damme,L.** (1989) *Comparative laboratory investigations on Haro, Grooved Cubes, Dolos and Tetrapods.* Research Report, Ministry of Public Works, Hydraulic Research Laboratory, Antwerp, Belgium.

TABLE 1 DAMAGE REPORTED TO SEAWALLS (Thomas and Hall 1992)

Damage reported to seawall	Number of occurrences	As percentage of all seawalls reported
Erosion of toe	63	12.3
Partial crest failure	26	5.1
Collapse/breach	16	3.1
Removal of revetment armour	19	3.7
Abrasion	16	3.0
Wash-out of fill material behind seawall	10	1.9
Concrete disintegration	9	1.7
Structural member failure	5	1.0
Landslip	5	1.0
Corrosion	3	0.6
Outflanking	3	0.6
Uplift of armouring	3	0.6
Settlement	2	0.4
Spalling of concrete	2	0.4
Damage to promenade	4	0.8
Concrete cracking	2	0.4
Total	188	36.6%

TABLE 2 STRUCTURAL CONFIGURATIONS INVESTIGATED

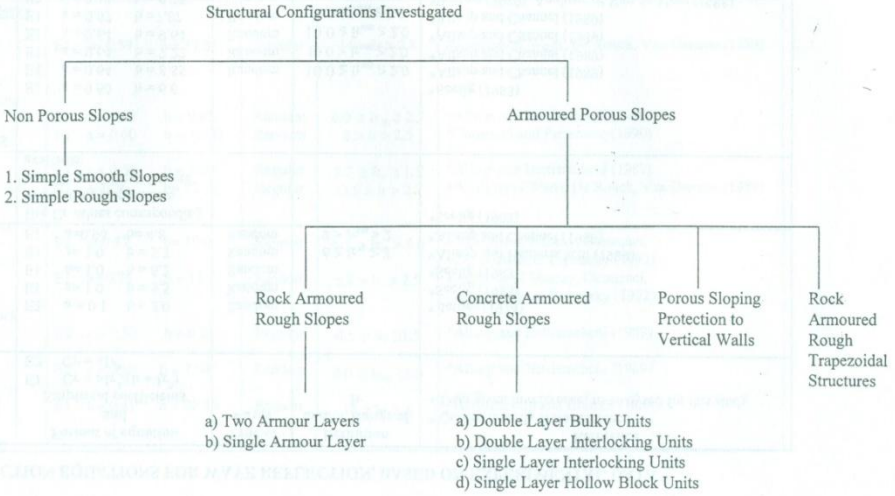

TABLE 3 PREDICTION EQUATIONS FOR WAVE REFLECTION, BASED ON EXPERIMENTAL DATA

Type of structure	Format of equation and Empirical coefficients E1 $Cr = aIr^2/(b + Ir^2)$ E2 $Cr = aIr^b$	Type of waves	Definition and/or Range of Ir	Reference * Quoted directly from reference + Data given in reference, re-analysed for this study
NON POROUS SLOPES				
Simple smooth slopes	E2 a = 0.1 b = 2.0	Random		*Battjes (1974)
	E1 a= 1.0 b = 5.5	Random		*Seelig (1983)
	E1 a= 1.0 b = 6.2	Random		*Seelig (1983)
	E1 a= 1.0 b = 5.7	Random	$6 \geq Ir_{op} \geq 3$	*Allsop and Hettiarachchi (1989)
	E1 a=0.96 b= 4.8	Random	$9 > Ir_{om} > 2$	*Allsop and Channel (1989)
Simple rough slopes	Use Cr values corresponding to a smooth slope unless specific model test data are available			*Seelig (1983)
ARMOURED POROUS SLOPES				
Rock armoured slopes				
Preliminary estimate	E1 a = 0.60 b = 6.6			*Seelig (1983)
Rock armour (2 layer)	E1 a = 0.64 b = 8.85	Random	$10.0 \geq Ir_{om} \geq 2.0$	*Allsop and Channel (1989)
Rock armour (1 layer)	E1 a = 0.64 b = 7.22	Random	$10.0 \geq Ir_{om} \geq 2.0$	*Allsop and Channel (1989)
Large rock (2 layer)	E1 a = 0.64 b = 9.64	Random	$10.0 \geq Ir_{om} \geq 2.0$	*Allsop and Channel (1989)
Large rock (1 layer)	E1 a = 0.67 b =7.87	Random	$10.0 \geq Ir_{om} \geq 2.0$	*Allsop and Channel (1989)
Rock armour	E2 a = 0.14 b = 0.73	Random	Ir_{op}	*Postma (1989), Analysis of Van de Meer (1988)
Rock armour	E2 a = 0.125 b = 0.73	Random	$9 > Ir_{op} > 2$	*Postma(1989), Analysis of Allsop and Channel (1989)

TABLE 3 contd....

Type of structure	Format of equation and Empirical coefficients E1 $Cr = aIr^2/(b + Ir^2)$ E2 $Cr = aIr^b$	Type of waves	Definition and/or Range of Ir	Reference * Quoted directly from reference + Data given in reference, re-analysed for this study
Concrete armoured slopes				
Double layer bulky				
Haro and Cube	E1 a= 0.59 b = 17.21	Regular	$14 > Ir > 2.8$	+Analysis of Wens, De Rouck, Van Damme (1989)
Double layer interlocking				
Tetrapod and Stabits	E1 a = 0.48 b = 9.62	Random	$6.0 \geq Ir_{op} \geq 2.5$	*Allsop and Hettiarachchi (1989)
Tetrapod	E1 a = 0.60 b = 12.00	Random	$8 > Ir > 2.5$	*Oumeraci and Partenscky(1990)
Dolos	E1 a = 0.56 b = 10.0	Regular	$5.5 \geq Ir_o \geq 1.5$	*Allsop and Hettiarachchi (1989)
Tetrapods and Dolos	E1 a=0.56 b= 22.32	Regular	$13.8 > Ir > 2.7$	+Analysis of Wens, De Rouck, Van Damme (1989)
Single layer interlocking				
Accropode	E1 a=0.82 b= 10.0	Regular	$6.1 > Ir_{sp} > 3.0$	+Analysis of Murray, Oumeraci, Zimmerman & Partensky (1992)
Accropode	E1 a= 0.79 b = 11.37	Random	$6.4 > Ir_s > 2.5$	+Analysis of Murray, Oumeraci, Zimmerman & Partensky (1992)
Single layer hollow block				
Cob	E1 a = 0.50 b = 6.54	Regular	$4.5 \geq Ir_o \geq 1.5$	*Allsop and Hettiarachchi (1989)
Shed and Diode	E1 a = 0.49 b = 7.94	Random	$6.0 \geq Ir_{op} \geq 3.0$	*Allsop and Hettiarachchi (1989)
Cob, Shed, Seabee and Hollow Block	E1 a = 0.41 b = 22.20	Regular	$16 \geq Ir_s \geq 4$	*Hettiarachchi and Holmes (1988)

TABLE 3 contd....

Type of structure	Format of equation And Empirical coefficients E1 $Cr = aIr^2/(b + Ir^2)$ E2 $Cr = aIr^b$	Type of waves	Definition and/or Range of Ir	Reference * Quoted directly from reference + Data given in reference, re-analysed for this study
ARMOURED POROUS TRAPEZOIAL STRUCTURES				
Rock armoured structures				
	E1 a = 0.57 b = 9.15	Regular	7 > Ir > 1.2	+Analysis of Gunbak (1979)
	E1 a = 0.40 b = 11.60	Regular	16 > Ir > 2	+Analysis of Sollit and Cross(1972)
	E1 a = 0.62 b = 21.71	Regular	9.5 > Ir >2.5	+Analysis of Sulisz (1985)
	E1 a = 0.65 b = 10.06	Regular	5 > Ir > 2	+Analysis of Hettiarachchi and Mirihagalla (1998)
Porous trapezoid consisting of hollow square blocks (Cobs)	E1 a = 0.40 b = 18.23	Regular	15 > Ir > 5.2	+Analysis of Hettiarachchi (1987)

TABLE 4 PREDICTION EQUATIONS FOR WAVE REFLECTION, BASED ON FIELD INVESTIGATIONS

Type of structure	Format of equation and empirical coefficients E1 $Cr = aIr^2/(b + Ir^2)$ E2 $Cr = aIr^b$	Type of waves	Depth range	Range of Ir	Reference
Rock armoured offshore breakwaters (*Gradient of the seaward face of the structure 1:1.1 fronted by a shallow sloping beach 1:50*)	E1 a = 0.65 b = 25 E1 a= 0.60 b = 35 E1 a= 0.64 b = 80	Random	d > 3.25 m 3.1 m ≥d ≥ 2.5 m 2.5 m > d	35 > Ir > 8 35 > Ir > 8 50 > Ir > 8	*Davidson,Bird, Bullock and Huntley (1994)
Berm breakwater (*Energy dissipation taking place on smooth impermeable slope of granite blocks (1:6) stretching seawards to a horizontal berm*)	E1 a = 0.42 b = 2.0	Random	d > 3.0 m	4.2 > Ir > 0.8	*Davidson, Bird, Bullock and Huntley (1994)

Note: * Quoted directly from reference
+ Data given in reference, re-analysed for this study

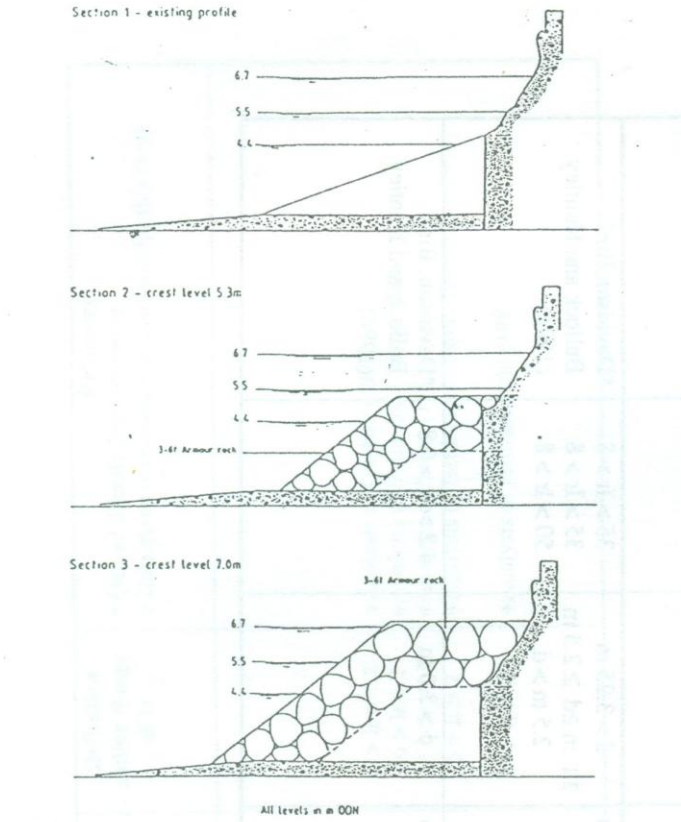

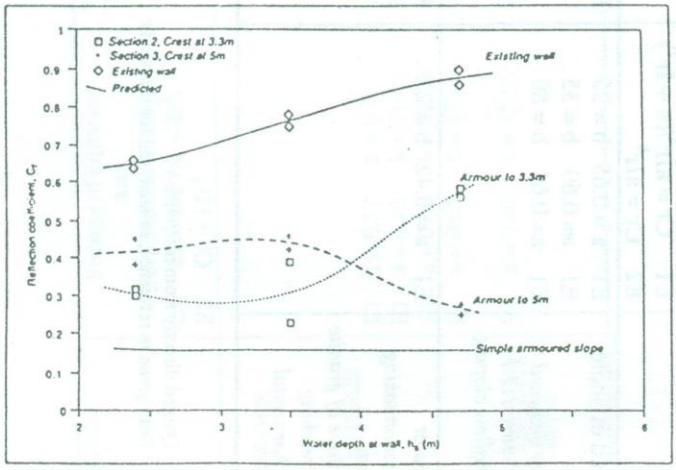

FIGURE 1
Reflection performance of rock protection to existing seawall

Allsop and Hettiarachchi (1989)

A SURFACE SOURCE SINGULARITY MODEL FOR TIME AVERAGED FLOW AROUND CYLINDRICAL STRUCTURES

A. G. T. Sugathapala
Dept. Mechanical Engineering, University of Moratuwa.

A SURFACE SOURCE SINGULARITY MODEL FOR TIME-AVERAGED FLOW AROUND CYLINDRICAL STRUCTURES

A. G. T. Sugathapala
Dept. Mechanical Engineering, University of Moratuwa.

ABSTRACT

A simple method of solution to the problem of two-dimensional separated flow around multiple-body circular cylindrical structures is presented. The method is applied to the case of two identical cylinders where the free-stream direction is perpendicular to the line joining the centers. The effect of the bodies and their wakes on the outer potential flow is modelled by surface source distributions over the front wetted surfaces. The flow in the wakes, generated by the source distributions, is ignored. The condition of the zero normal velocity is applied over the front surface to obtain an integral equation for the source strength. This equation is solved with the condition of finite velocities at the separation points to find the unknown source strength distribution and the positions of the separation points. The pressure distribution on the front wetted surface is then calculated through Bernoulli's equation. The pressure distribution on the rear surface exposed to the wake is assumed to be determined by the separation values. The effects of the distance between the bodies on the flow pattern, position of the separation points, wake under-pressure and the resultant forces are analysed. The most significant feature of the present flow model is that no empirical parameters are needed for the analysis. The empirical parameters used in other models, the back pressure coefficient and the positions of the separation points, can be predicted through the present model.

INTRODUCTION

Analysis of flow around and forces on bluff bodies is an important applied fluid mechanics problem. Aerodynamics of buildings and structures, hydrodynamics of under-water structures, flow around heat exchanger tube arrays are few examples. The flow around a bluff body at high Reynolds numbers is characterized by extensive boundary layer separation and formation of a broad wake behind the body. The boundary of the separated flow (so-called free shear layer) is thin and usually quite steady within a certain distance down stream of the separation points. The pressure in this near-wake region is approximately constant and lower than the free stream pressure. The body surface exposed to the wake is subjected to this uniform wake under-pressure. Further downstream the separated shear layers become unstable and roll up to form large scale eddies (vortices). This far-wake region is unsteady and highly turbulent. Therefore, even for steady on-coming flow, the resultant flow around a bluff body is unsteady. The body is then acted upon by time-dependent pressure loads. The mean forces are of particular interest and can be determined by averaging over a time much larger than the characteristic period of the unsteady flow (the vortex shedding periods). As a result of the wake under-pressure, the time-averaged mean forces acting on bluff bodies are relatively high and are mainly due to the non-symmetrical pressure distribution. At high Reynolds numbers contribution of the viscous forces is negligible.

Considerable progress has been made in the analysis of the flow past bluff bodies through the numerical solution of the complete Navier-Stokes equations. However results are restricted to laminar flow at low Reynolds numbers. Extensions to higher Reynolds numbers involve excessive computing time and suffers from uncertainties in turbulent modelling. A simple alternative approach is to utilize an inviscid flow

model that represents the important characteristics of the real flow. In fact the outer-flow region as well as the near-wake region could be considered as inviscid and irrotational (potential) and it is possible to model the outer flow and the pressure distribution on the body accurately by potential flow models. However, all such models involve empirical parameters, such as positions of the separation points and back pressure coefficient (which determines the wake under-pressure), since the separation of flow and formation of wake are governed by the viscous properties of the fluid and can not be expected to be modelled completely by inviscid approximations. The existing models for time-averaged mean flow around bluff bodies are briefly reviewed in the next section.

Almost all the existing bluff body potential flow models are limited to the case of flow around an isolated body. However in most of the practical applications fluid flow takes place around multiple bluff bodies (or a body near a solid wall), where the interaction between them are important. Another important application is model testing in wind tunnels where the flow takes place within a confined space. Analysis of such a flow problem is difficult since the phenomenon of flow separation and the interaction of bodies and wakes are very complicated.

The main purpose of this paper is to introduce a relatively simple potential flow model which can be applied to treat the flow around multiple-body circular cylindrical structures where the bodies are not in the wake regions of the others. A simple example of such a problem is that of the flow about two identical cylinders. In the case considered, the free stream direction is assumed to be perpendicular to the line joining the centers. The proposed method is an extension of the surface source singularity model presented by Hess (1973) for the case of flow past a circular cylinder. The effect of bodies and their wakes on the outer-flow is modelled by source distributions on the front wetted surfaces. The source strength distribution and the position of the separation points are determined by appropriate boundary and flow conditions, for a given distance between the centers. Prediction of the flow pattern, the pressure and velocity distributions are then straightforward. No empirical parameters are needed for the model and both positions of the separation points and back pressure coefficients can be predicted.

POTENTIAL FLOW MODELS

The salient features of uniform flow around long bodies of constant cross-sections suggests the possibility of modelling the time-averaged flow quantities such as velocity and surface pressure distribution using two-dimensional and incompressible potential flow models. These models basically fall into the following three categories:

(*a*) free-streamline models using conformal mapping,
(*b*) surface singularity models,
(*c*) free-streamline models with surface and wake singularities.

In each of these models back pressure coefficient is introduced as a free parameter (as well as the position of the separation points in the case of continuously curved body) in order to account for the essential features of a complicated process of viscous dissipation in the wake, and to replace the real wake flow by a simplified

model within the frame work of the potential theory. These flow models do not provide a good description of the far-wake region at all, and the validity will have to be justified by their agreement with experimental observation of the actual flow field near the body.

In the models under category (*a*), the free-streamlines (or surface of discontinuity in velocity) are taken as the idealization of the separating shear layers. In conventional models the shape of these lines are determined by a series of conformal transformations of complex velocity and complex potential planes to the physical plane, and thereby velocity and pressure distributions in the outer-flow regime are calculated (Wu 1972). More simplified modelling method was presented by Parkinson and Jandali (1970), where a circular cylinder in a transformation plane was used instead of complex velocity and complex potential planes. Calculation of the flow field around the circle is simple and the conformal transformation of the circle to the body shape in the physical plane results in the required solution. This method has been extended and applied successfully for the flow around a number of bluff body shapes (Yeung & Parkinson 1997). In general, all these methods are limited to two-dimensional flow around a few standard bluff body shapes (such as circular cylinder, flat plate) because the conformal mapping technique depends on knowing suitable transformations.

In the method of surface singularity modelling, the body surface is replaced by a distribution of flow singularities (sources or vortices). The strength of the singularity varies over the surface such that at every point on the boundary a prescribed boundary condition is satisfied. Comprehensive reviews of these methods were presented by Hess & Smith (1966) on surface source models and by Lewis (1981) on surface vortex models. A large class of solutions for potential flow around bodies (including multiple-body configurations) can be generated by this indirect method of solution. However, relatively few works deal with the problem of separated flow past bluff bodies. One such method is the model presented by Hess (1973), where only the front wetted surface of the body is replaced by a continuous source distribution. The flow from the source distribution models the effect of the wake on the outer potential flow. The most significant result of this model is that it gives the separation angle for the circular cylinder at 77.45° from the front stagnation point (which is close to the separation point for laminar boundary layer flow) and a back pressure coefficient of -0.96. In all the other models these two quantities are taken as free parameters. This model was extended by the present author by adding a down-stream sink to close the wake (Sugathapala 1996). Different positions of the sink correspond to different back pressure coefficients, thus permitting a wide range of solutions. The main contribution of this closed wake model is its application to unsteady flow. An open wake model gives infinite potential at the far field in the case of unsteady flow, which is physically inadmissible.

Free-streamline models with surface and wake singularities assume that the vorticity in the wake is concentrated in relatively thin shear layer so that the rotational wake can be modelled by pair of vortex sheets. The body surface too is replaced by a vortex (or source) distribution. The position of the vortex sheets (wake shape) is calculated by an iterative procedure. It is possible to extend this method to incorporate the influence of boundary layer displacement effects, viscous diffusion

and dissipation of the wake vorticity and other important features in the real wake (Mukherjea & Bandyopadhyay 1990).

SURFACE SINGULARITY MODEL FOR FLOW AROUND TWO CYLINDERS

Formulation of the Problem

Consider two-dimensional, incompressible flow, uniform at infinity, past two identical circular cylinders in parallel. The free-stream direction is assumed to be perpendicular to the plane of the axes of the cylinders. Let the radius of the cylinders be R, distance between centers be H and the free-stream velocity be U.

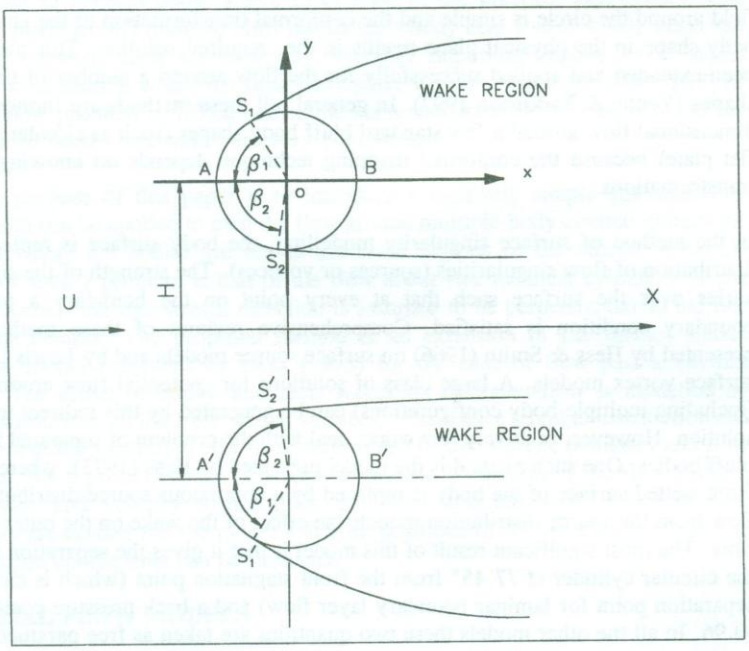

Figure (1) : Two Identical Cylinders in a Uniform flow.

The flow configuration and the selected coordinate axis system are shown in Figure (1). The effect of the bodies on the on-coming flow is modelled by source distributions over the front surfaces S_1AS_2 and $S_1'A'S_2'$ where the flow is attached. Flow from each source distribution occupies a semi-infinite region of finite width behind the corresponding body, which represents the shape of the wake. The separating shear layers in the real flow are assumed to be represented by the boundary of the source flow (free streamlines) and the flow inside the wake is ignored. The resulting flow is symmetrical about the X-axis, hence the source distributions on the two cylinders are identical. The strength of the source distribution $Q(\theta)$ per unit length and the positions of the separation points β_1 and β_2 can be

determined by the Neumann boundary condition of zero normal velocity on the surface of a cylinder and a condition that the tangential velocities are finite at the separation points.

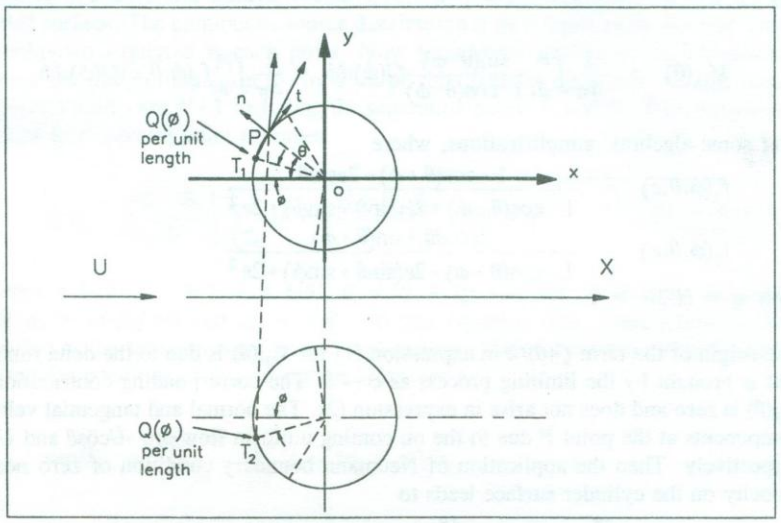

Figure (2) : Surface Source Distributions on Cylinders.

The velocities at the surface point P, induced by the source elements at the point T_1 on the same cylinder and the point T_2 on the other cylinder are given by the expressions

$$\delta V_1 = \frac{RQ(\phi)d\phi}{4\pi}\frac{\mathbf{T_1P}}{T_1P^2}$$

and

$$\delta V_2 = \frac{RQ(\phi)d\phi}{4\pi}\frac{\mathbf{T_2P}}{T_2P^2}$$

where,

$$\mathbf{T_1P} = R(\cos\phi - \cos\theta)\mathbf{i} - R(\sin\phi - \sin\theta)\mathbf{j}$$

and

$$\mathbf{T_2P} = R(\cos\phi - \cos\theta)\mathbf{i} + [H + R(\sin\phi + \sin\theta)]\mathbf{j}$$

with respect to the coordinate axis system x-y, $\mathbf{i}$ and $\mathbf{j}$ are the corresponding unit vectors and $-\beta_2 \le \phi \le \beta_1$, $-\beta_2 \le \theta \le \beta_1$ (see Figure (2)). The unit normal outward from the cylinder and the tangential vectors at P are

$$\mathbf{n} = -\cos\theta\mathbf{i} + \sin\theta\mathbf{j} \quad \text{and} \quad \mathbf{t} = \sin\theta\mathbf{i} + \cos\theta\mathbf{j}, \text{ respectively.}$$

Hence the normal and tangential velocities induced by the source elements are given by

$$\delta V_n = \mathbf{n}.\delta\mathbf{V_1} + \mathbf{n}.\delta\mathbf{V_2} \quad \text{and} \quad \delta V_t = \mathbf{t}.\delta\mathbf{V_1} + \mathbf{t}.\delta\mathbf{V_2}, \text{ respectively.}$$

After substituting above expressions, the resultant normal and tangential velocities at the point P due to the source distributions on the two cylinders can be evaluated by

integrating over the front wetted surfaces, as

$$V_{Qn}(\theta) = \frac{Q(\theta)}{2} + \frac{1}{4\pi}\int_{-\beta_2}^{\beta_1} Q(\phi)d\phi + \frac{1}{4\pi}\int_{-\beta_2}^{\beta_1} f_1(\phi,\theta,e)Q(\phi)d\phi \quad (1)$$

and

$$V_{Qt}(\theta) = \frac{1}{4\pi}\int_{-\beta_2}^{\beta_1} \frac{\sin(\theta-\phi)}{1-\cos(\theta-\phi)} Q(\phi)d\phi + \frac{1}{4\pi}\int_{-\beta_2}^{\beta_1} f_2(\phi,\theta,e)Q(\phi)d\phi \quad (2)$$

after some algebraic simplifications, where

$$f_1(\phi,\theta,e) = \frac{1-\cos(\theta+\phi)+2e\sin\theta}{1-\cos(\theta+\phi)+2e(\sin\theta+\sin\phi)+2e^2}, \quad (3)$$

$$f_2(\phi,\theta,e) = \frac{2e\cos\theta+\sin(\theta+\phi)}{1-\cos(\theta+\phi)+2e(\sin\theta+\sin\phi)+2e^2} \quad (4)$$

with $e = H/2R > 1$.

The origin of the term $Q(\theta)/2$ in expression (1) for $V_{Qn}(\theta)$ is due to the delta function that is brought by the limiting process as $\phi \to \theta$. The corresponding contribution on $V_{Qt}(\theta)$ is zero and does not arise in expression (2). The normal and tangential velocity components at the point P due to the on-coming uniform flow are $-U\cos\theta$ and $U\sin\theta$ respectively. Then the application of Neumann boundary condition of zero normal velocity on the cylinder surface leads to

$$2\pi\sigma(\theta) + \int_{-\beta_2}^{\beta_1} \sigma(\phi)d\phi + \int_{-\beta_2}^{\beta_1} f_1(\phi,\theta,e)\sigma(\phi)d\phi = \cos\theta, \quad (5)$$

where $\sigma(\theta) = Q(\theta)/4\pi U$ is the non-dimensional source distribution. This is a Fredholm integral equation of the second kind for the source distribution $\sigma(\theta)$. In general there is no difficulty of solving this equation for given β_1, β_2 and e, but a complete analytical solution is not possible since the kernel of the second integral depends on both ϕ and θ, and is not a simple function. Furthermore, a direct numerical solution too is not possible since the limits of the integration β_1 and β_2 (separation angles) are unknowns and have to be determined by some other considerations. It can be shown that at separation points as $\theta \to \beta_1$ and $\theta \to -\beta_2$, $V_{Qt}(\theta) \to \infty$ (see equation (2)), which is physically inadmissible, unless

$$\sigma(\beta_1) = 0 \quad \text{and} \quad \sigma(-\beta_2) = 0, \quad (6)$$

respectively. Substitution of these expressions into equation (5) leads to the expressions required to find the location of separation points, as

$$\cos\beta_1 = \int_{-\beta_2}^{\beta_1} [1 + f_1(\phi,\beta_1,e)]\sigma(\phi)d\phi \quad (7)$$

and

$$\cos\beta_2 = \int_{-\beta_2}^{\beta_1} [1 + f_1(\phi,-\beta_2,e)]\sigma(\phi)d\phi. \quad (8)$$

Now the complex fluid mechanics problem has reduced to a relatively simple mathematical problem of solving equations (5), (7) and (8) for $\sigma(\theta)$, β_1 and β_2, together with the conditions given in the equation (6), where $-\beta_2 \le \theta \le \beta_1$. Once these equations have been solved, calculations of the velocity and pressure field in the outer flow regime, pressure distribution on the wetted surface and the streamline patterns are straightforward.

Numerical Method of Solution

In the present analysis the solution of equation (5) is obtained numerically by the selection of a sufficient number of equi-spaced pivotal points distributed over the front wetted surface. The continuous source distribution is then replaced by discrete sources of unknown strengths at each point. Now trapezoidal integration is introduced to replace the integral equation (5) by a set of simultaneous equations. Let the number of pivotal points are $N+1$ including the separation points S_1 and S_2. Then equation (5) applied to i^{th} pivotal point becomes

$$2\pi\sigma_i + \left(\frac{\beta_1+\beta_2}{N}\right)\sum_{j=1,j\neq i}^{N-1}\sigma_j + \left(\frac{\beta_1+\beta_2}{N}\right)\sum_{j=1}^{N-1} f_1(\phi_j,\theta_i,e)\sigma_j = \cos\theta_i , \qquad (9)$$

where $i = 1, 2, \ldots, N\text{-}1$, $\sigma_i = \sigma(\theta_i)$, $\theta_i = -\beta_2 + (\beta_1+\beta_2)i/N$, $\phi_j = -\beta_2 + (\beta_1+\beta_2)j/N$ with $\sigma_0 = \sigma(-\beta_2)=0$ and $\sigma_N = \sigma(\beta_1)=0$ (see equation (6)). Application of above equation to the separation points at $i = 0$ and $i = N$ leads to the conditions required to find the positions of the separation points as

$$\cos\beta_1 = \left(\frac{\beta_1+\beta_2}{N}\right)\sum_{j=1}^{N-1}[1+f_1(\phi_j,\beta_1,e)]\sigma_j \qquad (10)$$

and

$$\cos\beta_2 = \left(\frac{\beta_1+\beta_2}{N}\right)\sum_{j=1}^{N-1}[1+f_1(\phi_j,-\beta_2,e)]\sigma_j . \qquad (11)$$

Note that these equations are equivalent to equations (7) and (8), respectively. Equation (9) represents N-1 number of linear equations for N-1 number of unknowns $\sigma_1, \sigma_2, \ldots, \sigma_{N-1}$ in the matrix form

$$[A_{ij}][\sigma_j] = [K_i], \qquad (12)$$

where $i, j = 1, 2, \ldots, N\text{-}1$.

An iteration procedure is employed to solve equations (10), (11) and (12). For a given value of e, equation (12) is solved for σ_j based on the method of LU factorization with assumed values for β_1 and β_2. Substitution of σ_j in equations (10) and (11) gives better approximations for β_1 and β_2. This procedure is performed till the solutions converge to the correct values with required accuracy. Since equation (5) is a Fredholm integral equation of the second kind, the diagonal elements of the coefficient matrix $[A_{ij}]$ are predominant. As a result the efficiency of the iteration process is high and has a rapid convergence. As an example, for almost entire range of values of e, the solutions converge in less than 10 iterations when $N=500$ with 0.001% accuracy. Only when e is very close to 1.0 (approximately $e<1.1$) the solution does not converge within 100 iterations. Anyway in most of the practical applications e is not very close to 1.0.

The change in the positions of the separation points with e is presented in Figure (3). It can be seen that as e decreases, β_1 decreases and β_2 increases which result in an

angular shift of the near-wake regions away from each other. When $e \gg 1$, both β_1 and β_2 approaches to 77.45°, the value corresponds to the isolated circular cylinder. The source distribution for the case $e = 1.5$ is given in Figure (4).

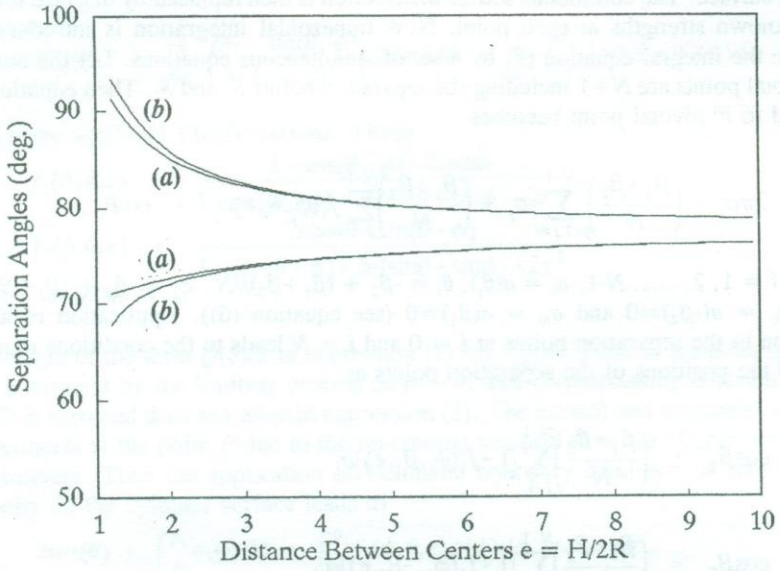

Figure (3) : Position of the Separation Points: (*a*)-Approximate Analytical Solution; (*b*)-Numerical Solution.

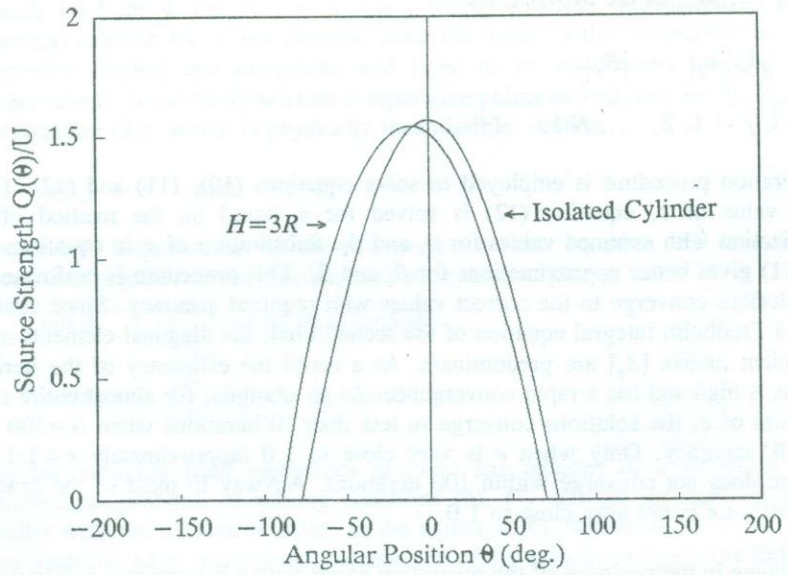

Figure (4) : Source Distribution on the Cylinder.

Approximate Analytical Solution

In the early stages of the present work, the author attempted to solve the integral equation (5) analytically, but failed to obtain a complete solution. However an approximate solution is possible, which closely agrees with the numerical result, especially when $e > 2$. This analytical work is reproduced in this section, as it will confirm the validity of the numerical results. In addition, the analysis will give a better insight into the problem and such analytical work will be useful as an academic exercise.

The main difficulty of obtaining an analytical solution to the integral equation (5) is the functional form of the kernel $f_1(\phi,\theta,e)$ of the second integral, given in equation (3). There the parameter $e = H/2R > 1$ and, in general, $f_1(\phi,\theta,e)$ is of order $\delta = 1/e < 1$. Hence one possible alternative approach in attempting an approximate solution is to expand $f_1(\phi,\theta,e)$ as a power series of δ and keep only the significant order terms, as

$$f_1(\phi,\theta,\delta) = \frac{2\delta\sin\theta + \delta^2[1-\cos(\theta+\phi)]}{2 + 2\delta(\sin\theta+\sin\phi) + \delta^2[1-\cos(\theta+\phi)]}$$
$$= \delta\sin\theta + \frac{1}{2}\delta^2[\cos(2\theta) - \cos(\theta-\phi)] + O(\delta^3). \quad (13)$$

The source distribution too may be expanded as a power series of δ in the form

$$\sigma(\theta) = \sigma_0(\theta) + \delta\sigma_1(\theta) + \delta^2\sigma_2(\theta) + O(\delta^3). \quad (14)$$

Substitution of expansions (13) and (14) in equation (5) leads to the following integral equations

$$2\pi\sigma_0(\theta) + \int_{-\beta_2}^{\beta_1}\sigma_0(\phi)d\phi = \cos\theta \quad (15)$$

$$2\pi\sigma_1(\theta) + \int_{-\beta_2}^{\beta_1}\sigma_1(\phi)d\phi = -\sin\theta\int_{-\beta_2}^{\beta_1}\sigma_0(\phi)d\phi \quad (16)$$

$$2\pi\sigma_2(\theta) + \int_{-\beta_2}^{\beta_1}\sigma_2(\phi)d\phi = -\sin\theta\int_{-\beta_2}^{\beta_1}\sigma_1(\phi)d\phi + \frac{1}{2}\int_{-\beta_2}^{\beta_1}[\cos(\theta-\phi)-\cos(2\theta)]\sigma_0(\phi)d\phi \quad (17)$$

correspond to the terms of O(1), O(δ) and O(δ^2), respectively.

Each of these equations is a Fredholm integral equation of the second kind and is of the simplest form. The solution to equation (15) is direct and given by

$$\sigma_0(\theta) = \frac{(\cos\theta - c_0)}{2\pi}, \quad (18)$$

where $c_0 = (\sin\beta_1 + \sin\beta_2)/(2\pi + \beta_1 + \beta_2)$. Equation (16) is solved after substituting for $\sigma_0(\theta)$ from (18), and the result is

$$\sigma_1(\theta) = -\frac{(c_1 + c_0\sin\theta)}{2\pi}, \quad (19)$$

where $c_1 = c_0(\cos\beta_1 - \cos\beta_2)/(2\pi + \beta_1 + \beta_2)$.

Similarly solution to equation (17) can be obtained, but in a more complicated form, as

$$\sigma_2(\theta) = a_0 + a_1\cos\theta + a_2\cos(2\theta) + b_1\sin\theta , \qquad (20)$$

where a_0, a_1, a_2, and b_1 are some known functions of β_1 and β_2. Same procedure may be adopted to derive expressions for other higher order terms but they are getting more and more complicated in form. Now substitution of above expressions in (14) gives the source distribution as a function of β_1, β_2 and δ. Then β_1 and β_2 can be calculated by the use of the conditions stated in expression (6) as

$$\cos\beta_1 = c_o+\delta(c_1+c_0\sin\beta_1) - \delta^2[a_0+a_1\cos\beta_1+a_2\cos(2\beta_1)+b_1\sin\beta_1] \qquad (21)$$

and

$$\cos\beta_2 = c_o-\delta(c_1 - c_0\sin\beta_2) - \delta^2[a_0+a_1\cos\beta_2+a_2\cos(2\beta_2)+b_1\sin\beta_2], \qquad (22)$$

up to order δ^2.

A simple iterative process is adopted to find the solutions to equations (21) and (22) for β_1 and β_2, at a given value of δ and the results are presented in Figure (3). The comparison with the numerical results shows that the approximate analytical method gives satisfactory results except in the range $\delta > 0.5$ (i.e. $e<2$) in which other higher order terms are needed for more accurate results.

Note that for the corresponding flow around an isolated cylinder, $\delta = 0$ (i.e. $e\to\infty$) equations (21) and (22) simplify to $\tan\beta = \beta + \pi$, where $\beta = \beta_1 = \beta_2$, for which the solution is $\beta \approx 77.45°$. The corresponding source distribution is given by $\sigma(\theta) = (\cos\theta - \cos\beta)/2\pi$ and is plotted in Figure (4).

SURFACE PRESSURE DISTRIBUTION AND FORCES

The pressure distribution in the flow external to the bodies and their wakes as well as on the front wetted surface of the bodies follow from the knowledge of the velocity field, given by the expression

$$C_p = \frac{p - p_0}{\frac{1}{2}\rho U^2} = 1 - \left(\frac{V}{U}\right)^2, \qquad (23)$$

where C_p is the pressure coefficient, p_0 is the free-stream pressure and V is the magnitude of the velocity at the point of consideration. Both uniform flow and the source distributions contribute to the velocity V and can be calculated for a known source distribution $\sigma(\theta)$. On the wetted surface of the cylinder $V = V_T(\theta) = U\sin\theta + V_{Qt}(\theta)$, where $-\beta_2 \le \theta \le \beta_1$ and $V_{Qt}(\theta)$, given in expression (2), is the contribution of the source distributions. Substitution of this expression in (23) leads to the surface pressure distribution as

$$C_p(\theta) = 1 - \left[\int_{-\beta_2}^{\beta_1}\left\{\frac{\sin(\theta-\phi)}{1-\cos(\theta-\phi)} + f_2(\phi,\theta,e)\right\}\sigma(\phi)d\phi\right]^2. \qquad (24)$$

Now the pressure coefficient at the separation points S_1 and S_2, which determine the pressure distribution in the near-wake, are given by $C_{pb1} = C_p(\beta_1)$ and $C_{pb2} = C_p(-\beta_2)$, respectively. Variation of these quantities with e is given in Figure (5).

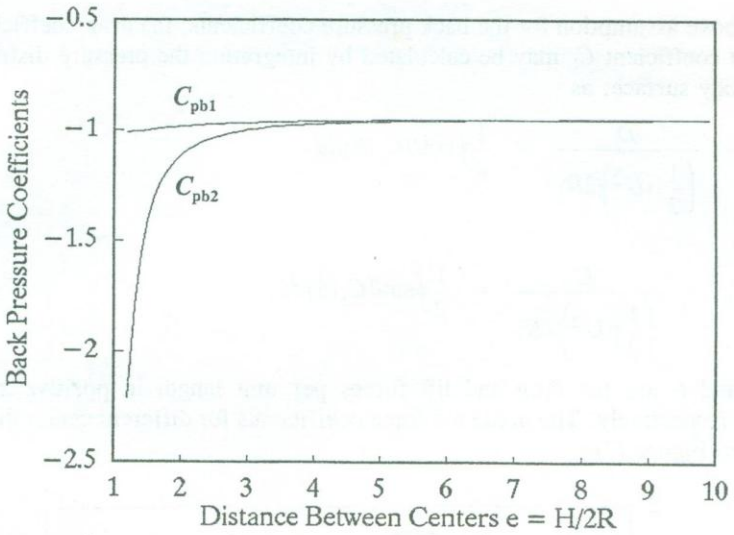

Figure (5) : Variation of Back Pressure Coefficients.

For an isolated cylinder ($e\to\infty$) $C_{pb1} = C_{pb2} = -0.95$, and for case of two cylinders both C_{pb1} and C_{pb2} are lower, resulting higher forces. The change in C_{pb1} is not very significant but C_{pb2} shows very high suction (between the cylinders) as $e\to1$. Since $C_{pb1} \neq C_{pb2}$ the pressure in the near-wake is not uniform which gives rises to some difficulty in predicting pressure loading on the rear surface of the cylinder exposed to the wake. It cannot be expected to predict this variation through potential flow modelling and some empirical information is needed for further calculations, especially to predict the forces. In the present analysis the back pressure coefficient $C_{pb}(\theta)$ is assumed to be varied linearly from C_{pb1} at $\theta=\beta_1$ to C_{pb2} at $\theta=-\beta_2$. For an example, pressure distributions on the cylinder for the case $e=1.5$ and for the case of an isolated cylinder are presented in Figure (6).

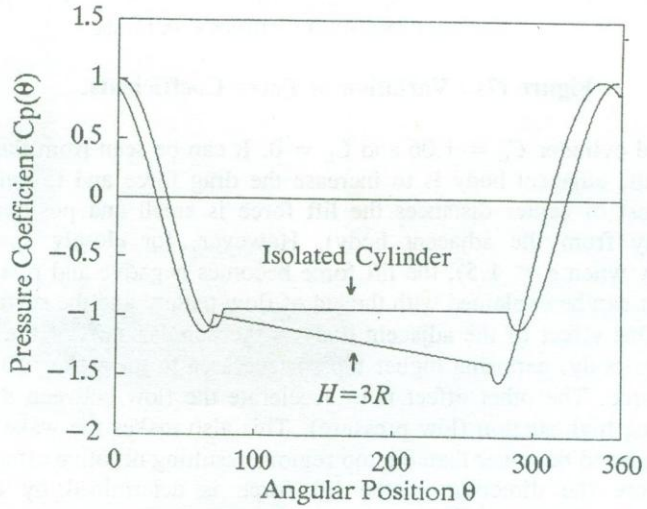

Figure (6) : Pressure Distribution on the Cylinder.

With the above assumption for the back pressure coefficients, the drag coefficient C_D and the lift coefficient C_L may be calculated by integrating the pressure distribution over the body surface, as

$$C_D = \frac{D}{\left(\frac{1}{2}\rho U^2\right)(2R)} = \frac{1}{2}\oint \cos\theta\, C_p(\theta)\, d\theta$$

and

$$C_L = \frac{L}{\left(\frac{1}{2}\rho U^2\right)(2R)} = \frac{1}{2}\oint \sin\theta\, C_p(\theta)\, d\theta,$$

where D and L are the drag and lift forces per unit length in positive x and y directions, respectively. The predicted force coefficients for different center distances are given in Figure (7).

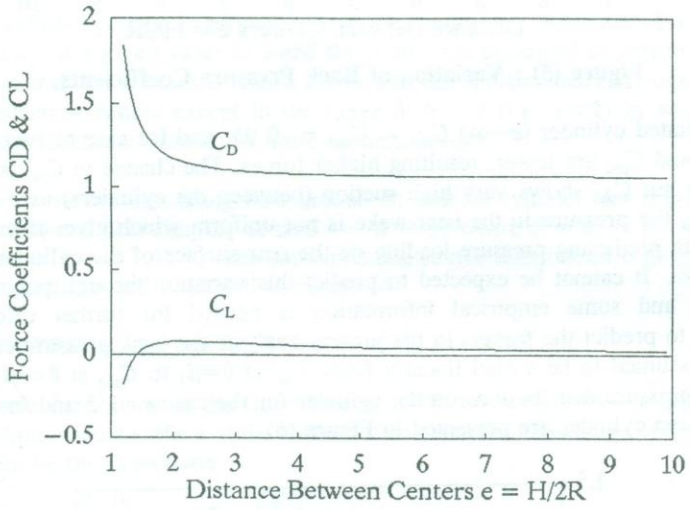

Figure (7) : Variation of Force Coefficients.

For an isolated cylinder $C_D = 1.06$ and $C_L = 0$. It can be seen from the Figure (7) the effect of the adjacent body is to increase the drag force and to generate a lift force. For most of center distances the lift force is small and positive (i.e. in a direction away from the adjacent body). However, for closely spaced bodies (approximately when $e < 1.5$), the lift force becomes negative and relatively high. This behaviour can be explained with the aid of flow pattern and the surface pressure distribution. One effect of the adjacent body is the angular shift of the near-wake, away from that body, exposing higher top surface area to the wake. This results in positive lift force. The other effect is to accelerate the flow between the cylinders thereby creating high suction (low pressure). This also makes the wake pressure in the bottom region to be lower than the top region, resulting negative effect on the lift force. Therefore the direction of the lift force is determined by the relative magnitudes of these two contributions.

PATTERN OF FLOW

Kinematic aspects of the flow (streamline pattern) is also important and will give a better qualitative understanding of the problem. Consider a point $P(x,y)$ in the outer flow field. The position of P relative to the source elements at T_1 and T_2 are represented in polar coordinates by (r_1, θ_1) and (r_2, θ_2), as shown in Figure (8).

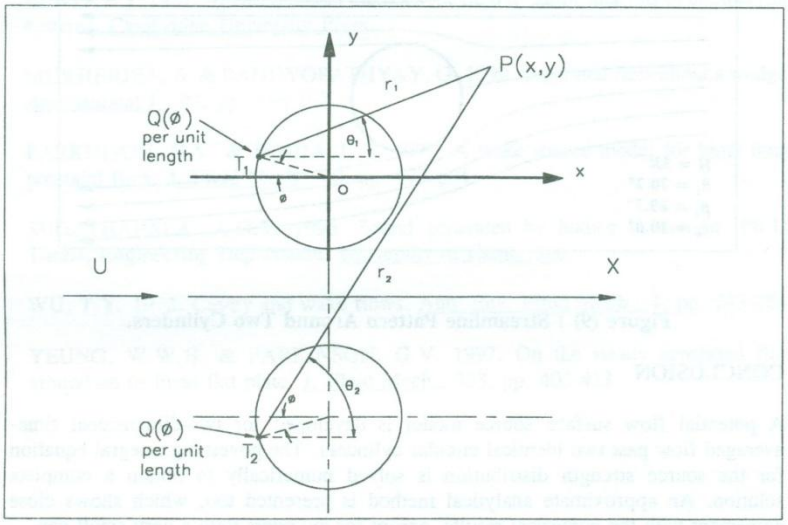

Figure (8) : Calculation of Streamline Pattern.

The complex potential function for the flow field is

$$F(z) = Uz + \frac{R}{2\pi}\int_{-\beta_2}^{\beta_1}\left[\ln\left(\frac{r_1 r_2}{R^2}\right) + i(\theta_1+\theta_2)\right]Q(\phi)d\phi.$$

Therefore the stream function, given by $\psi = Real\ \{F(z)\}$, is

$$\psi(x,y) = UR\left[\frac{y}{R} + 2\int_{-\beta_2}^{\beta_1}(\theta_1+\theta_2)\sigma(\phi)d\phi\right], \qquad (25)$$

where θ_1 and θ_2 are functions of x, y and ϕ. Now, on a streamline ψ is a constant and equation (25) can be solved to locate the position of the line. Here too a simple iteration procedure is used to find y for a given x. Note that θ_1 and θ_2 are multi-valued functions and therefore a suitable branch-cut(s) should be selected to make them single-valued. A set of streamlines around the cylinders can be obtained by selecting suitable values for the stream function. The value corresponding to the separation streamlines may be obtained through equation (25) by considering any point on the front wetted surface. The streamline pattern for the case of $e = 1.5$ is plotted in Figure (9), where the angular shift of the near-wake is clearly indicated.

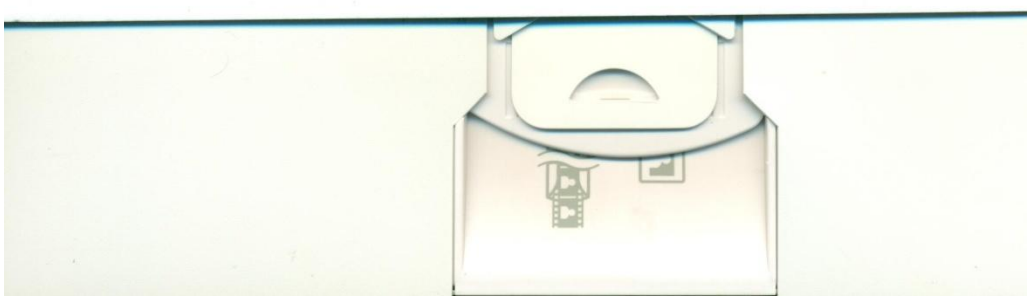

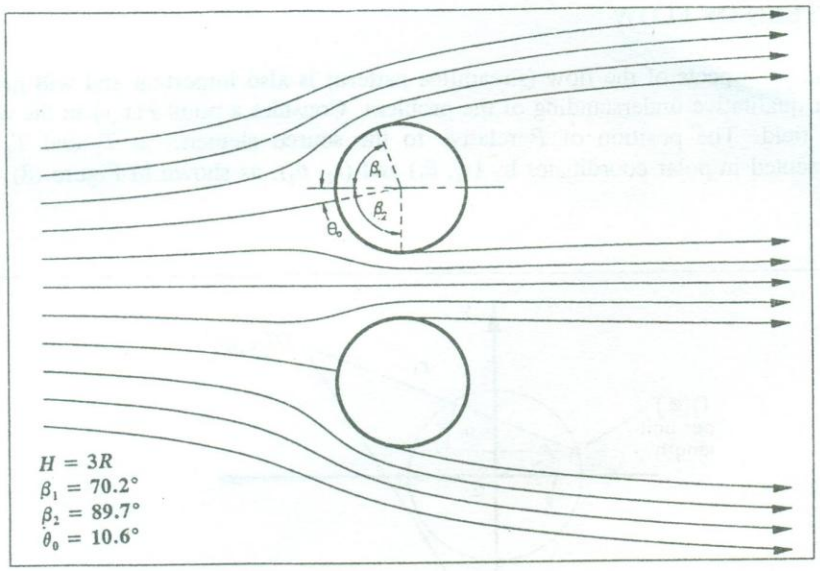

Figure (9) : Streamline Pattern Around Two Cylinders.

CONCLUSION

A potential flow surface source model is developed for two-dimensional time-averaged flow past two identical circular cylinders. The governing integral equation for the source strength distribution is solved numerically to obtain a complete solution. An approximate analytical method is presented too, which shows close agreement with the numerical results, except for cylinders with a very small gap.

The main advantages of the present model are that it is simpler to use and it does not require any empirical parameters. The model predicts the positions of the separating points and the corresponding back pressure coefficients. The results show that the effects of the presence of the adjacent body are to shift the separating points, resulting an angular shift of the near wake, and to create a non-uniform, higher wake under-pressure. These effects give rise to higher drag force on the body and generate a lift force.

The model can be extended readily for the general two-body problem of different body sizes with any flow direction respect to the bodies, if there is no direct interaction of the down-stream body with the wake of the up-stream one. In such situations there will be two integral equations for the source strength distributions on the two bodies with four unknown angular positions of the separation points. In principle, this method of analysis could be used for a general multi-body flow problem with any number of circular cylinders.

Finally, other possible use of the present model is worth mentioning. It is possible to calculate the effect of the presence of a plane solid surface or of blockage in a wind tunnel by using a system of images.

REFERENCES

HESS, J.L. 1973. Analytical solutions for potential flow over a class of semi-infinite two-dimensional bodies having circular-arc noses. J. Fluid Mech., 60, pp. 225-239.

HESS, J.L. & Smith, A.M.O. 1966. Calculation of potential flow about arbitrary bodies. Prog. in Aero. Sci., 8, pp. 1-138.

LEWIS, R.I. 1981. Vortex element methods for fluid dynamic analysis of engineering systems. Cambridge University Press.

MUKHERJEA, S. & BANDYOPATHYAY, G. 1990. Separated flow about a wedge. Aeronautical J., 94, pp. 196-202.

PARKINSON, G.V. & JANDALI, T. 1970. A wake source model for bluff body potential flow. J. Fluid Mech., 40, pp. 577-594.

SUGATHAPALA, A.G.T. 1996. Sound generated by bodies in motion. Ph.D. Thesis, Engineering Department, University of Cambridge.

WU, T.Y. 1972. Cavity and wake flows. Ann. Rev. Fluid Mech., 4, pp. 243-284.

YEUNG, W.W.H. & PARKINSON, G.V. 1997. On the steady separated flow around an inclined flat plate. J. Fluid Mech., 333, pp. 403-413.

DESIGN AND CONSTRUCTION OF A BENDING TESTER FOR TEXTILES

Nirmali Perera
Department of Textile & Clothing Technology, University of Moratuwa

DESIGN AND CONSTRUCTION OF A BENDING TESTER FOR TEXTILES

Nirmali Perera
Department of Textile & Clothing Technology, University of Moratuwa

ABSTRACT

Bending rigidity is an important physical parameter measured in Textiles. The drape and handle qualities of a textile are governed mainly by its bending and torsional characteristics. These can be changed only by using suitable softeners or various finishing agents. Many attempts have been made to develop instruments to measure the bending rigidity of textiles using various principles. The aim of some research activities is to relate the bending properties of constituent fibres and yarns to fabric properties. According to one school of thought properties such as bending, torsion, strength, friction and compression are measured to predict the overall drape and handle qualities of fabrics. Much work is being done in the objective evaluation of properties of textile structures which should replace subjective evaluation methods. Upto now there is no standard instrument to measure each of these parameters including the bending rigidity.

Although there are several commonly used methods for measuring the bending rigidity of yarns and fabrics, not all satisfy the desirable condition that a pure bending couple should be imparted to the test specimen. Such a method has an advantage over other methods in that the specimen experiences only a bending moment. The apparatus described in this work has been designed to impart an almost pure bending to the specimen under consideration over its entire length. Also it was attempted to ensure that the equipment is made versatile in as many aspects as possible.

A cyclic bending tester was designed and constructed to achieve the above mentioned aims. Unlike the earlier versions this tester was controlled by computer. The principle employed was that of the cloth bending tester designed by Livesey and Owen [1], later improved and extended by Abbott[2], Grosberg[3], Chapman[4] and Grey[5]. This tester was made with more precisely controlled movement and with greater sensitivity, adjustable to measure yarns and fibres and with overall control using an IBM Personal Computer.

DESIGN OF THE INSTRUMENT

In the design of the instrument, three main parts were put together to make up the composite apparatus. The three units are the rotating unit, the load measuring unit and the computer for overall control of the system.

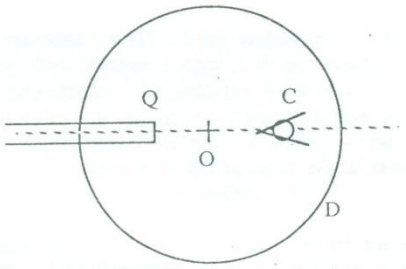

Figure 1.1 Schematic of the moving jaws and disc

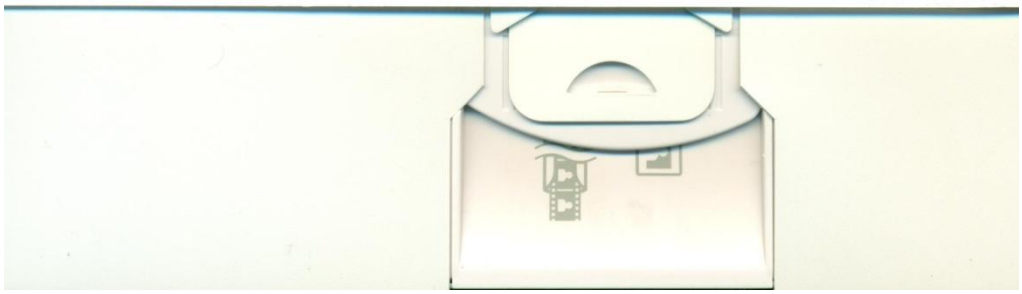

Many problems arose in the construction of the instrument and each of these are discussed. The bending unit consists of two sets of jaws, one stationary(Q) and the other able to rotate(C). The stationary set of jaws are fixed to the end of a very light lever, suspended at its centre by a wire that hangs from the load measuring unit. The movable jaws are fixed to a metal disc(D) with the nip of the jaws half the length of the sample away from the centre of rotation(O) of the disc. The disc is attached to the shaft of a stepper motor which drives the shaft. If the shaft and disc are concentric, then one end of the sample moves in an arc of a circle.

THE ROTATING UNIT

The Stepper Motor

The stepper motor rotates in finite steps and the motion is not strictly uniform. A matching gear box was used to produce nearly uniform speed of rotation. The software controlling the instrument was designed so that the rate of rotation of the shaft which is proportional to the rate of change of curvature in the specimen, can be fixed before the start of a test.

The curvature of the specimen at any given time is proportional to the angular position of the shaft and is calculated precisely by the step counter in the programme. Automatic and instantaneous reversal of the direction of bending was made possible by manipulating the software. The maximum angle of rotation can be set to any value in the range ±90° which enables a specimen of 5 mm length to attain a curvature of ±3 cm^{-1}, which is the usual limit in these experiments. If the specimen size was reduced, the maximum curvature can be increased further.

The Disc

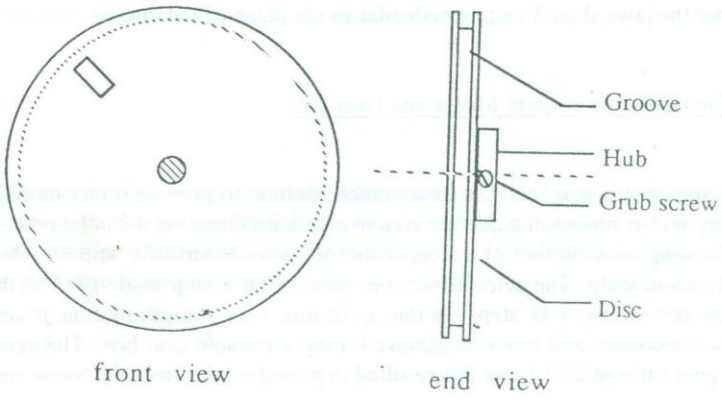

Fig 1.2 Slot and the groove in disc

A circular metal disc was used to fix the rotating jaws which are fitted on the shaft of the stepper motor. This is concentric with the disc and the distance from the centre of the disc to the nip point of the jaws is half the length of the test specimen. The disc has a slot in one place and a groove round its perimeter, the purposes of these features will be seen later.

The Movable Jaws

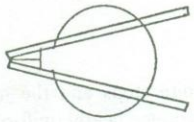

Fig. 1.3 Rotating jaws

The movable jaws consist of a bulldog clip which has been slightly modified by filling up the angle at its nip so that the specimen is mounted in a simple and effective way. The rotating jaws are rigidly attached to the circular disc by a bracket on which the jaws are fixed. A second slot is made in the disc and the bracket is fixed in it using two screws. Slight movement is possible within the slot in the unscrewed state in order to adjust the sample length as well as the height of the nip when required. The nip of the rotating jaws has to be level with the nip of the 'stationary' jaws. It is also necessary that the jaws should be perpendicular to the plane of the disc.

The Choice of Stepper Motor and Gear Box.

A step motor was found to be a suitable method to provide rotary motion and since the step motor moves in a definite step in a definite direction it can be precisely controlled. The step-wise motion of a stepper motor becomes virtually smooth when the motor is driven quickly. The selected stepper motor had a step angle of 7.5° thus completing one revolution in 48 steps. In this apparatus, very smooth motion at very slow speeds was necessary and this was achieved using a suitable gear box. The gear box used had a gear ratio of 250:1 and this resulted in providing the smooth motion required.

Overcoming the Backlash in Gears

As expected, it was found that the gear box used with the stepper motor produced a considerable backlash. To overcome this problem the gears were biased by means of a string wound round the disc and sitting inside the groove at its rim mentioned earlier. One of the ends of the string is knotted through a hole let into the groove, and the string, on leaving the disc is passed over a fixed pulley and then allowed to hang freely with a small weight at the end. This weight is about 50 grams which would keep the string taut and therefore suited the purpose. This arrangement counteracts the backlash produced by the gears. With the correct length of string there will be no problems of fouling the pulley nor striking the base, within the extremes of the test limits, which is a quarter of a revolution in either direction from the rest position.

Verifying the Rest Position

The rest position is defined as the situation when the two nip points of the jaws, the specimen, the lever and the centre of the rotating shaft all lie on the same horizontal axis. At the rest position, the angle of rotation is zero which in turn corresponds to a zero curvature. The rest position of the rotating jaws is determined by the zero position of the shaft which is verified by means of an optical sensor fixed in the slot in the disc mentioned earlier.

This enables the shaft to be driven in any direction and to be stopped at the geometrical rest position, which is determined by the optical sensor. When the lever(carrying the specimen in the jaws) is suspended the load cell reads a force. This is cancelled out by balancing electronically. When the specimen is inserted between the moving set of jaws, the load cell reading is checked and the shaft and specimen adjusted until the original reading is obtained.

Since the expected record of moment s curvature is a hysteresis curve, it was therefore decided to set the starting point of a test at the middle of the scale.

Optical Sensor

An optical sensor was fixed to the frame of the instrument in such a position that when the slot passes through the sensor, an optically activated signal is received by the computer and the rotation is stopped. Then the disc will be at its reference position. The slot was so positioned that the rotation was not inhibited while a test was on.

THE LOAD MEASURING UNIT

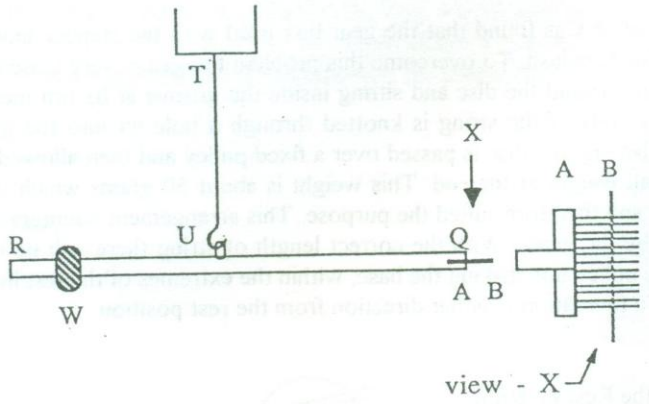

Fig 1.4 Arrangement for measuring the force on the load cell

This unit consists of a load cell type of transducer to measure the strain. In this case a load cell of an Instron Tensile Tester was used. A long lever is suspended from the hook which carries at one end the "fixed" jaws, and at the other a movable counter weight. At the rest position, just before a test is carried out, the lever, the jaws and the specimen should be horizontal. When the shaft rotates and bends the specimen, the balance of the system is upset, and the load cell will immediately measure the change in force that takes place. The change in the force on the load cell measures the changes in bending moment that occur with changing curvature. This force in analogue form is amplified and converted to a digital value and recorded by the computer. An A/D converter was used to convert the analogue signal produced by the load cell into a digital signal.

Strain-Gauge Amplifier

The strain-gauge amplifier was a precisioned, purpose built amplifier with low drift characteristics and with stable amplification.

The Lever

The theoretical analysis suggests that the lever should be as light as possible and that the distance from the specimen to the point of suspension should be more than 10 times the length of specimen. If not the error due to the moment produced by the weight of the lever becomes significant. This is a very critical feature of this apparatus as there is a possibility of the centre of gravity of the system moving slightly forwards or backwards during a test.

Hooks and Connections

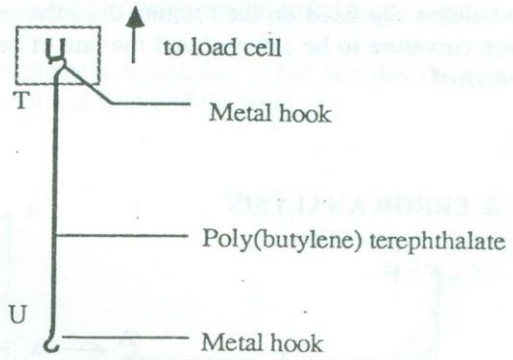

Fig. 1.5 Hooks and the lever arrangement

The top end of a long hook is rigidly fixed to a hook that exists on the strain gauge within the cell. The arm of the hook is a string made up of poly(butylene terephthalate) which has an insignificant moisture regain and very low creep characteristics.

THE CONTROLLING DEVICE

An IBM PC is used to control the motor. The motor can be rotated, at the required speed, in both clockwise and anti-clockwise directions. In the cyclic bending test, the motor is rotated until a pre-determined maximum curvature is reached and then driven in both directions until the cycle is completed.

While the test proceeds, a Load - Curvature curve can be plotted on the video display unit of the computer. By manipulating the software, initial bending rigidity could be calculated.

The computer is used to calibrate the instrument, store and retrieve information and data associated with experiments and to calculate the results of the experiment.

Test procedure

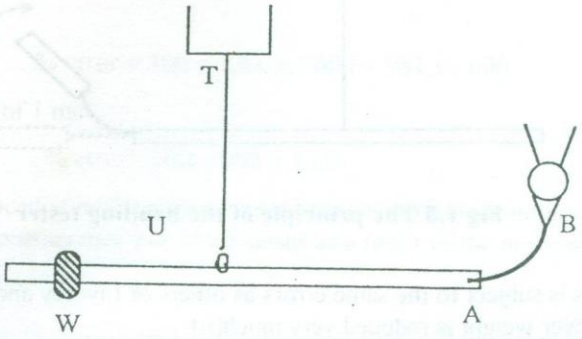

Figure 1.6 Bent sample during the course of the test

When the specimen is inserted into the jaws attached to the tube with the other end held by the bulldog clip fixed on the rotating disc, the sample is ready for test. When the maximum curvature to be assumed and the rate of bending have been decided the test can be started.

THEORY & ERROR ANALYSIS

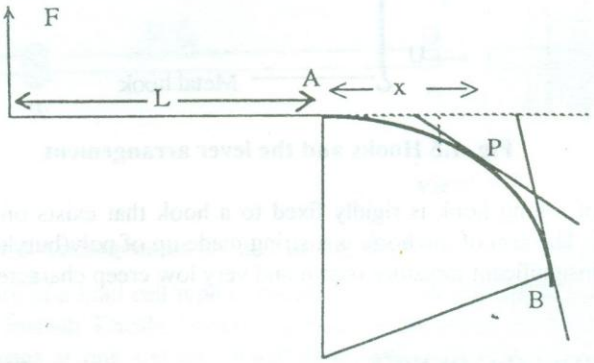

Fig 1.7 Representation of forces in specimen while bending

AB is the specimen and P is a point situated at a horizontal distance x from A. Assume that the specimen AB bends to form an arc of a circle having a radius of r, then,

$$\text{Moment(M) about P} = F(L + x)$$

where F is the resultant force on the load cell. From this we see that, if $x << L$, M will be nearly constant along the length of the specimen.

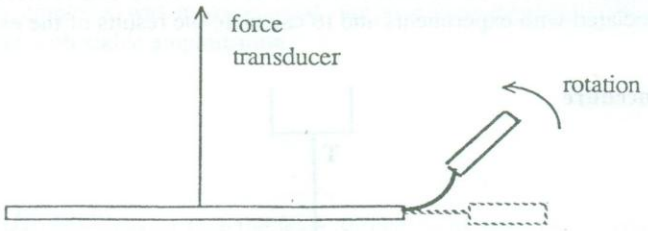

Fig 1.8 The principle of the bending tester

This apparatus is subject to the same errors as others of Livesey and Owen type but the effect of the lever weight is reduced very much[6].

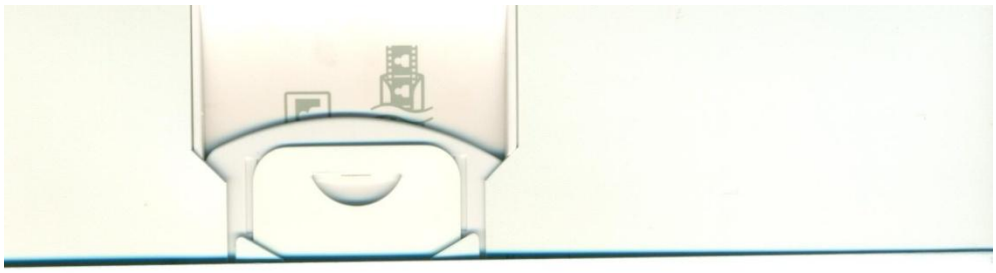

If the lever was uneven and the centre of gravity did not coincide with the geometrical centre, this was overcome by using a counter-weight to balance the lever at its point of suspension.
There could be an unwanted moment arising due to the fact that the centre of gravity of the lever is not at the geometrical centre of the lever.

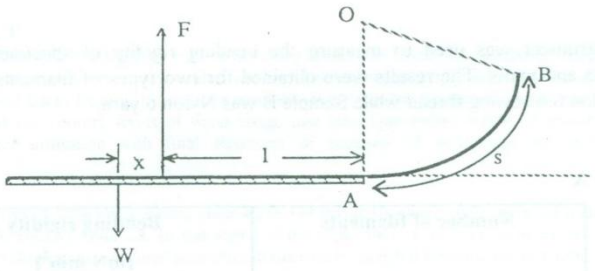

Fig 1.9 Lever with centre of gravity not in the geometrical centre

Suppose the centre of gravity is at a distance ***s*** from the geometrical centre. Then, taking moments about B,

$$M = F(l + \rho\sin\alpha) - W(x + l + \rho\sin\alpha)$$
$$= (F - W)(l + \rho\sin\alpha) - W.x$$

When x = 0, the "correct" moment is

$$M_c = (F - W)(l + \rho\sin\alpha) = B/\rho$$
$$\therefore \text{ \% error} = W.x.100/M_c$$
$$= 100W.x /(F - W)(l + \rho\sin\alpha)$$
$$= 100\ W.x.\ \rho\ /\ B$$

If W = 9.81 mN ($\equiv$ 1 g)

M_c = 600 mN mm

$$\text{\% error} = 100 \times 9.81.\ x\ /\ 600 = 981\ x\ /\ 600$$

If ***x*** is in the order of 1 mm,

$$\text{\% error} = 981\ /\ 600 = 1.6\%$$

If the lever is balanced at its suspension point, using a movable counterweight, there will be another erroneous moment which arises as a result of the movement of the lever, during a test

It can be shown that this movement is normally less than 1/4(specimen length) which is = 0.25 ***s***.

When the lever is balanced, it can be shown that the maximum moment of this force about the specimen is approximately 0.16 mN mm when W = 1 g. This is very small in comparison with M.

RESULTS

The instrument was used to measure the bending rigidity of specimens made of filaments and yarns. The results were obtained for two types of filaments. Sample A was Nylon 6.6 sewing thread while Sample B was Nylon 6 yarn.

Sample A

Number of filaments	Bending rigidity ($mN\ mm^2$)
20	929
10	464

Sample B

Number of filaments	Bending rigidity ($mN\ mm^2$)
20	384
10	192

The instrument was calibrated using a specimen made of shim metal and within the limits of the experiment, the results obtained were very promising. Further the results obtained for sample filaments were compatible with calculated values for bending rigidity.

References

1. LIVESEY, R. G. & OWEN, J. D., J. Text. Inst., **55** (1964) T516-530
2. ABBOTT, G. M., Ph.D. Thesis, University of Leeds, (1968)
3. ABBOTT, G. M. & GROSBERG, P., Text. Res. J., **36** (1966) 928-30
4. CHAPMAN, B. M. Text. Res. J, **41** (1971) 705-7
5. GREY, S. J., Ph.D. Thesis, University of Leeds, (1978)
6. PERERA, N., Ph.D. Thesis, University of Leeds, (1991)

INVESTIGATION OF THE USE OF WATER BY THE TEXTILE INDUSTRY IN SRI LANKA-PART 1

NGH.de Silva
Dept. of Textile & Clothing Technology
University of Moratuwa.

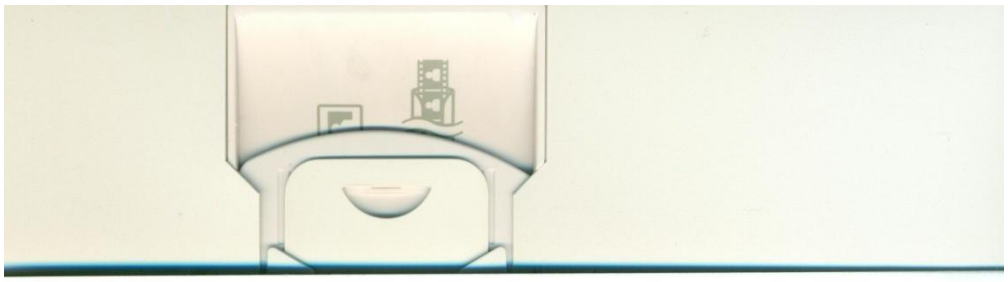

INVESTIGATION OF THE USE OF WATER BY THE TEXTILE INDUSTRY IN SRI LANKA-PART 1

N.G.H.de Silva
Dept. of Textile & Clothing Technology
University of Moratuwa.

ABSTRACT

The textile sector is one of the high water consuming operations among all industries. Studies on water use by their respective textile industries have been conducted by many countries such as USA, India and Great Britain. Information available facilitates the finisher to realise the actual position about the country levels of water usage and take appropriate action, if required, to optimise water utilisation with final objectives of economy of production and pollution prevention.

This study has to cover as much a wide cross section of textile finishing facilities to get a realistic view about the country situation. In this Part 1 of the paper four of the biggest mills have been surveyed and information presented according to the widely accepted formats, i.e. in terms of unit operations of finishing treatments by the number of litres per kilogram (l/kg) processed. Information has also been presented in terms of the variable parameters such as machine type, dye class type or chemical type for better analytical possibility. The finisher would then be able to decide on any conservation measures necessary by comparison with (target) figures available from various sources.

It is intended to cover the medium and some small scale textile finishing facilities in the next part of this study to complete the full cross-section of the Sri Lankan textile finishing sector.

INTRODUCTION

The major use of water in textile manufacture may take place at any one, or more than one, of the many stages of production as indicated in Fig.1 depicting a typical manufacturing procedure.

From what is known of the wet processing of textiles in the industry, large quantities of water are used for Desizing, Scouring, Bleaching, Mercerising, Dyeing and Printing. Relatively a smaller proportion of these large quantities of water acts as a vehicle to transport process chemicals to the substrate and a much greater proportion is utilised for washing off the solubilised impurities and residual process chemicals. In this study, therefore, more attention was due on the afore-mentioned wet processes.

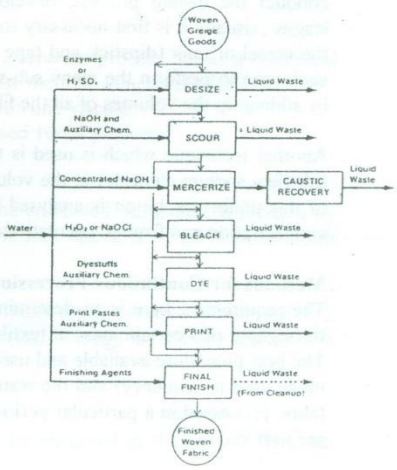

Fig.1 Typical woven fabric finishing process flow diagram

Not much published information on the topic of water usage world-wide was available when this investigation was started a few years back. Some information of specific water usage is presently available from India[1], UK[2] and the USA[3].

No published information is available on water usage studies on the Sri Lankan textile wet processing industry sector. This study in water usage in the major textile mills of Sri Lanka was started as undergraduate and postgraduate Diploma projects[4] to fulfil this requirement. Measurements and observations have been made under normal factory running conditions on the major water consuming wet processes in 4 of the largest integrated mills in Sri Lanka. Wherever possible measurements of process water was carried out separately from the wash water used in each major wet process.

METHODS OF MEASUREMENT

The study of water usage and expression of measured data are based on unit processes viz. Desizing, Scouring, Bleaching, Mercerisation, Dyeing and Printing. In the case of Dyeing, both "batch" and "continuous" types and machinery are used in the industry and since it is known that generally the different batch type machines use widely varying material to liquor ratios (MLR), the water consumption data have been presented in terms of different types of such machinery used.

Methods for Batch-Processing Machinery

In this situation since the same machine is used several times one after the other to conduct the dyeing process, development of colour, many rinses and soaping stages ; usually it is first necessary to calculate the volume from the dimensions of the vessel or tank (dipstick and tape method). Then the height of the fillings used each time to perform the many sub-steps in the total dyeing operation is obtained by adding up the volumes of all the fillings used.

Another technique which is used is the dissolution of a known weight of soluble salt (like sodium chloride) in the volume of water in the tank and a known volume of this uniform solution is analysed by standard analytical techniques for the salt concentration and from it calculate the total volume of water.

Methods for Continuous-Processing Machinery

The requirement here is to determine the total volume of water used during the throughput of a certain mass of textile material.
The best procedure available and used was to measure the tank / vessel volume (of those used in sequence) and the water flow-rate while recording the total mass of fabric processed in a particular period and there from calculate the specific volume per unit mass.

In counter-current washing ranges, the measurement is still easier, where either the input of effluent is measured and used against the total mass of fabric throughput for a particular period.

PRESENTATION OF RESULTS

The most widely available water usage figure in textile wet processing is the "overall specific consumption"; that is the total amount of water used by all processes in finishing divided by the total weight of material processed in the plant. Such data invariably shows very wide ranging values such as 5 to above 500 litres per kg[5], which may result from big differences in the extent and complexity of the processes involved. However when the range of values of overall specific water consumption varies widely; the average value for the industry as a whole has limited significance. It is of little assistance to the individual finisher except as a very broad guide who has to look more closely at his own data and at the relevance of comparable or target figures if he is to attempt a more logical approach to water use and conservation. Consequently it would be more meaningful to investigate the individual unit processes obtained by dividing the overall wet processing into different process steps by their objectives and wherever possible consider the major types of machinery using widely varying material to liquor ratios (MLR). In this investigative study this approach was followed and information is presented on the basis of unit processes. Further, wherever possible the process water (used to bring the process chemical and other auxiliaries in contact with the textile) and wash water (used to remove any solubilised or emulsified impurities or residual process chemicals etc. from the textile) measurements have been taken separately.

Water Usage in Unit Processes

Desizing of Fabric

All the four mills use enzyme for size removal. For details refer Table 1.

Scouring of Fabric

Mill nos. 1 & 3 do not perform scouring as a separate process but as a combined process with bleaching. The other two mills use the following methods (Table 2) :

1. Continuous open-width treatment for cotton and viscose.
2. Jet treatment for polyester/cotton blends and 100% polyester.

Bleaching of Fabric

Peroxide is used as the bleaching agent in the combined scour-bleach process by mill nos. 1 & 3, while hypochlorite is used in mill nos. 2 & 4, all in open-width continuous state. For details see Table 3.

Mercerising of Fabric

Caustic Soda treatment in concentrated form under tension is used in mill nos. 1, 2 & 3, while mill no. 1 gives a milder treatment (causticising) for viscose fabrics. See Table 4 for details.

Dyeing of Fabric

Three dyeing methods by machine type can be observed in the study. They are dealt with separately.

Jig Dyeing

Reactive, direct and vat dye classes are used on cotton fabrics with a wide range of usage depending on the type of dye used and washing method. See Table 5 & 6 for deatails.

Pad Dyeing

"Cold pad batch" (CPB) which is a semi-continuous method using reactive dye is performed at mill nos. 1, 2 & 3. See Table 7 for details.

Jet Dyeing

Two mills, nos. 3 & 4, used this method for dyeing polyester and its blends with disperse dyes. See Table 8 for details.

Printing of Fabrics

Mill no. 1 uses Flat bed screen printing (machine) method and Rotary printing (machine) method for printing viscose fabrics where washing off is performed in a washing range and by beam washing for both methods. Mill no. 2 uses only Roller printing (machine) method for cotton fabrics. Mill no. 3 uses both Flat bed screen printing (machine) method and Rotary printing (machine) method for printing cotton fabrics. Mill no. 4 uses both Flat bed screen printing (manual) method and Rotary printing (machine) method for polyester/cotton blend fabrics and 100% cotton fabrics respectively. See Table 9 for details.

Water Usage in Textile Washing

In general it is observable in all steps of wet processing that the processing baths use comparatively low or very low water, as against the subsequent wash processes (see Table 10), where the water consumed in the washes are indicated as a percentage of the total.

The jig and jet machines normally are designed to use low material to liquor ratios. On the jig, water consumption in the chemical bath tends to be kept down by the constraint imposed by chemical consumption since chemicals are added according to the volume of water in the bath (in grams per litre). In the ensuing washing baths this constraint is absent and hardly any attempt is made to keep the wash water volumes to the lowest practicable limit. Sometimes the washing baths are kept overflowing (running) and consequently relatively high usage values are unavoidable for washing, obviously making the total specific wash consumption unnecessarily high. (see Table 11).

In continuous processing too, similar situations arise, where the chemical bath usage is low but subsequent washing, which may be again continuous or batchwise such as in jigs, may use running baths in the soaper range or washing range and overflow washing in the consecutive jig washing steps respectively. If running baths are not used, generally for jig and soaper/washing range the usage of wash water and the total usages would be very much lower.

In the jet, the expected theoretical usage should be only slightly higher than the jig although the distribution of chemical bath usage and the wash bath usage would not be very wide. The total values may go up if full capacity of material is not processed in each jet, since generally a fixed volume of water is entered into the jet for each processing stage.

Two further features observed in jig wet processing is the tendency to use a fixed length and the lack of consideration of the fabric weight per unit length

Generally, dyeing processes vary widely, continuous dyeing being the lowest. Although no fully continuous dyeing is observed in this study, among methods of continuous padding followed by batching periods for dye fixation (cold pad batch-CPB - Table 7) could be observed for reactive dye application. These are considered as semi-continuous processes. The other two methods (machine-wise) are jig dyeing (Table 5) and jet dyeing (Table 8) which have slightly higher and much higher values respectively. The range of values in each type of method overlaps those of others and on closer analysis it is apparent that water usage is influenced by the type of dyestuff (see Table 6). This is so because of complex process requirements for the application of different dye classes even when the same type of equipment is used. Moreover when applying the same dye using the same machine, there can be wide variation in total water usage due to the dyer's preference in the washing process, with more or less the same usage value of dye application process. This is observed in jig dyeing using reactive dye (see table 7), where in mill no.2 the average washing usage and total usage are 12.8 and 16.2 l/kg while in mill no.4 they are 36.15 and 87.8 l/kg respectively. On further examination of the latter usages, the excessive wash water usage is seen to be attributable to 5 consecutive washes out of a total of 8 washes being given with overflow (running) in the jig bath. Opportunities for considerable savings would probably be available here, by a study of the efficiencies of static and running rinses in washing off the unfixed dye and residual chemicals in the fabric.

A similar situation is observed with the "Cold Pad Batch" dyeing method (see Table 7) where the range of total water is 13.5 - 181.3 l/kg. The lowest here is 13.5 l/kg where washing is done in jumbo-jig and all other instances washing is carried out in a range of tanks either with or without counter current and many tanks having overflow at different flow rates.

In jet dyeing (see table 8), where washes are given in the same machine and since the usable volume of water is variable within limits and no overflow is possible; variation in total water usage is low. Any significant variations could be attributed to the non-consideration of volume changes in relation to the density of the fabric load.

Table 11 indicates the average and range values that have been obtained in this study, illustrating the effect of machine type on water usage for the consecutive unit processes. The last column gives the best values which are the lowest in the range. Using these figures it is possible to calculate the cumulative usage for a particular manufacturing sequence, say for a bleached white fabric by just adding the average values or best values (target values) that have been used in the sequential unit operations from the grey state to the bleached state. It is possible also to find the cumulative usage where all operations have been conducted either fully continuously or batchwise or even when a mix of both these methods have been used. The Table 12 illustrates these clearly. Here the plain figures are average totals and those in brackets are the lowest in the range values which could be taken as the best attainable (could be considered as target figures).

Taking the example of a dyed fabric which has undergone the sequential unit operations of desizing by fully continuous method; combined scour-bleach

(gram/metre). Consequently in a jig operation, correspondingly higher water consumptions are observed for lighter fabrics, if the liquor volume used is not altered accordingly.

In continuous washing operations, there is a similar tendency to run a machine with a fixed water through-flow rate, but no adjustment of processing speeds are made to achieve constant mass throughput rate of fabric. This results in higher specific water consumption on lighter fabrics; in real effect the machine loading may be considered as reduced on such situations. This means that the lowest in the range of usage values of water in any process, generally relate to conditions of maximum machine loading. It may be considered as prudent to use these lowest usage values as "target figures"' derived from practical analysis with the existing system of processing.

CONCLUSIONS

General Comparison of Results

All the four mills in the study use the enzyme method for desizing in a semi-continuous manner except one mill (i.e. mill No.2) which is continuous. Values of desizing in all four mills are generally low and fairly similar, but mill No. 4 has higher consumption figures than the other three as seen by the total usage of mill No. 4 varying between 47.9 and 78.7 l/kg. This is observed to be due to high wash process values caused by overflow in all the four tanks of the counter current washing method defeating the main objective of this washing method. (Table 1).

The scouring process is not separately carried out in two of the mills (Nos. 1 & 3) but they use a combined scour-bleach. The other two mills impregnate fabric with caustic soda, steam, give dwell time for scour actions and wash in a range of tanks. Mill no. 2 washes in a 5 tank range with overflow in all 5 tanks having comparatively low flow rate, while mill no.4 performs the wash in a 4 tank counter current range with overflow in 3 of the tanks at a high rate. The latter mill is observed to be using overflow in a counter current washing system defeating its very purpose itself. However both the mills have comparatively low usages although it is possible to reduce it further by cutting down the overflows.

Bleaching is brought about by two different agents, viz. Peroxide and hypochlorite, the former generally using less water than the latter. Peroxide is used in two mills (Nos. 1 & 3) to perform the combined scour-bleach and the variation on water usage is observed to be due to overflow in all 5 tanks of washing in mill no.1 while the no.3 mill used counter current without overflow. In hypochlorite bleaching also the washing is observed to be practised with overflow in the washing range including counter current washing. This latter process carried out in mill no. 4 for PE/Co fabrics thereby give high usages which could be cut down.

Usage figures for mercerising are fairly low (Table 4) and among them the total usage value of 44.06 l/kg at mill no. 3 stands out high. On scrutiny it is found to be due to non-adjustment of processing speeds to bring about a constant mass throughput rate of fabric in the washing operation, i.e. lower weight per unit length fabrics should be run faster through the washes. This will give reduced usage in wash process.

(peroxide) by fully continuous method, followed by dyeing by jig method the cumulative total of average water usage would be (5+26+36=) 67 l/kg while target figures would be (4+11+16) 31 l/kg. (Arrived at using the data in Table 12).

Comparison with other sources

Some information on water usage figures are available from other sources. They are Indian[1] , British[2] and American[3] sources. Table 13 illustrates some average values and ranges of water usage that allow comparison of similar processes, taken from these sources and the present survey in Sri Lanka.

The unit process of desizing from all sources are low, particularly the average value for the Indian mill and the lowest value of the range for the British mills.

The next process of kier boil (scour) and washing gives similar low figures for both Indian and British and slightly higher for Sri Lankan and the highest for American.

For hypochlorite bleaching, again the lowest values are for the Indian mills, the next is Sri Lanka followed by the British mills, yet at tolerable level while the American mill figure is extraordinarily high. The alternative bleaching process with peroxide does not indicate any figures for India while Sri Lankan are the lowest (combined scour/bleach), next higher being the British followed by American mills.

Mercerising which is an optional process, usage figures are similar and low for the British and Sri Lankan mills, followed by Indian mills and the highest in America.

Dyeing water usage figures for jigs using vat dyes are lowest in India, while British and American were much higher with Sri Lankan mills a close second lowest.

A general observation on the information available in table 13 is the overall low figures for the Indian processes while the American figures are observed to be about four times greater. The Sri Lankan and British figures on the whole tend to be 1.3 and 1.6 times greater than that of the Indian. This comparison although interesting is not very precise due to known and unknown variations in and between the processes. However they show the trend and possibilities and opportunities for reducing water usage.

References

1) Gopujkar , S.S. Water Usage in Textile Mills. International Dyer and Textile Printer 1970: 144 P.47
2) Textile Research Conference Members. The use of water by the textile industry WIRA 1973.
3) Burford , M.G. et al. Industrial waste surveys of two New - England cotton finishing mills. NEI . WPCC report .(New England) 1953.
4) Sarath , Dharmapriya et al, Balakrishnan et al , Jayasuriya et al. Critical study of water consumption in the finishing department and suggestions for conservation at mill 1, 2, 3 & 4. P.G. Diploma & B.Sc. (Eng.) Textile Final Year Research Projects. University of Moratuwa
5) Little, A.H. Use and conservation of water in textiles J.S.D.C., 1971: 87 P137.

Table 1 - Desizing Of Fabric

Mill	Method	Material	Agent	Water Usage : l/kg Process	Wash	Total
(1)	Impregnate open width, batch into rolls, rotate for 4 hours and wash off. (semi-cont.)	100% Cotton	Enzyme	5.2	9.9	15.1
		-do-	-do-	3.2	13.3	15.5
		100% Viscose	-do-	3.0	9.4	12.4
		-do-	-do-	3.1	9.4	12.5
		Mill Average		*3.6*	*10.5*	*13.9*
		Mill Range : 12.4 - 15.5				
(2)	Impregnate, dwell 20-45 minutes in scray and wash. (cont.)	100% Cotton	Enzyme	1.0	3.5	4.5
		-do-	-do-	0.9	3.2	4.1
		65/35 P/V	-do-	1.0	4.5	5.5
		Mill Average		*0.97*	*3.7*	*4.7*
		Mill Range : 4.1 - 5.5				
(3)	Pad-roll 2 hours & 3 washes,(c.c.) (semi-cont.)	100% Cotton	Enzyme	0.7	6.4	7.1
		100% Viscose	-do-	1.2	5.9	7.1
		Mill Average		0.95	6.2	7.1
		Mill Range : 7.1				
(4)	Impregnate, openwidth batch 2 hours, wash off in 4-tank (c.c.) range with overflow in all 4.(semi-cont)	100% Cotton	Enzyme	1.3	(c.c) 50.5	51.8
		100% Cotton	-do-	1.4	(c.c) 46.5	47.9
		PE / Co	-do-	1.4	(c.c) 65.3	66.7
		PE / Co	-do-	1.3	(c.c) 68.0	69.3
		PE / V	-do-	1.6	(c.c) 76.7	78.3
		PE / V	-do-	1.7	(c.c) 77.0	78.7
		Mill Average		*1.5*	*64.0*	*65.5*
		Mill Range : 47.9 - 78.7				
		All Mill Average		*1.8*	*21.1*	*22.8*
		Range of All Mills : 4.1 - 78.7				

c/c = Counter Current Wash

Table 2 - Scouring Of Fabric

Mill	Method	Material	Water Usage : l/kg Process	Wash	Total
(1)	No separate scouring. For combined scour-bleach, see bleaching.				
(2)	Impregnate open-width with caustic soda, steam, dwell 45 min, wash in 5 tank range with overflow in all	100% Cotton	0.62	38.15	38.77
		PE / Viscose	0.62	17.49	18.11
		Mill Average	*0.62*	*27.82*	*28.44*
(3)	No separate scouring. For combined scour-bleach, see bleaching.				
(4)	Jumbo jig. (batch). Caustic impregnation. Steam 2 hours, wash in 4 tank c.c. range with overflow in 3 tanks.	100% Cotton	11.14	44.48	55.62
	Jet scour & Wash. (batch)	PE/Co suiting	8.27	16.53	24.8
	Jet scour & Wash. (batch)	100% PE	16.48	32.96	49.44
		Mill Average	*11.96*	*31.32*	*43.29*
	All Mill Average		*6.29*	*29.57*	*35.87*
		Range of All Mills : 18.11-55.62			

Table 3 - Bleaching Of Fabric

Mill	Method	Material	Water Usage : l/kg Process	Wash	Total
(1)	Peroxide (continuous) Impregnate, dwell 90min. at 90-100°C and wash in 5 tank range with overflow in all 5 (combine scour-bleach).	100% Cotton	0.88	44.74	45.62
		100% Viscose	0.85	34.71	35.56
		Mill Average	*0.87*	*39.73*	*40.59*
(2)	Hypochlorite Impregnate, dwell 45 min scray, wash in 6 tank range with overflow in 3 tanks.	100% Cotton	0.12	24.50	24.6
		PE / Viscose	0.12	37.57	39.3
		Mill Average	*0.12*	*31.04*	*31.95*
(3)	Caustic Soda-Peroxide Combined Scour-Bleach (continuous) with counter-current (c/c) washing.	100% Cotton	0.8	c/c10.60	11.4
		100% Cotton	0.8	c/c10.75	11.5
		Cotton/Viscose	0.8	c/c 9.75	10.6
		Mill Average	*0.8*	*10.37*	*10.8*
(4)	Continuous Hypochlorite Impregnate, J-box dwell 45 min, wash in 4 tank range with overflow in 3 tanks. As above in Jumbo, wash in 4 tank counter-current range with overflow in all 4 tanks.	100% Cotton	0.69	18.97	19.7
		PE/Co	13.8	68.76	82.5
		Mill Average	*7.25*	*43.82*	*51.1*
		All Mill Average	*2.25*	*31.2*	*33.6*
		Range of All Mills : 10.6 - 82.5			

Table 4 - Mercerising Of Fabric

Mill	Material	m/Kg Fabric	m/min. m/c speed	Water Usage : l/kg Process	Wash	Total
(1)	Cotton Pad-chain	9.1	60	3.45	c/c19.10	22.55
	Viscose Jig (Causticising)	6.1		0.75	29.35	30.10
		Mill Average		*2.1*	*24.2*	*26.33*
(2)	Cotton			1.1	24.54	25.64
		Mill Average		1.1	24.54	25.64
(3)	Cotton (CD14)	3.5		0.63	14.63	15.26
	Cotton (CD30)	7.5		1.50	42.56	44.06
	Cotton (CD20)	4.3		0.49	12.53	13.04
	PE / Co	4.1		0.42	13.75	14.17
		Mill Average		*0.76*	*20.87*	*21.63*
		All Mill Average		*1.39*	*23.2*	*24.52*
		Range of All Mills : 13.04 - 44.06				

c/c = Counter Current Wash

Table 5 - Effect Of Dyestuff In Jig Dyeing

Dyestuff Class	Specific Water Consumption l/kg	
	Average	Range
Reactive	34	16 - 88
Direct	18	18
Vat	58	42 - 73

Table 6 - Jig Dyeing Of Fabric

				Water Usage : l/kg		
Mill	Method	Material	Dye	Process	Wash	Total
2	Jig dye & Wash	Cotton	Reactive	1.70	14.27	15.97
2	Jig dye & Wash	Cotton	Reactive	1.43	14.97	16.40
2	Jig dye & Wash	Cotton	Reactive	3.38	12.78	16.2
4	Dye Cotton part in Jig & wash 8 times with overflow in 5.	PE / Co	Reactive	1.67	86.15	87.82
		All Mill Average		*2.05*	*32.04*	*34.09*
4	Jig dye & Wash	Cotton	Direct	2.72	14.99	17.70
		All Mill Average		*2.72*	*14.99*	*17.70*
2	Jig dye & Wash	PE /Co	Vat	1.75	40.44	42.19
4	Jig dye & Wash	PE /V	Vat	1.3	71.42	72.70
	All Mill Average			*1.5*	*55.93*	*57.45*
	All Mill Average for all dyes			*2.1*	*34.30*	*36.40*
	Range of all mills : 15.9 - 87.8					

Table 7 - Pad Dyeing Of Fabric

				Water Usage : l/kg		
Mill	Method	Material	Dye	Process	Wash	Total
3	CPB -Wash c.c. in 6 tank soaper with overflow in 3	Cotton	Reactive	0.92	74.64	75.56
3	CPB -Wash c.c. in 6 tank soaper with overflow in 3	Viscose	Reactive	0.99	44.47	45.46
2	CPB - Wash in jumbo jig	Cotton	Reactive	0.55	12.96	13.51
2	CPB -Wash in soaper of 13 tanks with overflow in 11		Reactive	0.55	28.54	29.09
1	CPB -Wash c.c. in 6 tanks with overflow in all.		Reactive	0.86	94.74	95.60
1	CPB -Wash c.c. in 6 tanks with overflow in all.		Reactive	0.96	180.3	181.30
		All Mill Average		*0.81*	*72.60*	*73.40*
		Range of all Mills : 13.5 - 181.3				

CPB = Cold Pad Batch c/c = Counter Current Wash

Table 8 - Jet Dyeing Of Fabric

				Water Usage : l/kg		
Mill	Method	Material	Dye	Process	Wash	Total
4	PE dye in Jet & wash	PE / Co 3.4 m/kg	Disperse	8.27	16.25	24.82
4	PE dye in Jet & wash	PE / V 7.4 m/kg	Disperse	8.86	35.44	44.30
		Mill Average		*8.57*	*25.88*	*34.56*
3	PE dye in Jet & wash	100%PE 8.3 m/kg	Disperse	6.62	41.6	48.22
3	PE dye in Jet & wash	100% PE 8.3m/kg	Disperse	5.25	17.87	23.12
3	PE dye in Jet & wash	100%PE 9.1 m/kg	Disperse	5.64	42.28	47.92
		Mill Average		*5.84*	*33.92*	*39.75*
		All Mill Average		*7.21*	*29.89*	*37.16*
		Range of all mills		*23.12 - 48.22*		

Table 9 - Printing Of Fabric

Mill	Material	Flat Bed Print m/c / Manual Water Usage (l/kg)			Roller or Rotary Print m/c Water Usage (l/kg)			Avg. Total
		Process	Wash	Total	Process	Wash	Total	(All)
1	Cotton	12.5	35.2 (R)	47.7	31.5	35.2 (R)	66.7	57.2
		12.5	46.7 (B)	59.2	31.5	46.7 (B)	78.2	68.7
1	Viscose				20.9	29.9 (R)	50.8	50.8
					20.9	22.7 (B)	43.6	43.6
Mill Average		*12.5*	*41.0*	*53.5*	*26.2*	*33.6*	*48.9*	*55.1*
Mill Range : 43.6 - 78.2								
2	Cotton				0.7	28.5	29.2	29.2
Mill Average					*0.7*	*28.5*	*29.2*	*29.2*
3	Cotton	18.6	64.8	83.4	10.2	64.8	75.0	79.2
Mill Average		*18.6*	*64.8*	*83.4*	*10.2*	*64.8*	*75.0*	*79.2*
4	Cotton				N/A	28.6	28.6	28.6
	PE/Co	N/A	16.7	16.7				16.7
Mill Average			*16.7*	*16.7*		*28.6*	*28.6*	*22.7*
Mill Range : 16.7 - 28.6								
All Mill Average		*15.6*	*40.8*	*51.2*	*12.4*	*38.9*	*45.4*	
Range of All Mills : 16.7 - 83.4								

R = Washing Range B = Beam Washing

Table 10 - Distribution Of Water Usage Between Processing Baths & Washing

Processing Method		Average Specific Water Usage (l/kg)			Wash as a % of Total
		Process	Wash	Total	
Continuous	Desizing	1.0	3.7	4.7	78.7
	Scouring	0.6	27.8	28.4	97.8
	H_2O_2 bleach	0.8	25.1	25.9	96.9
	NaOCl bleach	3.7	37.4	41.5	90.1
	Dyeing	0.9	49.6	50.5	98.2
Semi-cont.	Desizing	2.0	26.9	28.9	93.1
Jig	Scouring	11.4	44.5	55.9	79.6
	Dyeing	2.1	34.3	36.4	94.2
Jet	Scouring				
	H_2O_2 bleach	12.4	24.7	37.1	66.6

Table 11 - Effect Of Machine Type On Water Use

Process	Machine Type (method)	Specific Water Use l/kg	
		Avg.	Range
Desizing	Continuous	5	4 - 6
	Semi-continuous	29	7 - 79
Scouring	Continuous	28	18 - 39
	Jumbo Jig	56	
	Jet	43	25 - 56
Bleach			
Peroxide Bleach	Continuous	26	11 - 46
Combined Scour Hypochlorite	Continuous (J box)	28	20 - 39
	Jumbo Jig	83	
Mercerising	Continuous	24	13 - 44
Dyeing	Continuous	73	14 - 181
	Jig	36	16 - 88
	Jet	56	25 - 88
Washing	Continuous	40	10 - 65
	Jig	27	16 - 38
	Jet	47	25 - 98

Table 12 - Continuous *vs.* Batch processing - Water Usage (l/kg)

Unit Processes	Continuous		Batchwise	
	Fully	Semi	Jig	Jet
Desizing	5 (4)	29 (7)	-	-
Scouring		28 (18)	56	37 (25)
Bleach (peroxide)/Scour	26(11)	-	-	-
Bleach (hypochlorite)	28 (20)	-	83	-
Mercerising	22.5	-	-	-
Dyeing	-	73 (14)	36 (16)	56 (25)

NB. : The plain figures denote average totals and those in brackets the lowest of the range values.

Table 13 - Comparison Of Available Water Usage Figures

	Water Usage (litres/kilogram)							
Unit Process	Present Survey		American		Indian		Great Britain	
	Avg.	Range	Avg.	Range	Avg.	Range	Avg.	Range
Desizing & Washing	23	04-79	21	17-25	11	-	26	1.4-47
Kier boil (Scour) & Washing	36	18-56	68	24-111	24	22-25	25	5-46
Hypochlorite Bleach & Washing	42	11-83	310	276-343	11	-	68	21-173
Continuous Peroxide Bleach	26	20-83	90	-	-	-	38	13-64
Mercerising	25	13-44	77	-	60	27-92	26	11-57
Jig Dyeing : vat	58	42-73	102	-	35	-	82	38-196

POSITIVE ENVIRONMENTAL MANAGEMENT VIA WASTE MINIMIZATION IN A TEXTILE WASHING FACILITY.

Samudrika Wijayapala and NGH de Silva
Department of Textile & Clothing Technology
Ajith de Alwis
Department of Chemical Engineering

POSITIVE ENVIRONMENTAL MANAGEMENT VIA WASTE MINIMIZATION IN A TEXTILE WASHING FACILITY.

Samudrika Wijayapala and NGH de Silva
Department of Textile & Clothing Technology
Ajith de Alwis
Department of Chemical Engineering

ABSTRACT

Existing and developing national environment protection regulations have made it mandatory for all industries to establish a treatment system for wastewater to bring down all toxic, hazardous and offensive components to specified levels before releasing to the environment.

The paper looks at the garment washing industry in the textile sector. The industry sector today uses significant quantities of water and none of the factories utilise waste minimisation nor water recycling techniques. A washing plant is analysed with the objective of promoting water recycling and waste minimisation practices. Initially typical practices are given, followed by a water balance for the system. Results of the water audit presented here forms the first essential element of the waste minimisation process.

The method suggested look at the iron removal process to utilise ground water and then (eliminating water transport needs) to advance filtration to make recycling feasible. Iron is the key limiting factor in utilising the available ground water supply. These steps would preserve the water resource and would eliminate the current wasteful practices adopted by the industry.

INTRODUCTION

Textiles and Sri Lankan history have close connection with evidence available to suggest the practice of this industry (craft) from the very beginning. However , modern mechanised textile manufacturer is a post independent development in Sri Lanka. Today the industry has come to be a dynamic export oriented sector and since 1986 it has become the No.1 export earner overtaking the traditional export of tea. Textile industry has become a vital contributor to the national economy today with textiles, wearing apparel and leather products totalling 40.6 % of the industrial output.

According to the Ministry of Industrial Development (MID) , there were 845 garment factories at the end of 1996. Of the factories begun under the 200 garment factory programme,154 factories were in commercial operation, while six factories were closed down or merged during the year, mainly due to managerial problems. The export earnings of these factories were estimated at Rs. 44,659 million in 1996 and showed an increase of Rs. 4,300 million. The industry is of vital importance to the national economy. However, the industry has a bad reputation relative to its environmental performance, especially the garment finishing (dyeing, special effect washing) plants. This paper discusses the garment washing plants and proposes an environmentally friendly alternative operational method.

The number of washing plants in the country is about 60 and the number is considered inadequate to serve the need. Due to the bad environmental image , the siting of washing plants had been a problem and difficulties had been experienced in obtaining permission from regulatory agencies (i.e. CEA).

GARMENT WASHING PROCESS

The washing operation must meet stringent quality standards which are difficult to formulate in a quantitative manner. Today, the garment washing houses must meet the demanding fashion needs of the denim garment wearers. Beyond the stages of acid wash , stone wash etc. customers now demand that the environmentally unfriendly stone washing method be replaced with enzyme washing. Understanding the action of enzymes is of paramount importance to all those who are working with enzyme wash , in order to obtain optimum effects from these rather costly products. The Sri Lankan industry currently uses many methods as well have still not transformed to new methods completely.
Only garments made out of fabric having a high mass per unit area such as the following fabric types are generally subjected to these washing processes.

- Heavy weight twills
- Medium weight twills
- Light weight twills
- Chambrays
- Cotton knits (heavy weight)
- Denims

However, to improve as their negative environmental image different strategies have to be adopted and put in to practice. The advantage is that in implementing waste minimisaton practices the industry stands to benefit as well as the environment. It is with the view that the project is being carried out. Benefits to the industry will result in better performance resulting in stronger trade performance. The positive environmental performance in addition will bring in positive community response an asset of much value.

Conventional washing of garments (or fabrics) is performed usually to remove impurities (soil) accrued as a result of wearing. However industrial 'garment washing' is performed in order to develop or impart certain predetermined visual effects, sometimes ,together with specific handle. This can therefore be considered as 'Special effect washing' .

Conventional washing is performed for the purpose of cleaning where hardly any destruction (strength, colour) of the fabric/garment takes place. On the other hand in the 'Special effect washing' some destruction of strength and low to high destruction of colour are associated with the various effects produced after washing. Consequently it is important to consider the residual levels of strengths in the garment after washing to make them last long enough when in consumer use .The severity of the wash effect has to be reduced for the low mass per unit area fabrics, so that sufficient residual strength could be retained in the garment fabric without reducing the utility period of the article.

A typical "special effect washing" sequence flowchart is given in Figure 1.
The figure also indicates the environmental impacts at various stages of the washing operation.

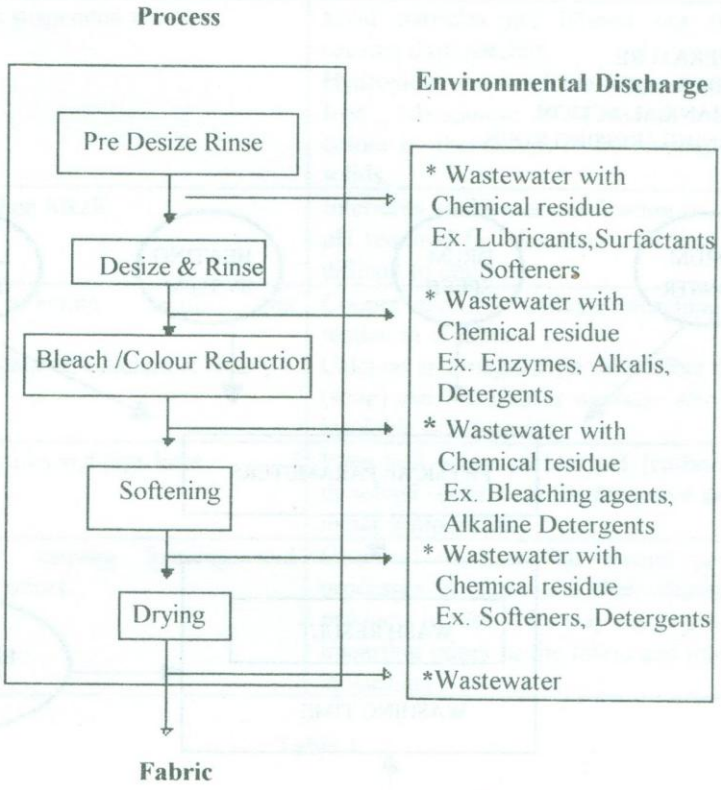

Fig. 1 - Special effect washing in the garment industry.

Effect Of Garment Quality On Washing

Large quantities of garments are subjected to industrial washing and a variety of units exist to achieve this. Washing imparts certain desired quality effects to the garments. The final product quality can vary significantly due to the way the washing process is carried out. The wash effect is dependent on a number of process parameters as shown in Figure 2.
Possible problems or faults arising as a result of inappropriate physical conditions and / or parameters being used in the washing procedures are summarised in Tables 1 and 2 (de Silva 1996,1997).

The process typically uses water and other chemicals and quality problems can result in the finished products from the presence of impurities in water and / or deviation in process steps when utilising chemicals.

There are many changes that could be implemented in washing plants for improving their efficiencies and performance.

PROCESS PARAMETERS THAT GOVERN THE WASH EFFECT

- TYPE OF DENIM
- ENZYME DOZE
- TIME
- pH
- TEMPERATURE
- LIQUOR RATIO
- MECHANICAL ACTION
- CLEANING / RINSING STEPS

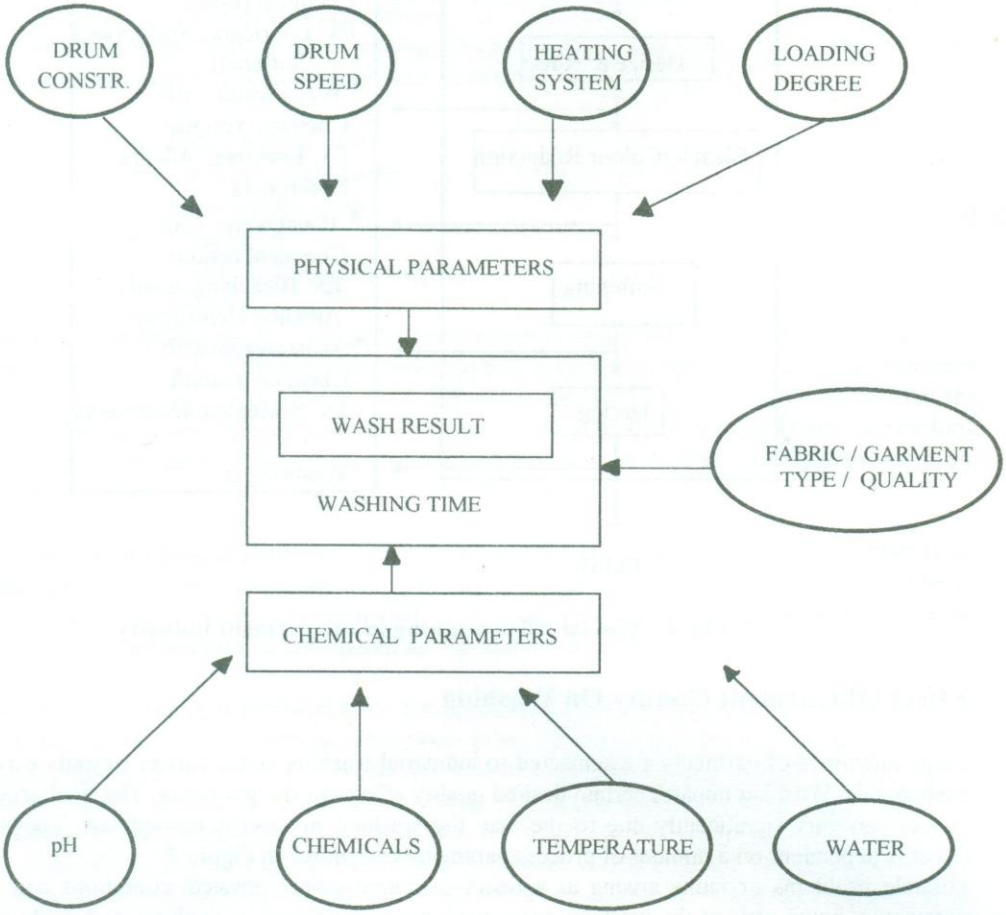

Figure 2

QUALITY PARAMETER	EFFECT OF DEVIATION
1. Freedom from suspended solids	Solid particles get filtered out on fabric causing dark patches. Hydroxides and insoluble soaps of metals like Iron , Manganese & Aluminum may impart colour by themselves or by binding coloured solids.
2. Excess of acid or Alkali	Interferes with water purification pH required for bleaching , enzyme washing difficult to control.
3.Substances affecting textile wet processing e.g. Iron, Manganese, Calcium & Heavy metals.	Copper and Iron activate bleaching causing tendering of fabric. Calcium and magnesium salts affect detergent (soap) use, i.e. Causes wastage, also produce insoluble salt deposits.
4. Corrosion of tanks and pipe lines	Even soft water of low pH (carbon dioxide dissolved water) can be corrosive destroying metal components.
5 Substances causing foaming and unpleasant odors.	Chemical residues that escape purification processes or algae and their decomposition products in reservoirs may cause problems of imparting odors to the fabric and interference in washing

Table 1

CASE STUDY

A textile washing plant situated in the Ratmalana - Moratuwa area is considered as a typical example. Water is an essential component for the process. However, for this plant water cannot be obtained from the ground due to the presence of iron and it is sourced externally.
Ground water samples were obtained from two existing tube wells. Iron and Manganese are the two critical elements that were tested for their concentrations.
An analysis of ground water on the site is given in Table 3.The results indicate that the problems would arise only from the presence of Iron.

Water Sample	Iron (mg/l)			Manganese (mg/l)		
	Test value	Reqd value	% reduction	Test value	Reqd value	% reduction
Tube well No 1	0.15	0.02	86.7	Nil	0.02	--
Tube well No 2	0.69	0.02	97.1	Nil	0.02	--
Bowser	0.06	0.02	66.7	Nil	0.02	--

Table 3

STEPS & FUNCTIONS	CHEMICALS USED	PROBLEMS	SOLUTION
1. **PRE-DESIZE RINSE** * Wets out Garment * Relaxes fabric * Removes Soluble substances	Non - ionic lubricants Non - ionic surfactants Non - ionic softeners	If not wetted out may : * cause uneven desizing * cause streaks & creases	proper water level water too hot was lubricant added
2. **DESIZE** *removes size ingrediants * removes excess dye & contaminants * relaxes fabric further	Amylase & non-ionic surfactants Anionic/ Non ionic surfactant and heat Peroxide with alkaline detergent Alkaline detergent Alkalis (NaoH,KOH,Na_2Sio_3) Hot water	size if not completely removed will cause : * uneven abrasion * dark spots * streaks , crease marks	For proper size removal * ensure proper water level * add sufficient enzyme and chemicals * keep pH within range * keep water temperature within range * prolong desize cycle * optimize desize cycle i.e. enzyme dose, load, timing
3. **ABRASION / ENZYME** * removes colour * softens fabric * produces faded , aged look	Cellulase enzyme Cellulase + stone Non ionic surfactants , Buffers (pH)	* uneven abrasion ,steaks & crease marks * too much abrasion * too little abrasion	* ensure proper water level * check temperature & pH * shorten cycle time * prolong cycle time
4. **BLEACH / COLOUR REDUCTION** * clean up fabric * removes colour * bleaches fabric	Alkaline detergent Anionic / Non ionic S.A. blend Peroxide + alkaline detergent Hypochlorite + Alkaline detergent and antichlor Hypochlorite then peroxide Hot water	*white spots & streaks *Excess fabric strength loss *uneven bleaching	dilute all chemicals and add * Never add chemicals direct on top of garments bwhen drum not rotating * with hypochlorite keep pH 8 to 11 * with peroxide keep pH 6-10 * optimize abrasion step for time and enzyme dose * Check temperature and pH before adding bleach chemical * optimise bleach time and concentration * check pH prior to adding bleach compound.
5. **SOFTENING** * gives fabric soft handle * eases removal of wrinkles in dryer	Cationic softeners Cationic silicones Non- ionic polyethylene emulsion Emulsified silicon fluid.	* No soften handle * greasy, slimy feel or scum spots on fabric * spots on fabric	* optimise softener dose * check pH before softener addition (cationics pH 4-6, others 7-8) * silicone emulsion unstable, use fresh products * pH may be too high for stability, reduce pH

Table 2

In the present operational situation, wash water is purchased from outside and the effluent is discharged after wastewater treatment as below :-

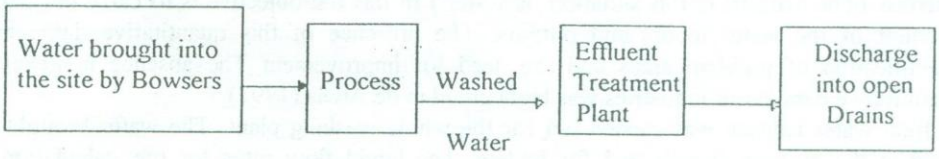

Figure 3

As can be seen the water passes through the plant only once. There is considerable effort on purchasing and transporting water to the site. This water supplies the needs of all plant personnel as well. The purchasing figures show that there is a minimum of 24 vehicle (bowsers) runs every day. Every other hour a bowser arrives at the factory constituting of 2 vehicle runs. This is a considerable addition of traffic volume to the area considering the already congested roads. If the ground water in tube well no.2 is to be used a removal figure of 97% iron is necessary. However even the bowser water is not of satisfactory quality, thus the company should work at having an Iron removal plant.

The map (Fig. 4) indicates the ground water quality as to the presence of Iron. The selected plant falls into the region 'not suitable' to have a washing plant if direct use of ground water is intended.

Thus if a plant is placed in the area the facility should have a treatment plant to achieve satisfactory quality if one is to use ground water. Otherwise transportation of water from an outside area will have to be resorted to. However, this may still involve some treatment as can be seen from the distribution of iron in groundwater in Sri Lanka

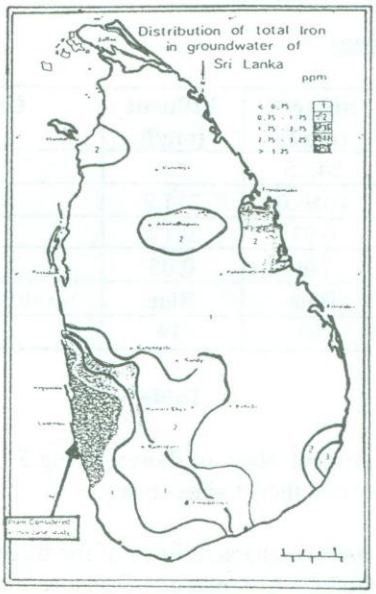

Figure 4

4. WATER AUDIT

The water audit aims to identify all inputs of water with outputs. This is a material balance exercise (The material in this situation is water.) In this the objective is to carry out detailed account of the water inputs and outputs. The presence of this quantitative data enables identification of problem areas and the need for improvement The absence in general of quantitative data in our industries was highlighted in de Alwis (1997)
A total water balance was carried out for the whole washing plant. The water brought in is used in the process directly and for boilers. The liquid flow rates for this calculation was measured by using two types of instruments.

1. Flumes (Portaflow MKII , Micronics) - Instrument for measuring open channel water flow rates (Effluent flow rate from the factory was measured)

2. Area Velocity Flow Meter (ISCO 4250 , Electronics) - Instrument for measuring closed channel water flow rates.

Steam flow rates were taken by the use of pipe diameters and the pressure gauge readings from the steam flow rate charts. The condensate is not recovered and is drained away.

Tabulated results from the water balance carried out is given in Table 4.

The results show that there are losses in the systems which had not been possible to identify. High accuracies are never the target of a material balance though 99% accuracy is quite useful. Such high accuracies are rarely achievable in practice specially in situations where diversity of practices and equipments exist. Normally accepted tolerance range for a material balance is 10%. The exercise shows that the estimated consumption and the effluent generation to fall into this acceptance range.

5.0 Wastewater & Treatment

Effluent Characteristics	Influent (mg/l)	Effluent (mg/l)	CEA Standards (mg/l)	Standards
BOD	242.5	52.0	60	Satisfactory
COD	1056.0	211.2	250	Satisfactory
Iron (Fe)	0.03	0.17	-	-
Manganese (Mn)	Nil	0.05	-	-
Colour	Blue	Blue	No stds available for colour	
Temperature (^{o}C)	30	38	30	Satisfactory

Table 5

The current wastewater treatment plant is shown in Fig.5. The effluent is treated using a flocculant coagulating system and then drained away.

The influent characteristics and the characteristics of the treated effluent are given in Table 5. This also indicates the required CEA standards (discharge standards for inland surface water) for comparison.

TOTAL WATER BALANCE			
Operation	**Estimated water consumption (l/day)**	**Estimated steam consumption (kg/day)**	**Estimated effluent (l/day)**
Enzyme washing	43,000	1880	41,775
Softening	16,200	344	15,863
Normal washing	2,800	154	2,250
E/S washing	109,200	3,539	108,700
Only softener	45,000	743	44,681
b/washing	25,200	813	25,110
Normal wash - B	15,400	608	12,920
Floor washing	**30,000**		**30,000**
Total	256,800	**8,081**	281,302
Actual Amount	**307,200**		319,680
Undefined Consumption / Loss	**6.64%**		**8.9%**

Table 4

Assumptions and Calculations

1. Condensed steam **(8,081 kg)** is discharged into Effluent stream

2. Steam Consumed $= (cp_f Xm_f + cp_l Xm_l) (T_0 - T_r)/ h_s$
   $cp_f =$ **1.4 KJ/kg** $cp_l =$ **4.2 KJ/kg** & m_f . m_l are fabric and liquid weight.

3. Moisture Content of fabrics
   Raw fabric - 7%
   After wet process - 43 %
   After Hydro extraction - 22%
   After Drying - 7%

4. Measured Value of Raw water inlet **207,200 kg/day** and From Bowsers **100,000 kg/day.**

The influent iron concentration is as per requirement of the washing plant. However the effluent value indicates a higher Fe value. This result was shown in all samples analysed. The cause of this is probably due to ageing pipe water etc.

CURRENT WASTEWATER TREATMENT PLANT

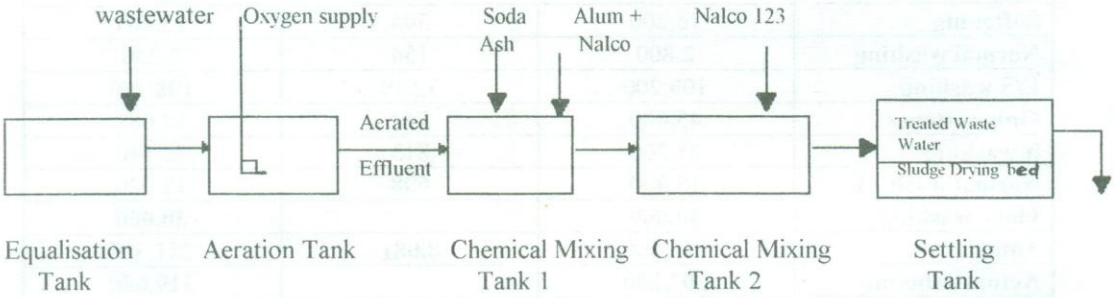

Figure 5

DISCUSSION

The results suggest that there are improvements that could be done to improve its performance. These steps also will benefit the company balance sheet. Some suggestions are as follows. Only brief statements are given as further work is progressing in this area.

i) Iron can be removed from groundwater using the following operations . This eliminates the transport of water from outside.
   a) Physico - Chemical Treatment-
      -pH of the water from tube wells are increased by adding KOH or NaOH
      -Aeration is done.
      -Allow it to precipitate (by using alum & Polymer coagulant)
      -Then it is sent through filter beds.

   b) Ozone Treatment -
      Ozone treatment is an option available for water treatment. It is a powerful oxidation mechanism. This can be utilised both in water and wastewater treatment. The difference would be the process retention time. The design details for iron removal are as follows.

      1ppm (mg/l) requires **0.43ppm** O_3 .
      Thus for the removal Ozone requirement is - **0.288 mg/l.**

ii) More controls should be added to the plant to monitor water consumption and use. This can be done via proper monitoring through instrumentation.
iii) Condensate should be recovered and reused back in the process.
iv) Effluent treatment plant should be streamlined to reduce effluent characteristics to get the effluent within CEA limits. Waste generation and treatment could make possible the introduction of water recycle steps, thus reducing input water quantity.
v) Plant piping and layout needs modifications to support waste minimisation.

Reference -

The gazette of the Democratic Socialist Republic of Sri Lanka 1990.02.02
De Alwis (1997); Hazardous waste management in Sri Lanka, Presentation of the symposium on Research for Industry.- Moratuwa Sri lanka.
De Silva (1996) ; Seminar presentation "An Outline of Garment Washing"
De Silva (1997) ; Seminar presentation "Basics of Garment Washing"
Central Bank Report(1995)
ARJUNA's Atlas of Sri Lanka.

BILLEST : COMPUTER AIDED ESTIMATING SOFTWARE

Dr. A.A.D.A.J. Perera, Department of Civil Engineering

BILLEST : COMPUTER AIDED ESTIMATING SOFTWARE

Dr. A.A.D.A.J. Perera, Department of Civil Engineering

The concepts of Computer Aided Estimating were first presented as far as late 1970 and very good software is now available. However, the use of Computer Aided Estimating Software in the Sri Lanka's construction industry is still at a very low level. Some organisations do use systems based on spreadsheets, databases and programs but lack facilities beyond the calculations of unit rates and preparation of simple bills of quantities. One of the main reasons for the limited use of Computer Aided Estimating software is the price, which is generally more than Rupees three hundred thousand. The software available is developed in other countries and has the problem of proper implementation.

With this background, Billest Computer Aided Estimating system was developed with the prime objective of offering software at a reasonable price and to suit estimating and tendering methods of Sri Lanka. Special effort was made to develop a system with very user friendly working methods and to avoid difficult procedures such as coding which is common in many Computer Aided Estimating Systems. Billest software was developed using Visual Basic Programming language and EXCEL spread sheets database.

The system maintains a library for the unit rate calculations, which can be updated for price variations of materials, labour, plant and subcontract items. If necessary separate libraries can be maintained for Building works and Civil Engineering works. Facilities are available to insert new library items for unit rates, new material, labour, plant and subcontract items. The operation manual and all the technical help required are incorporated into the system.

New BOQs can be created and descriptions can be imported from old project files or from the unit rate library. If descriptions and units are identical to the library items pricing will be done automatically. Otherwise pricing can be done by matching BOQ items and items in the library. Once the pricing is complete, a complete list of items of materials, labour, plant and subcontract items will be created and these could be updated to suit a particular project. Further last minute tendering adjustments such as mark-up, discounts can be made. Facilities are available to obtain reports of material usage and material where used. Finally, cash flow of the project considering cash flow variables can be performed using Billest software.

MEASUREMENT OF OCEAN WAVE HEIGHT USING A CAPACITANCE-BASED LIQUID LEVEL SENSOR

G. K. Watugala, W. A. Dilhara, N. G. D. I. Perera, K.K.K. C. Ariyathilake, S. C. R. Perera
Department of Mechanical Engineering
University of Moratuwa

MEASUREMENT OF OCEAN WAVE HEIGHT USING A CAPACITANCE-BASED LIQUID LEVEL SENSOR

G. K. Watugala, W. A. Dilhara, N. G. D. I. Perera, K.K.K. C. Ariyathilake, S. C. R. Perera
Department of Mechanical Engineering
University of Moratuwa

ABSTRACT

A digital liquid level measuring gauge has been designed, constructed and laboratory tested. The prototype gauge is specially made for ocean wave height measurement, but the underlined principle can be extended to level measurements in other situations.

The gauge consists of a field unit anchored at the location where the ocean wave height is to be measured, and a base unit stationed in land.. The base unit can be connected to a computer to download wave height data for analysis.

The field unit (see Fig.) consists of (1) an air-filled torus-shaped fully submerged platform anchored to sea bed, (2) a level sensing column hinged to the platform, and (3) a control box with electronic circuits, a radio transmitter, and rechargeable batteries. The anchoring is done in such a way that the mean sea level is roughly at the centre of the level sensing column. The sensing columns should be longer than twice the amplitude of sea waves. The control circuits perform many tasks: it converts the variation of capacitance between the two vertical tubes in the sensing column to variable frequency radio signal; it determines the sampling periods and sampling rates; it also communicates with the base unit by radio signals. The field unit is designed to consume very little power and the rechargeable batteries alone can power the unit for 10 days.

The base unit consists of a radio receiver, control circuits, and an interface. This unit can receive radio signals from the field unit which must be within 2 km. It decodes radio signals and obtains digital wave height data for transmission to a computer using the parallel port.

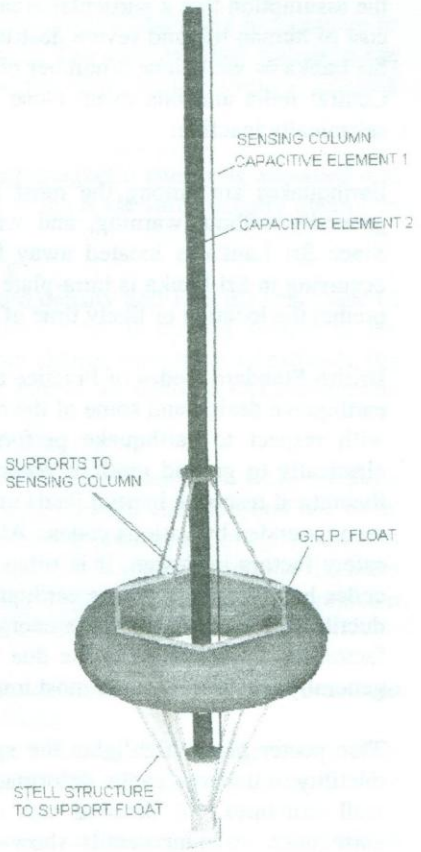

EARTHQUAKE RESISTANT DETAILING OF REINFORCED CONCRETE STRUCTURES

D F U Perera*, M T R Jayasinghe**,
* Stems Consultants (pte) Ltd.
** Department of Civil Engineering, University of Moratuwa.

EARTHQUAKE RESISTANT DETAILING OF REINFORCED CONCRETE STRUCTURES

D F U Perera*, M T R Jayasinghe**,
* Stems Consultants (pte) Ltd.
** Department of Civil Engineering, University of Moratuwa.

There are two major factors that discourage the use of earthquake resistant design and detailing of structures constructed in Sri Lanka. They are the belief that the earthquake resistant structures will cost a lot more than the normal structures and the misconception that Sri Lanka is located at area where no earthquakes will occur. On many occasions, the assumption that a particular area is seismically inactive has been proven wrong at the cost of human life and severe destruction to the infrastructure of an area. This is true for Sri Lanka as well since a number of earthquakes have been reported in the recent past in Central India and one event close to Sri Lanka which have hitherto be considered as seismically inactive.

Earthquakes are among the most awesome of natural forces. They occur suddenly, generally without warning, and within 10-20 seconds can turn cities into wasteland. Since Sri Lanka is located away from well known plate boundaries, any earthquake occurring in Sri Lanka is intra-plate type. In an intraplate area, it is almost impossible to predict the location or likely time of an earthquake event.

British Standard Codes of Practice used in Sri Lanka for structural design does not cover earthquake design and some of the reinforcement details widely adopted are not desirable with respect to earthquake performance. Dynamic analysis of structures responding elastically to ground motions recorded during severe earthquakes have shown that the theoretical response inertial loads may be much greater than the static design lateral loads recommended by various codes. Although this difference is too large to be reconciled by safety factors in design, it is often seen that structures designed to the lateral loads of codes have survived severe earthquakes. This can be attributed mainly to the ability of ductile structures to dissipate energy by post-elastic deformations helped by such other factors as a reduced response due to increased damping. The ductility of members is generally considered as the most important factor.

This poster paper highlights the special details that are required to provide sufficient ductility to undergo cyclic deformations without collapse for framed structures and shear wall structures. A detailed cost comparison carried out between normal details and earthquake resistant details show that the cost increase due to adopting earthquake resistant details would only be in the order of 2% of the overall cost of the project or it could even be less.

ELECTROMAGNETIC EFFECTS ON A HUMAN BRAIN DUE TO CELLULAR PHONES

I. J. Dayawansa
Department of Electronic & Telecommunication Engineering
University of Moratuwa.

ELECTROMAGNETIC EFFECTS ON A HUMAN BRAIN DUE TO CELLULAR PHONES

I. J. Dayawansa
Department of Electronic & Telecommunication Engineering
University of Moratuwa.

Electromagnetic waves of frequencies between 825MHz and 960MHz are used in Cellular Technology. These waves contain high energy. Constant exposure to such radiation is a cause for public health concern.

Work is being carried out to analyse the effects on the human brain due to exposure to electromagnetic waves from the use of cellular phones. The user receives signals at the high frequency end and transmits signals at the low frequency end, within the allowed frequency band.

The key issue in this problem is how much of electromagnetic energy is absorbed and where it is deposited. The Specific Absorption Rate or the **SAR** value usually quantifies this. At a specific location,

$$SAR = [\sigma |E|^2] / \rho$$

where σ is the tissue conductivity, ρ is the tissue mass density and **E** is the rms value of the internal electric field intensity. Thus the localized SAR is directly related to the electric field intensity at that location. Therefore our efforts have been to estimate the electric field intensity distribution inside the brain, due to an incident electromagnetic wave.

We modeled the brain by "cubic spheres" and solved the electromagnetic wave equation for incident "uniform plane waves". The equation is an integral equation and has to be solved using numerical techniques. Using the **Method of Moments**, the integral equation was solved and the electric field distribution obtained for a specific value of incident electric field. As the σ, ε & ρ values for the human brain were not available, the relevant values for a dog's brain were used to estimate the SAR values.

Our preliminary results indicate that the SAR values are very small inside the brain and that the values are higher near the outer layers of the brain.
The SAR value increases with increasing incident field. Near a cell boundary, the mobile unit operates at a high power level and therefore produces a high field intensity. This would increase the SAR value significantly.
The SAR value also increases with decreasing frequency and the mobile unit transmits at a lower frequency.

Future Prospects for a New Industry

Nirmali Perera
Department of Textile & Clothing Technology

Future Prospects for a New Industry

Nirmali Perera
Department of Textile & Clothing Technology

Abstract

Textile Industry in a global context is looking at new fibres, new applications, new developments in the New Millenium. This Sri Lankan industry hitherto is only consolidating its garment industry which in year 2005 will be facing many challenges with the changes taking place in the World Trade Scenario.

Textiles are defined as fibrous assemblies traditionally used for the making up of apparel. Textiles are also used in shoes, handbags and head gear apart from what is draped on the human body. Textiles are commonly and traditionally used for many household purposes too. The Sri Lankan Industry is operating at this end of the market where the non traditional textiles used in a number of other applications are increasing in its importance. These applications are smaller in scale but are very much higher in value.

As a single group these could be referred to as Technical Textiles. It is time that we focus our attention to these unexplored market niches in the Textile Industry.